**UNIVERSITY OF THESSALY**
**SCHOOL OF ENGINEERING**
**DEPARTMENT OF MECHANICAL & INDUSTRIAL ENGINEERING**

Master Thesis

# STRUCTURAL MODAL IDENTIFICATION METHODS BASED ON EARTHQUAKE-INDUCED VIBRATIONS

by

**NIKOLAOU IOANNIS**

Diploma in Mechanical & Industrial Engineering, University of Thessaly, 2006

A Thesis
Submitted in Partial Fulfillment of the
Requirements for the Degree of
Master of Science
(in Mechanical & Industrial Engineering)
2008

Institutional Repository - Library & Information Centre - University of Thessaly
24/04/2024 00:02:26 EEST - 3.141.244.201

ΠΑΝΕΠΙΣΤΗΜΙΟ ΘΕΣΣΑΛΙΑΣ
ΒΙΒΛΙΟΘΗΚΗ & ΚΕΝΤΡΟ ΠΛΗΡΟΦΟΡΗΣΗΣ
ΕΙΔΙΚΗ ΣΥΛΛΟΓΗ «ΓΚΡΙΖΑ ΒΙΒΛΙΟΓΡΑΦΙΑ»

Αριθ. Εισ.: 6450/1
Ημερ. Εισ.: 18-07-2008
Δωρεά: Συγγραφέα
Ταξιθετικός Κωδικός: Δ
624.176 2
ΝΙΚ

Institutional Repository - Library & Information Centre - University of Thessaly
24/04/2024 00:02:26 EEST - 3.141.244.201

**ΠΑΝΕΠΙΣΤΗΜΙΟ ΘΕΣΣΑΛΙΑΣ**
**ΠΟΛΥΤΕΧΝΙΚΗ ΣΧΟΛΗ**
**ΤΜΗΜΑ ΜΗΧΑΝΟΛΟΓΩΝ ΜΗΧΑΝΙΚΩΝ ΒΙΟΜΗΧΑΝΙΑΣ**

Μεταπτυχιακή Εργασία

# ΑΝΑΠΤΥΞΗ ΜΕΘΟΔΩΝ ΑΝΑΓΝΩΡΙΣΗΣ ΙΔΙΟΜΟΡΦΙΚΩΝ ΧΑΡΑΚΤΗΡΙΣΤΙΚΩΝ ΚΑΤΑΣΚΕΥΩΝ ΥΠΟ ΣΕΙΣΜΙΚΑ ΦΟΡΤΙΑ

υπό

**ΝΙΚΟΛΑΟΥ ΙΩΑΝΝΗ**

Διπλωματούχου Μηχανολόγου Μηχανικού Βιομηχανίας, Π.Θ., 2006

Υπεβλήθη για την εκπλήρωση μέρους των
απαιτήσεων για την απόκτηση του
Μεταπτυχιακού Διπλώματος Ειδίκευσης
2008



Institutional Repository - Library & Information Centre - University of Thessaly
24/04/2024 00:02:26 EEST - 3.141.244.201

© 2008 Νικολάου Ιωάννης

Η έγκριση της μεταπτυχιακής εργασίας από το Τμήμα Μηχανολόγων Μηχανικών Βιομηχανίας της Πολυτεχνικής Σχολής του Πανεπιστημίου Θεσσαλίας δεν υποδηλώνει αποδοχή των απόψεων του συγγραφέα (Ν. 5343/32 αρ. 202 παρ. 2).



Institutional Repository - Library & Information Centre - University of Thessaly
24/04/2024 00:02:26 EEST - 3.141.244.201

This research in this thesis was partially supported by funds provided by the Egnatia Odos A.E. This support is gratefully acknowledged.



Institutional Repository - Library & Information Centre - University of Thessaly
24/04/2024 00:02:26 EEST - 3.141.244.201

**Εγκρίθηκε από τα Μέλη της Πενταμελούς Εξεταστικής Επιτροπής:**

| | |
|---|---|
| Πρώτος Εξεταστής (Επιβλέπων) | Δρ. Παπαδημητρίου Κωνσταντίνος<br>Καθηγητής, Τμήμα Μηχανολόγων Μηχανικών Βιομηχανίας, Πανεπιστήμιο Θεσσαλίας |
| Δεύτερος Εξεταστής | Δρ. Σταματέλλος Αναστάσιος<br>Καθηγητής, Τμήμα Μηχανολόγων Μηχανικών Βιομηχανίας, Πανεπιστήμιο Θεσσαλίας |
| Τρίτος Εξεταστής | Δρ. Τσόπελας Παναγιώτης<br>Αναπληρωτής Καθηγητής, Τμήμα Πολιτικών Μηχανικών, Πανεπιστήμιο Θεσσαλίας |
| Τέταρτος Εξεταστής | Δρ. Νατσιάβας Σωτήριος<br>Καθηγητής, Τμήμα Μηχανολόγων Μηχανικών, Αριστοτέλειο Πανεπιστήμιο Θεσσαλονίκης |
| Πέμπτος Εξεταστής | Δρ. Πανέτσος Παναγιώτης<br>Διδάσκων Π. Δ. 407/80, Τμήμα Αρχιτεκτόνων Μηχανικών, Πανεπιστήμιο Θεσσαλίας |



Institutional Repository - Library & Information Centre - University of Thessaly
24/04/2024 00:02:26 EEST - 3.141.244.201

# Ευχαριστίες

Πρώτα απ' όλα, θέλω να ευχαριστήσω τον επιβλέποντα της μεταπτυχιακής εργασίας μου, Καθηγητή κ. Παπαδημητρίου Κωνσταντίνο, για την πολύτιμη βοήθεια και καθοδήγησή του κατά τη διάρκεια της μεταπτυχιακής εργασίας μου. Επίσης, είμαι ευγνώμων στα υπόλοιπα μέλη της εξεταστικής επιτροπής της μεταπτυχιακής εργασίας μου, Καθηγητές κκ. Σταματέλλο Αναστάσιο, Τσόπελα Παναγιώτη, Νατσιάβα Σωτήριο και Πανέτσο Παναγιώτη για την προσεκτική ανάγνωση της εργασίας μου και για τις πολύτιμες υποδείξεις τους. Ευχαριστίες οφείλω σε όλους τους προπτυχιακούς και μεταπτυχιακούς φοιτητές του Εργαστηρίου Δυναμικής Συστημάτων και φίλους μου για την άριστη συνεργασία που είχαμε κατά τη διάρκεια της παρούσας μεταπτυχιακής εργασίας. Ιδιαίτερες ευχαριστίες οφείλω στον συμφοιτητή και φίλο Ντότσιο Βαγγέλη για την πολύτιμη βοήθειά του σε θέματα προγραμματισμού σε περιβάλλον Matlab αλλά και σε πολλά θέματα σχετικά με τη συγγραφή της παρούσας εργασίας. Ευχαριστώ τους φίλους(ες) μου Δανιήλ, Πέτρο, Ματούλα, Μαριλένα, Πατρίτσια, Θωμά και Στέλιο για την ηθική υποστήριξή τους και για τις ωραίες στιγμές που περάσαμε. Πάνω απ' όλα, είμαι ευγνώμων στους γονείς μου, Νικόλαο και Βασιλική καθώς και στην αδελφή μου Σοφία για την ολόψυχη αγάπη και υποστήριξή τους όλα αυτά τα χρόνια καθώς και για τη δυνατότητα που μου έδωσαν να συνεχίσω τις σπουδές μου.

Ιωάννης Νικολάου



Institutional Repository - Library & Information Centre - University of Thessaly
24/04/2024 00:02:26 EEST - 3.141.244.201

# STRUCTURAL MODAL IDENTIFICATION METHODS BASED ON EARTHQUAKE-INDUCED VIBRATIONS

## Abstract

The problem of identification of the modal parameters of a structural model using earthquake-induced vibration measurements is addressed. It is based on a weighted least-squares approach using multiple-input multiple-output measured time histories at the base supports and at selected locations of a structure. The identification is performed in the time domain and in the frequency domain. Existing modal identification methods have been extended in this work to treat generalized non-classically damped modal models. The case of classically damped modal models is treated as a special case.

The identification of the modal parameters (modal frequencies, modal damping ratios, modeshape components and participation factors) is accomplished by introducing a three step approach: in the first step, a stabilization diagram is constructed containing frequency and damping information. Next, the modeshape components and participation factors are found in a second least-squares step, based on the user selection of the stabilized poles. Finally, in order to improve the estimation of the modal characteristics especially for the challenging case of closely spaced and overlapping modes, a third step concerning the fully nonlinear optimization problem is addressed. Computational issues involving the solution of the optimization problems and the evaluation of analytical expressions of the gradients of the objective functions are also discussed.

The validation of the proposed methodologies and algorithms is presented using simulated data from a 3 DOF and a 10 DOF spring mass chain model. The methodologies are next applied for the identification of the modal characteristics of two bridges, the R/C bridge of Egnatia Odos located at Polymylos, Greece, and the Vincent Thomas cable suspension bridge located at Los Angeles, USA. Results provide qualitative and quantitative information on the dynamic behaviour of the bridge systems and their components under earthquake-induced vibrations.



Institutional Repository - Library & Information Centre - University of Thessaly
24/04/2024 00:02:26 EEST - 3.141.244.201

## Contents

**Chapter 1: Introduction** ..... 1

1.1 Research Context ..... 1

1.2 Outline – Organization of the Thesis ..... 4

**Chapter 2: Linear System Analysis in Time Domain** ..... 6

2.1 Introduction ..... 6

2.2 Formulation for Classically-Damped Models ..... 7

2.3 State Space Formulation of non-Classically Damped Models ..... 8

2.3.1 The eigenvalue problem ..... 8

2.3.2 Orthogonality conditions ..... 9

2.4 Observation equations ..... 11

2.5 Modal model ..... 12

2.5.1 State space equations ..... 12

2.5.2 Observation equations ..... 13

2.5.3 Summary of modal model equations ..... 15

2.6 Special case: Classically damped model ..... 17

**Chapter 3: Time Domain Methods for Identification of Non-classically Damped Modal Models of StructuresLinear System Analysis in Time Domain** ..... 19

3.1 Introduction ..... 19

3.2 Formulation as a Least-Squares Optimization Problem ..... 20

3.3 Formulation Using Active and Fixed Modes ..... 24

3.4 Simplifications Explaining Quadratic Dependence on Modal Characteristics ..... 25

3.5 Analytical Expression of the Gradient of the Objective function ..... 28

3.6 Special Case: Classically Damped Modal Models ..... 31

3.6.1 Formulation of the Objective Function ..... 31

3.6.2 Analytical Expression of the Gradient of the Objective function 36

3.7 Modal Sweep Approach ..... 38

**Chapter 4: Frequency Domain Methods for Identification of Non-classically Damped Modal Models** ..... 39

4.1 Introduction ..... 39



Institutional Repository - Library & Information Centre - University of Thessaly
24/04/2024 00:02:26 EEST - 3.141.244.201

4.2 Modal model – Frequency domain ..... 40
4.3 Stabilization Diagrams (First Step) ..... 41
4.3.1 Common Denominator Model ..... 41
4.3.2 Error Function ..... 43
4.3.3 Reduced Normal Equations ..... 44
4.4 Formulation as a Weighted Least-Squares Optimization Problem ..... 46
4.5 Second Step (First Approach) ..... 48
4.5.1 Simplifications Explaining Quadratic Dependence on Modal Characteristic ..... 51
4.5.2 Analytical Expression of the Gradient of the Objective function ..... 55
4.6 Second Step (Second Approach) ..... 57
4.6.1 Simplifications Explaining Quadratic Dependence on Modal Characteristics ..... 61
4.6.2 Analytical Expression of the Gradient of the Objective function ..... 65
4.7 Third Step (Nonlinear Optimization) ..... 72
4.8 Appendix ..... 73
4.8.1 System Of Linear Algebraic Equations (First Approach of Second Step) ..... 73
4.8.2 System Of Linear Algebraic Equations (Second Approach of Second Step) ..... 79
**Chapter 5: Applications** ..... 83
5.1 Introduction ..... 83
5.2 Response of Structures Subjected to Multiple Base Excitation ..... 83
5.3 Validation of Modal Identification Algorithm using Simulated Data ..... 86
5.4 Polymylos Bridge, Greece ..... 93
5.4.1 Bridge Description and Instrumentation ..... 93
5.4.2 Modal Identification ..... 95
5.5 Vincent Thomas Bridge, Los Angeles, California ..... 102
5.6 Appendix ..... 110
**Chapter 6: Conclusions** ..... 113
**References** ..... 115



Institutional Repository - Library & Information Centre - University of Thessaly
24/04/2024 00:02:26 EEST - 3.141.244.201

# CHAPTER 1

# Introduction

## 1.1. Research Context

Identification is the process of building an accurate, simplified mathematical model for a system based on a set of input and output measurements. The particular problem of system identification of the modal parameters of a linear structural model by using dynamic data, commonly referred to as experimental modal analysis (Ewins, 2000), has received much attention during the years, because of the importance of the modal characteristics in understanding the dynamic behaviour of the structure and designing the structure to meet certain performance criteria. Also the modal characteristics are useful in model updating, structural control and health monitoring applications. Applications exist for a wide range of structures, such as in aerospace and automotive industries, where modal tests are performed on extensively instrumented spacecrafts, aircrafts, vehicle bodies and train bodies by using precisely controlled excitations for determining the modal parameters. Civil structures, mainly buildings, bridges, off-shore structures and dams also appear the need for identification strategies, so as to understand their behaviour as well as assert damage caused either by earthquake, wind, or aging and to prevent further deterioration.

A great number of structures require certain specifications for safe and precise operation conditions, which usually form the most significant design parameters. In order to ensure a constantly accepted and reliable performance of a system, the knowledge of its dynamic behavior becomes essential in either case of operational or unpredictable extreme loads. For newly build structures, as well as for the ones that are already in operation for some time, the measurement of their dynamic properties, such as natural frequencies, damping factors and modeshapes is well desired, so as for the prediction of their behavior using a reliable model to be feasible.

It is worth pointing out that measured modal characteristics are used in model updating and in damage detection efforts (Papadimitriou et al., 1997). The basic idea is that commonly measured modal parameters (notably modal frequencies, mode shapes, and modal damping) are functions of the physical properties of the structure (mass, damping, and stiffness). Therefore, changes in the physical properties, such as reductions in stiffness resulting from the onset of cracks or loosening of a connection, will cause detectable changes in these modal properties. These changes in modal characteristics can be used to detect damage and identify its location and severity.

This thesis is concerned with the application of the identification process to civil engineering structures based on their earthquake-induced vibrations. The evaluation of the actual dynamic characteristics of civil engineering structures through measurements of their dynamic response has been attracting an increasing research effort worldwide (Wilson 1986, Werner et al. 1987,



Institutional Repository - Library & Information Centre - University of Thessaly
24/04/2024 00:02:26 EEST - 3.141.244.201

Safak E (1993), Lus e. al. 1999, Chaudhary et al. 2000, Chaudhary et al. 2002, Smyth et al. 2003, Arici and Mosalam 2003, Lin et al. 2005, Liu et al. 2005, Siringoringo and Fujino 2007). For the case of earthquake-induced vibrations, the modal characteristics are estimated from the measured portion of the excitation occurred to the structure and the measured vibration responses. These measurements are usually the acceleration of the structure obtained by accelerometers optimal placed on the structure (Papadimitriou et al., 2002). It has been observed from response measurements of large structures to potentially damaging excitations that the dynamic properties of many structures are markedly different during response to strong ground motion than in small amplitude ambient and forced vibration tests. Hence, it is of considerable interest and importance to extract information about structural behavior from strong motion data.

Measured response data of civil engineering structures from earthquake-induced vibrations offer an opportunity to study quantitatively and qualitatively their dynamic behaviour within the resulting vibration levels. These vibration measurements can be processed for the estimation of the modal characteristics, as well for the calibration of corresponding (finite element) models used to simulate their behaviour. The information for the identified modal models and the updated finite element models is useful for validating the assumptions used in model development or for improving modelling, analysis and design procedures. Also, such information is useful for structural health monitoring purposes.

Modal identification algorithms provide estimates of the modal frequencies, modal damping ratios and modeshapes at the measured DOFs using classically-damped or non-classically damped modal models. For the case of earthquake-induced vibrations, modal identification methods have been developed in time domain (Beck 1978; Beck and Jennings 1980) and in frequency domain (McVerry 1980), based on a minimization of the measure of fit between the time history or its Fourier transform of the acceleration responses estimated from the measurements and the corresponding ones predicted from a classically-damped modal model of the structure. Beck (1978) and Beck and Jennings (1980), had presented an output-error approach for the identification of linear, time-invariant models from strong motion records, through the minimization of a measure of fit including displacement, velocity and acceleration records. McVerry (1980), has applied an output-error approach in the frequency domain, using the Fast Fourier Transform of the acceleration response time histories to estimate the modal properties through least-squares matching. Werner et al. (1987) formulated a methodology in the time domain for the case of measured input excitation, such as earthquake excitation, for an elastic system with classical normal modes and with motion measurements from any number of input and system response degrees of freedom. Their procedure was an extension of the least-squares-output-error method which was used by Beck (1978). Extensions for identifying non classically-damped modal models in the frequency domain have also been developed by Chaudhary et al. (2000). Tan and Cheng (1993) proposed an iterative identification algorithm, which was based on the modal sweep concept and the band-pass filtering process, to identify the modal parameters of a non-classically damped linear structure from its recorded earthquake



Institutional Repository - Library & Information Centre - University of Thessaly
24/04/2024 00:02:26 EEST - 3.141.244.201

response. Mahmoudabadi et al. (2006) developed a method for parametric system identification in frequency domain for classically and non-classically damped linear systems subjected up to six components of earthquake ground motions, which is able to work in multi-input/multi-output (MIMO) case.

For structural modal identification techniques, there exist certain limitations to the robustness and reliability, such as:

- ***Insufficient measurement data:*** the response of a structure is usually measured at only a small number of locations (limited number of sensors), which gives little information about the full modeshapes of the structure. Another issue is the usually limited range of the exciting frequency band that hides some of the system's dynamic properties. From a testing standpoint it is more difficult to excite the higher frequency response of a structure, as more energy is required to produce measurable response at these higher frequencies than at the lower frequencies. In addition, sensors are not always placed at the optimal locations to give the best possible information for the excited system.

- ***Coupling of modes:*** within the measured frequency range of response it is often difficult to identify all the modes contributing to the measured response because of coupling between the modes that are closely spaced in frequency. This difficulty is observed more commonly at the higher frequency portions of the spectrum where the modal density is typically greater.

- ***Measurement error:*** the dynamic data measurements always consist of bias errors (noise) at some extent, caused either by faulty instruments, changes in the environmental conditions during testing, or poor preprocessing of the initial data (*bias* from windowing of the data). The effect of noise on the modal approach is that it limits the number of modes that can be estimated reliably, for there exists a deterioration of the signal-to-noise ratio for the higher modes. Thus, the modal parameters could be identified for only the dominant modes in the measurement records.

- ***Non-uniqueness:*** the lack of sensitivity of the measurement quantities to small changes in the modal parameters to be identified.

- ***Ill-Conditioning:*** when the number of parameters is larger than needed or when the available measurements are relatively limited, then the optimal solution to the identification problem appears not to be unique.

The methods developed by McVerry (1980) in the frequency domain and Beck and Jennings (1980) in the time domain, are extended in this work to treat non-classically damped modal models, since damping may not be proportionally distributed in various structural components. For the special case of bridges, non - proportionally damping appears due to the energy dissipation mechanism provided locally by the elastomeric bearings and the foundation soil. For base isolated buildings, non proportional damping may appear due to the energy dissipation mechanism provided locally by the isolation system. Output-error methods are used in which the



Institutional Repository - Library & Information Centre - University of Thessaly
24/04/2024 00:02:26 EEST - 3.141.244.201

optimal values of the modal parameters are obtained by minimizing the discrepancy between measured responses and the predicted responses of the system. Time domain output error methods process the response time histories measured from a network of sensors (e.g. accelerometers), while frequency domain output error methods process the Fourier transforms of the measured response time histories.

A novel aspect of this thesis is the use of a three step approach to solve the error optimization problem. The first step provides estimates of the modal frequencies and modal damping ratios by solving a system of linear algebraic equations. Stabilization diagrams are used to distinguish between physical and mathematical modes. The second step provides estimates of the modeshapes and the participation factors by solving a system of linear algebraic equations. The first two steps usually give accurate estimates of the modal characteristics. A third step is added to improve this estimates, if needed by efficiently solving the full nonlinear optimization problem with initial estimates of the modal parameters those obtained from the first and second steps.

## 1.2. Outline – Organization of the Thesis

In this thesis modal identification methodologies for estimating the dynamic modal characteristics of civil engineering structures have been developed using earthquake induced vibration measurements.

Chapter 2 uses a linear system theory with the objective to describe the solution of the system in the time and frequency domains in terms of the modal coordinates. Several mathematical models are discussed that can be used to describe the dynamical behavior of a structure with a limited number of parameters. The formulation is presented for the general case of non-classically damped modes. The classically damped case is then formulated as a special case. Both continuous and discrete time formulations are presented.

In Chapter 3, a time domain methodology is presented for identifying the modal and other parameters of non-classically damped modal models describing a system's response characteristics based on earthquake-induced vibration data. An output error formulation is presented, in which the selected modal parameters are derived through least-squares matching of the acceleration time history estimated from the modal model to the measured acceleration at specific points within the structure. A time domain methodology for identifying the modal and other parameters of classically damped modal models is also presented.

In Chapter 4, a frequency domain methodology is presented for the identification of the modal and other parameters of non-classically damped modal models describing a system's response characteristics based on earthquake-induced vibration data. The identification of the modal parameters is performed using frequency domain data. An output error formulation is presented, in which the selected modal parameters are derived through least-squares matching of the



Institutional Repository - Library & Information Centre - University of Thessaly
24/04/2024 00:02:26 EEST - 3.141.244.201

Fourier transform of the response predicted from the modal model to the Fourier transform of the measured response acceleration at specific points within the structure, over a specified frequency band.

In Chapter 5, the modal identification methods are applied to identify the modes of civil engineering bridges subjected to different input acceleration components arising from the multiple supports. For this, the equation of motion governing the response of bridges when subjected to different excitations from the multiple supports is revealed and shown to fall into the category of linear structures used to develop the modal identification method. Next, the modal identification algorithms in time domain and in frequency domain are validated using simulated support (base) acceleration response time histories generated from a 3DOF and a 10DOF spring mass chain model. Finally, the implementation of the modal identification methodologies is presented for two bridges using available earthquake recordings. The first bridge is the R/C bridge of Polymylos which is part of the Egnatia Odos motorway system in Greece. Recordings are available for the low level, magnitude $M_L = 4.6$, earthquake event that occurred on 21/2/2007 (2:04:38 GMT) at a distance 35km Northeast of the bridge. The second bridge is the Vincent Thomas cable suspension Bridge located at Los Angeles. Earthquake recordings are available from the 1987 Whittier earthquake of magnitude $M_L = 6.1$.

Chapter 6 concentrates on the observations and conclusions that resulted from this work. It also focuses on several aspects concerning the area of modal model identification that need further attention.



Institutional Repository - Library & Information Centre - University of Thessaly
24/04/2024 00:02:26 EEST - 3.141.244.201

# CHAPTER 2

# Linear System Analysis in Time Domain

## 2.1 Introduction

This section uses linear system theory to solve the equations of motion that govern the response (displacement, velocity and acceleration) of structures. Modal analysis is used to describe the response at the measured (observable) degrees of freedom of the structure in terms of the eigenproperties (eigenvalues and eigenvectors) and the excitation. The analysis is used in subsequent Chapters for solving the inverse problem of identifying the eigenproperties given input-output measurements.

Using a spatial discretization method, such as finite element analysis, the equations of motion for a linear structure are given by the following set of $n$ second order differential equations

$$M\ddot{\underline{q}}(t)+C_0\dot{\underline{q}}(t)+K\underline{q}(t)=L\underline{u}(t) \tag{2.1}$$

where $\underline{q}(t)\in\mathbb{R}^{N_{out}\times 1}$ is the displacement vector, $M$, $C_0$ and $K\in\mathbb{R}^{n\times n}$ are respectively the mass, damping and stiffness matrices, $\underline{u}(t)\in\mathbb{R}^{N_{in}\times 1}$ is the applied force vector at the $N_{in}$ DOFs, and $L\in\mathbb{R}^{n\times N_{in}}$ is a matrix comprised of zeros and ones that maps the $N_{in}$ excited DOFs to the $n$ output DOFs. Throughout the analysis, it is assumed that the system matrices $M$, $C_0$ and $K$ are symmetric.

Linear system theory is used with the objective to describe the solution of the system in the time domain in terms of the modal coordinates. The formulation is presented for the general case of non-classically damped modes. The classically damped case is then formulated as a special case. Both continuous and discrete time formulations are presented. All results given in this Chapter are well known. Their presentation is given herein in order to make this Thesis self-contained.

The presentation is divided into the following sections. Section 2.3 gives known modal analysis results for formulating the response of the structure in terms of real modal coordinates for a classically-damped model (2.1). Sections 2.3 to 2.5 extend the formulation to the general case of a non-classically damped model (2.1). For this, the state space form of system (2.1) is used and the corresponding complex-valued modal analysis results are presented. Section 2.6 gives a summary of the formulas that describe the response of the structure at the measured locations in terms of the complex eigenproperties (eigenvalues and eigenvectors).



Institutional Repository - Library & Information Centre - University of Thessaly
24/04/2024 00:02:26 EEST - 3.141.244.201

## 2.2 Formulation for Classically-Damped Models

Assuming that the structure is classically damped and that the system matrices $M$, $C_0$ and $K \in \mathbb{R}^{n\times n}$ are symmetric, the solution for the displacement response $\underline{q}(t) \in \mathbb{R}^{N_{out}\times 1}$ in the modal space can be written in the form:

$$\underline{q}(t) = \sum_{r=1}^{N} \underline{\phi}_r \xi_r(t) = \Phi \underline{\xi}(t) \tag{2.2}$$

The modal coordinates $\xi_r(t)$ are given by the modal equations

$$\ddot{\xi}_r(t) + 2\zeta_r \omega_r \dot{\xi}_r(t) + \omega_r^2 \xi_r(t) = \underline{\phi}_r^T L \underline{u}(t) \tag{2.3}$$

where $\omega_r$ is the modal frequency, $\zeta_r$ is the modal damping ratio and $\underline{\varphi}_r$ is the modeshape vector for the $r$ mode. The modeshapes $\underline{\varphi}_r, r = 1,\ldots,n$, are real and satisfy the orthogonality conditions

$$\underline{\phi}_r^T M \underline{\phi}_s = \delta_{rs} \qquad ,r = 1,\ldots,n,\ s = 1,\ldots,n \tag{2.4}$$

$$\underline{\phi}_r^T K \underline{\phi}_s = \omega_r^2 \delta_{rs} \qquad ,r = 1,\ldots,n,\ s = 1,\ldots,n \tag{2.5}$$

where $\delta_{rs} = \begin{cases} 1, & r = s \\ 0, & r \neq s \end{cases}$ (2.6)

is the Kronecker delta. Equivalently, in matrix form the orthogonality condition (2.4) and (2.5) are written as

$$\Phi^{\mathrm{T}} M \Phi = I \tag{2.7}$$

$$\Phi^{\mathrm{T}} K \Phi = \Omega^2 \tag{2.8}$$

where $\Phi = \begin{bmatrix} \underline{\phi}_1 & \cdots & \underline{\phi}_n \end{bmatrix}$ is the matrix of modeshapes and $\Omega^2$ is a diagonal matrix of the squares of the modal frequencies given by

$$\Omega^2 = \begin{bmatrix} \omega_1^2 & & 0 \\ & \ddots & \\ 0 & & \omega_n^2 \end{bmatrix} \tag{2.9}$$

Note that all variables involved in the classically damped analysis presented in this section are real and the modal equation are second order differential equations. In contrast, the variables



Institutional Repository - Library & Information Centre - University of Thessaly
24/04/2024 00:02:26 EEST - 3.141.244.201

in the classically damped modal analysis presented in Section 2.3 are in general complex, while the modal equations are first order differential equations. It can be shown that the two formulations for describing the response in the modal space are equivalent.

## 2.3 State Space Formulation of non-Classically Damped Models

In the general case where the system is non-classically damped the set of equations (2.1) must be converted to a set of first order state space formulation. This is accomplished by introducing the complementary equation

$$M\dot{\underline{q}}(t) = M\dot{\underline{q}}(t) \tag{2.10}$$

and the state vector

$$\underline{x} = \begin{bmatrix} \underline{q} \\ \dot{\underline{q}} \end{bmatrix} \tag{2.11}$$

Equations (2.1) and (2.10) can be written in the state space form

$$P\dot{\underline{x}} + Q\underline{x} = \begin{bmatrix} L \\ 0 \end{bmatrix} \underline{u}(t) \tag{2.12}$$

where the matrices $P$ and $\mathrm{Q}$ are given by

$$P = \begin{bmatrix} C_0 & M \\ M & 0 \end{bmatrix}, \quad \mathrm{Q} = \begin{bmatrix} K & 0 \\ 0 & -M \end{bmatrix} \tag{2.13}$$

### 2.3.1 The eigenvalue problem

The eigenvectors $\underline{\psi}_r$ and the corresponding eigenvalues $\lambda_r$ satisfy the eigenproblem

$$(P\lambda + Q)\underline{\psi} = \underline{0} \tag{2.14}$$

The eigenvalues $\lambda_r$ and the eigenvectors $\underline{\psi}_r$ are complex and it can be shown that if $\lambda_r$ and $\underline{\psi}_r$ are the eigenvalues and eigenvectors of the eigenproblem then $\lambda_r^*$ and $\underline{\psi}_r^*$ are also eigenvalues and eigenvectors of the same eigenproblem.

Introducing the eigenmatrix $\Psi = \left[\underline{\psi}_1 \ \cdots \ \underline{\psi}_n \ \underline{\psi}_1^* \ \cdots \ \underline{\psi}_n^*\right] \in C^{2n\times 2n}$ it can easily be shown (Natsiavas 1999) that the eigenmatrix of the eigenproblem (2.14) is given by



Institutional Repository - Library & Information Centre - University of Thessaly
24/04/2024 00:02:26 EEST - 3.141.244.201

$$\Psi = \begin{bmatrix} \Phi & \Phi^* \\ \Phi\Lambda & \Phi^*\Lambda^* \end{bmatrix} \in \mathbb{C}^{2n\times 2n} \tag{2.15}$$

where $\Phi$, $\lambda$ satisfy the second order eigenproblem

$$M\Phi\lambda^2 + C_0\Phi\lambda + K\Phi = 0 \tag{2.16}$$

The eigenvalues $\lambda_r$ are given by

$$\lambda_r = -\zeta_r\omega_r \pm j\omega_r\sqrt{1-\zeta_r^2} \tag{2.17}$$

where

$$\omega_r = |\lambda_r| \qquad \text{and} \qquad \zeta_r = -\frac{\mathrm{Re}\{\lambda_r\}}{\omega_r} \tag{2.18}$$

The eigenvalue matrix for the first order linear system (2.12) is given by

$$\Lambda_c = \begin{bmatrix} \Lambda & 0 \\ 0 & \Lambda^* \end{bmatrix} = diagonal \in C^{2n\times 2n} \tag{2.19}$$

where $\Lambda$ is the diagonal matrix

$$\Lambda = \begin{bmatrix} \lambda_1 & & 0 \\ & \ddots & \\ 0 & & \lambda_n \end{bmatrix} \tag{2.20}$$

### 2.3.2 Orthogonality conditions

The complex eigenvectors satisfy the orthogonality condition

$$\Psi^T P\Psi = diag\left[a_r\right] \tag{2.21}$$

that can by written as

$$P = \Psi^{-T} diag\left[a_r\right]\Psi^{-1} \tag{2.22}$$

The eigenvectors also satisfy the orthogonality condition

$$\Psi^T Q\Psi = diag\left[\beta_r\right] \tag{2.23}$$



Institutional Repository - Library & Information Centre - University of Thessaly
24/04/2024 00:02:26 EEST - 3.141.244.201

that respectively can by written as

$$Q = \Psi^{-T} diag[\beta_r] \Psi^{-1} \tag{2.24}$$

Pre-multiplying (2.14) by $\underline{\psi}^T$ yields

$$\underline{\psi}^T P \underline{\psi} \lambda + \underline{\psi}^T Q \underline{\psi} = 0 \tag{2.25}$$

and solving for $\lambda$ gives

$$\lambda = -\frac{\underline{\psi}^T Q \underline{\psi}}{\underline{\psi}^T P \underline{\psi}} \tag{2.26}$$

For the r-th eigenvalue and eigenvector, the last expression gives

$$\lambda_r = -\frac{\underline{\psi}_r^T Q \underline{\psi}_r}{\underline{\psi}_r^T P \underline{\psi}_r} \tag{2.27}$$

The r-th eigenvalue is finally given by

$$\lambda_r = -\beta_r / \alpha_r \tag{2.28}$$

where

$$\begin{aligned} \beta_r &= \underline{\psi}_r^T Q \underline{\psi}_r \\ \alpha_r &= \underline{\psi}_r^T P \underline{\psi}_r \end{aligned} \tag{2.29}$$

and the eigenvalue matrix is given by

$$\Lambda_c = diag\left[1/a_r\right] diag[\beta_r] \tag{2.30}$$

The normalized state space formulation is obtained by pre-multiplying equation (2.12) by $P^{-1}$.

$$P^{-1} = \begin{bmatrix} 0 & M^{-1} \\ M^{-1} & -M^{-1} C_0 M^{-1} \end{bmatrix} \tag{2.31}$$

The normalized state space equations take the form



Institutional Repository - Library & Information Centre - University of Thessaly
24/04/2024 00:02:26 EEST - 3.141.244.201

$$\dot{\underline{x}} = A_c \underline{x} + B_c \underline{u}(t) \tag{2.32}$$

where

$$A_c = -P^{-1}Q = \begin{bmatrix} 0 & M^{-1} \\ M^{-1} & -M^{-1}C_0M^{-1} \end{bmatrix} \begin{bmatrix} K & 0 \\ 0 & -M \end{bmatrix} = \begin{bmatrix} 0 & I \\ -M^{-1}K & -M^{-1}C_0 \end{bmatrix} \tag{2.33}$$

is the state space matrix and

$$B_c = -P^{-1} \begin{bmatrix} L \\ 0 \end{bmatrix} = \begin{bmatrix} 0 & M^{-1} \\ M^{-1} & -M^{-1}C_0M^{-1} \end{bmatrix} \begin{bmatrix} L \\ 0 \end{bmatrix} = \begin{bmatrix} 0 \\ -M^{-1}L \end{bmatrix} \tag{2.34}$$

Based on the eigenproblem (2.14) and pre-multiplying (2.14) by $P^{-1}$ yields

$$(-P^{-1}Q - \lambda I)\underline{\psi} = \underline{0} \;\Rightarrow\; (A_c - \lambda I)\underline{\psi} = \underline{0} \tag{2.35}$$

For the r-th eigenvalue and eigenvecor, the last expression can be written in the form

$$A_c \underline{\psi}_r = \lambda_r \underline{\psi}_r, \qquad r = 1, \ldots, 2n \tag{2.36}$$

In matrix form, the set of $2n$ equations (2.36) can by written in the form

$$A_c \Psi = \Psi \Lambda_c \tag{2.37}$$

that gives

$$A_c = \Psi \Lambda_c \Psi^{-1} \tag{2.38}$$

Formulation (2.37) shows that the matrices $\Lambda_c$ and $\Psi$ contain the eigenvalues and eigenvectors of the state space matrix $A_c$.

## 2.4 Observation equations

Let $\underline{y}(t)$ be the response vector of interest. These responses, in general case, are a linear combination of the accelerations, velocities and displacements of the system. The generalized observation equation is given in the form

$$\underline{y}(t) = C_a \ddot{\underline{q}}(t) + C_v \dot{\underline{q}}(t) + C_d \underline{q}(t) \tag{2.39}$$



Institutional Repository - Library & Information Centre - University of Thessaly
24/04/2024 00:02:26 EEST - 3.141.244.201

By writing $\ddot{\underline{q}}(t)$ as a function of $\dot{\underline{q}}(t)$ and $\underline{q}(t)$ using (2.1) and substituting in (2.39) yields

$$\underline{y}(t) = C_c \underline{x} + D_c \underline{u}(t) \tag{2.40}$$

where

$$C_c = \left[ C_d - C_\alpha M^{-1} K \mid C_v - C_\alpha M^{-1} C_0 \right] \tag{2.41}$$

and

$$D_c = C_\alpha M^{-1} L \tag{2.42}$$

## 2.5 Modal model

### 2.5.1 State space equations

For the realization of modal analysis method the following transformation is introduced

$$\underline{x}(t) = \Psi \underline{\xi}(t) \tag{2.43}$$

where $\underline{\xi}$ is the vector of the main modal coordinates. Substituting eq. (2.43) in (2.32) and pre-multiplying by $\Psi^{-1}$ the following expressions are obtained

$$\Psi \dot{\underline{\xi}} = A_c \Psi \underline{\xi} + B_c \underline{u}(t) \tag{2.44}$$

or equivalently

$$\dot{\underline{\xi}} = \Psi^{-1} A_c \Psi \underline{\xi} + \Psi^{-1} B_c \underline{u}(t) \tag{2.45}$$

Using the eigenvalue problem (2.37), one finally obtains the equations

$$\dot{\underline{\xi}} = \Lambda_c \underline{\xi} + L_c \underline{u}(t) \tag{2.46}$$

where

$$L_c = \Psi^{-1} B_c \tag{2.47}$$

The last equation (2.46) is the state space equations for the modal coordinates $\underline{\xi}(t)$. The $L_c$ term can be simplified using equation (2.22) which is solved with respect to $\Psi^{-1}$ to yield

$$\Psi^{-1} = diag\left[ 1/a_r \right] \Psi^T P \tag{2.48}$$



Institutional Repository - Library & Information Centre - University of Thessaly
24/04/2024 00:02:26 EEST - 3.141.244.201

By substituting the last expression in (2.47) and using (2.15) and (2.13) results in

$$L_c = \Psi^{-1} B_c = diag\left[ 1/a_r \right] \Psi^T P \begin{bmatrix} 0 \\ M^{-1} L \end{bmatrix} = \\ = diag\left[ 1/a_r \right] \left[ \begin{array}{c|c} \Phi & \Phi^* \\ \hline \Phi\Lambda & \Phi^*\Lambda^* \end{array} \right]^T \begin{bmatrix} C_0 & M \\ M & 0 \end{bmatrix} \begin{bmatrix} 0 \\ M^{-1} L \end{bmatrix} \tag{2.49}$$

Carrying out the matrix multiplications, the above equation finally simplifies to

$$L_c = diag\left[ 1/a_r \right] \begin{bmatrix} \Phi^T \\ \Phi^{*T} \end{bmatrix} L \tag{2.50}$$

The $L_c$ matrix is the participation factor matrix. Using modal coordinates equations (2.50) result in

$$\dot{\xi}_r(t) = \lambda_r \xi_r(t) + \frac{1}{\alpha_r} \underline{\phi}_r^T L \underline{u}(t), \qquad r = 1, \ldots, n \tag{2.51}$$

$$\dot{\xi}_{n+r}(t) = \lambda_r^* \xi_{n+r}(t) + \frac{1}{\alpha_{n+r}} \underline{\phi}_{n+r}^{*T} L \underline{u}(t) \tag{2.52}$$

with

$$\xi_{n+r} = \xi_r^* \quad \text{and} \quad \alpha_{n+r} = \alpha_r^* \tag{2.53}$$

Note that the complex equation (2.52) is the complex conjugate of the complex model equation (2.51).

### 2.5.2 Observation equations

The response $\underline{y}(t)$ defined in (2.40) can be expressed using modal coordinates by substituting the transformation (2.43) in (2.40) to yield

$$\underline{y}(t) = C_c \Psi \underline{\xi}(t) + D_c \underline{u}(t) \tag{2.54}$$

or equivalently

$$\underline{y}(t) = V_c \underline{\xi}(t) + D_c \underline{u}(t) \tag{2.55}$$

where



Institutional Repository - Library & Information Centre - University of Thessaly
24/04/2024 00:02:26 EEST - 3.141.244.201

$$V_c = C_c \Psi \tag{2.56}$$

The matrix $V_c$ is called the modal response matrix (output – observation) and can be simplified using equations (2.41) and (2.15) into the form

$$V_c = \left[ C_d - C_\alpha M^{-1} K \;\vdots\; C_v - C_\alpha M^{-1} C_0 \right] \left[ \begin{array}{c:c} \Phi & \Phi^* \\ \hdashline \Phi\Lambda & \Phi^*\Lambda^* \end{array} \right] \tag{2.57}$$

Let us now consider the following three special cases:

a) The response $\underline{y}(t)$ consists of the displacements only, that is $C_a = C_v = 0$ and $C_d \neq 0$. The $V_c$ matrix takes the final form

$$V_c = \left[ C_d \;\vdots\; 0 \right] \left[ \begin{array}{c:c} \Phi & \Phi^* \\ \hdashline \Phi\Lambda & \Phi^*\Lambda^* \end{array} \right] = C_d \left[ \Phi \;\vdots\; \Phi^* \right] \tag{2.58}$$

b) The response $\underline{y}(t)$ consists of the velocities only, that is $C_a = C_d = 0$ and $C_v \neq 0$. The $V_c$ matrix takes the final form

$$V_c = C_v \left[ \Phi\Lambda \;\vdots\; \Phi^*\Lambda^* \right] \tag{2.59}$$

c) The response $\underline{y}(t)$ consists of the accelerations only, that is $C_v = C_d = 0$ and $C_a \neq 0$. The $V_c$ matrix takes the final form

$$\begin{aligned} V_c &= -C_\alpha \left[ M^{-1} K \;\vdots\; M^{-1} C_0 \right] \left[ \begin{array}{c:c} \Phi & \Phi^* \\ \hdashline \Phi\Lambda & \Phi^*\Lambda^* \end{array} \right] \\ &= -C_\alpha \left[ M^{-1} K\Phi + M^{-1} C_0 \Phi\Lambda \;\vdots\; M^{-1} K\Phi^* + M^{-1} C_0 \Phi^*\Lambda^* \right] \end{aligned} \tag{2.60}$$

that can be simplified further using the eigenproblem (2.16). Specifically, from (2.16) one has

$$M^{-1} K\Phi + M^{-1} C_0 \Phi\Lambda = -\Phi\Lambda^2 \tag{2.61}$$

or equivalently by taking complex conjugates

$$M^{-1} K\Phi^* + M^{-1} C_0 \Phi^*\Lambda^* = -\Phi^*\Lambda^{*2} \tag{2.62}$$

Substituting the last two expressions into (2.60), $V_c$ is given by

$$V_c = C_\alpha \left[ \Phi\Lambda^2 \;\vdots\; \Phi^*\Lambda^{*2} \right] \tag{2.63}$$



Institutional Repository - Library & Information Centre - University of Thessaly
24/04/2024 00:02:26 EEST - 3.141.244.201

### 2.5.3 Summary of modal model equations

Summarizing, for the case of general non classically damped systems, the modal model consists of the modal state space equations (2.46) and the modal observation equations (2.55), that is,

$$\dot{\underline{\xi}} = \Lambda_c \underline{\xi} + L_c \underline{u}(t) \tag{2.64}$$

$$\underline{y}(t) = V_c \underline{\xi}(t) + D_c \underline{u}(t) \tag{2.65}$$

where

$$\underline{\xi}(t) = \begin{Bmatrix} \xi_1(t) \\ \vdots \\ \xi_n(t) \\ \xi_1^*(t) \\ \vdots \\ \xi_n^*(t) \end{Bmatrix} \in C^{2n\times 1} \tag{2.66}$$

is the modal coordinates vector

$$\Lambda_c = \begin{bmatrix} \Lambda & 0 \\ 0 & \Lambda^* \end{bmatrix} \tag{2.67}$$

is the matrix that consists of the complex eigenvalues $\lambda_r$ of the system,

$$L_c = \Psi^{-1} B_c = diag\left[ 1/a_r \right] \begin{bmatrix} \Phi^T \\ \Phi^{*T} \end{bmatrix} L \in C^{2n\times N_{in}} \tag{2.68}$$

is the participation factor matrix,

$$\underline{u}(t) \in \mathbb{R}^{N_{in}} \tag{2.69}$$

is the independent vector of excitations,

$$D_c = C_a M^{-1} L \in \mathbb{R}^{N_o \times N_{in}} \tag{2.70}$$

is a matrix that is zero if no accelerations are contained in the response vector $\underline{y}(t)$, and $V_c \in C^{N_o \times 2n}$ is a matrix given by

$$V_c = C_d \begin{bmatrix} \Phi & \Phi^* \end{bmatrix} \qquad \text{for displacements} \tag{2.71}$$



Institutional Repository - Library & Information Centre - University of Thessaly
24/04/2024 00:02:26 EEST - 3.141.244.201

$$V_c = C_v\left[\Phi\Lambda \quad \Phi^*\Lambda^*\right] \qquad \text{for velocities} \tag{2.72}$$

$$V_c = C_a\left[\Phi\Lambda^2 \quad \Phi^*\Lambda^{*2}\right] \qquad \text{for accelerations} \tag{2.73}$$

Consider next the case for which $C_d$, $C_v$ and $C_a$ in (2.39) are observation matrices that assign a correspondence between the model degrees of freedom and the observation (measured) degrees of freedom. In this case note that:

$$U = C_d\Theta = \left[\underline{u}_1 \quad \cdots \quad \underline{u}_n\right] \tag{2.74}$$

is the eigenvector matrix at the desirable (measured) degrees of freedom that are included in the response vector $\underline{y}(t)$ for the displacements. Similarly, taking into account that $\Lambda$ is diagonal yields

$$C_v\Theta\Lambda = \left[\lambda_1\underline{u}_1 \quad \cdots \quad \lambda_n\underline{u}_n\right] \tag{2.75}$$

is the eigenvector matrix at the desirable degrees of freedom that are included in the response vector $\underline{y}(t)$ for the velocities. Similarly, taking into account that $\Lambda^2$ is a diagonal matrix,

$$C_a\Theta\Lambda^2 = \left[\lambda_1^2\underline{u}_1 \quad \cdots \quad \lambda_n^2\underline{u}_n\right] \tag{2.76}$$

is the eigenvector matrix at the desirable degrees of freedom that are included in the response vector $\underline{y}(t)$ for the accelerations.

Based on the above formulations the response $\underline{y}(t) \in \mathbb{R}^{No}$ at the $N_o$ degrees of freedom of the linear model is given by

$$\underline{y}(t) = \left[U \quad U^*\right]\underline{\xi}(t) + D_c\underline{u}(t) \tag{2.77}$$

where

$$U = \left[\underline{u}_1, \ldots \underline{u}_n\right] \in C^{N_o \times n} \tag{2.78}$$

is the eigenvector matrix at the desirable degrees of freedom. Consequently, the system response for either displacements or velocities or accelerations is fully defined when the elements of the matrices $\Lambda_c$, $L_c$, $U$ and $D_c$ are known.

From the previous analysis, it is evident that the response $\underline{y}(t)$ of the linear structure at selected degrees of freedom can be completely defined by knowing the parameters set $\underline{\theta}$ that includes all entries involved in the matrices $\Lambda_c$, $L_c$, $V_c$ and $D_c$.



Institutional Repository - Library & Information Centre - University of Thessaly
24/04/2024 00:02:26 EEST - 3.141.244.201

## 2.6 Special case: Classically damped model

The aforementioned equations for the general case of non-classically damped system are simplified in this paragraph for the case of classically damped systems and assuming that the structure matrices $M$, $C_0$ and $K \in \mathbb{R}^{n\times n}$ are symmetric. From the analysis of classically damped structures with symmetric matrices, it is known that the response is given by

$$\underline{q} = \underline{\phi} e^{\lambda t} \tag{2.79}$$

where $\underline{\phi} \in \mathbb{R}^n$ is a real modeshape vector. In this case the matrix of modeshapes $\Phi \in \mathbb{R}^{n\times n}$, defined in (2.15), is also a real matrix.

Consequently, substituting in (2.15) the complex modeshape matrix, $\Psi$ is given by

$$\Psi = \begin{bmatrix} \Phi & \Phi \\ \Phi\Lambda & \Phi\Lambda^* \end{bmatrix} \tag{2.80}$$

Substituting the above equation into the orthogonality condition (2.21) yields

$$diag\left[a_r\right] = \Psi^{\mathrm{T}} P \Psi = \begin{bmatrix} diag\left[2\omega_r\sqrt{1-\zeta_r^2}\right] & 0 \\ 0 & -diag\left[2\omega_r\sqrt{1-\zeta_r^2}\right] \end{bmatrix} \tag{2.81}$$

and substituting (2.81) in (2.68) yields

$$L_c = -j\begin{bmatrix} diag\left[2\omega_r\sqrt{1-\zeta_r^2}\right] & 0 \\ 0 & -diag\left[2\omega_r\sqrt{1-\zeta_r^2}\right] \end{bmatrix}^{-1} \begin{bmatrix} \Phi^T \\ \Phi^T \end{bmatrix} L \tag{2.82}$$

Using (2.51) and (2.52), the modal coordinates $\xi_r(t)$ and $\xi_r^*(t)$ are written in the form

$$\dot{\xi}_r(t) = \lambda_r \xi_r + \frac{1}{2\omega_r j\sqrt{1-\zeta_r^2}} \underline{\phi}_r^T L \underline{u}(t) \tag{2.83}$$

$$\dot{\xi}_r^*(t) = \lambda_r^* \xi_r^* + \frac{1}{-2\omega_r j\sqrt{1-\zeta_r^2}} \underline{\phi}_r^T L \underline{u}(t) \tag{2.84}$$

The system of equation (2.83) and (2.84) can thus be written in the complex form (2.64) where $L_c$ is an *purely imaginary* matrix given by (2.82). Using (2.55) to (2.57) and (2.80), the response vector $\underline{y}(t)$ is given by the observation equation

$$\underline{y}(t) = V_c \underline{\xi}(t) + D_c \underline{u}(t) \tag{2.85}$$



Institutional Repository - Library & Information Centre - University of Thessaly
24/04/2024 00:02:26 EEST - 3.141.244.201

where

$$V_c = C_c \begin{bmatrix} \Phi & \Phi \\ \Phi\Lambda & \Phi\Lambda^* \end{bmatrix} \tag{2.86}$$

$$C_c = \left[ C_d - C_\alpha M^{-1} K \mid C_v - C_\alpha M^{-1} C_0 \right] \tag{2.87}$$

$$D_c = C_\alpha M^{-1} L \tag{2.88}$$



Institutional Repository - Library & Information Centre - University of Thessaly
24/04/2024 00:02:26 EEST - 3.141.244.201

# CHAPTER 3

# Time Domain Methods for Identification of Non-classically Damped Modal Models of Structures

## 3.1 Introduction

In this chapter, a time domain methodology is presented for identifying the modal parameters of non-classically damped modal models used to describe the response of linear structures subjected to multiple base excitations. The modal parameters to be identified include the modal frequencies, the modal damping ratios, the modeshapes and the participation factors. The proposed structural modal identification methodology is applicable to civil engineering structures such as buildings, towers, bridges, offshore structures, etc., subjected to earthquake excitations. The identification methodology uses measured input acceleration time history data at the base degrees of freedom and output acceleration time history data at the model degrees of freedom of the structure. An output error formulation is presented, in which the modal parameters are identified through least-squares matching between the output measured acceleration time histories and the acceleration time histories predicted by a modal model of the structure subjected to the measured base input acceleration time histories. In addition, a time domain methodology for identifying the modal and other parameters in the special case of classically damped modal models is also presented.

This chapter discusses several mathematical models that can be used to describe the dynamical behavior of a structure with a limited number of parameters. From an engineering point of view the modal model of a structure provides the best physical understanding. However, since this model is highly non-linear in its parameters most identification algorithms do not directly identify the model parameters. Instead, the modal parameter estimation methods proposed in this chapter identify state space models from the experimental measurements. In the next sections, the relation between these models and the modal parameters are discussed.

This chapter is divided into the following sections. In Section 3.2 an output error formulation is presented as a weighted least squares optimization problem in the time domain. In Section 3.3 the formulation of the objective function for non-classically damped systems is presented using active and fixed modes in order to implement a modal sweep approach similar to one presented in Werner et al. (1987) for classically damped systems. Section 3.4 gives simplifications which explain the quadratic dependence of the objective function on the modal characteristics and in Section 3.5 analytical expressions of the gradient of the objective function are given. In Section 3.6 the special case of classically damped modal models is presented. In Subsection 3.6.1 the formulation of the objective function for classically damped modal models is presented using active and fixed modes, and in Subsection 3.6.2 analytical expressions of the gradient of the



Institutional Repository - Library & Information Centre - University of Thessaly
24/04/2024 00:02:26 EEST - 3.141.244.201

objective function are given. Finally, in Section 3.7 the modal sweep approach which is used for the implemented optimization routine is presented.

## 3.2 Formulation as a Least-Squares Optimization Problem

Let $\underline{y}(k\Delta t,\underline{\theta})$ be a vector of the response of a linear structure obtained from a modal model involving a parameter set $\underline{\theta}$ and $m$ modes. The variable $\Delta t$ denotes the time discretization step and $k=\{1,2,\ldots,N\}$ is an index set. The parameters in $\underline{\theta}$ include the modal characteristics such as modal frequencies, modal damping ratios, and modeshape components at the measured locations, modal participation factors, and other parameters that completely define the response vector $\underline{y}(k\Delta t,\underline{\theta})$.

A modal model output-error identification approach seeks the optimal values of the parameter set $\underline{\theta}$ that minimize a measure of fit between the modal model predictions $\underline{y}(k\Delta t,\underline{\theta})$ and the corresponding response $\underline{\hat{y}}(k\Delta t)$ estimated from the measured data. That is, the modal model identification is formulated as a minimization problem of finding the values of $\underline{\theta}$ that minimizes the measure of fit

$$J(\underline{\theta})=\frac{1}{V}\sum_{k=0}^{N}\left[\underline{y}(k\Delta t;\underline{\theta})-\underline{\hat{y}}(k\Delta t)\right]^{T}\left[\underline{y}(k\Delta t;\underline{\theta})-\underline{\hat{y}}(k\Delta t)\right] \tag{3.1}$$

where

$\underline{\hat{y}}$: measured response time histories at the $N_{in}$ measured DOF

$\underline{y}$: response time histories at the measured $N_{out}$ DOF predicted by the modal model

$\Delta t$: sampling time interval of the digital acceleration

$N$: total number of sample data over the response duration $T$

$k$: the time index set at time $t=k\Delta t$

$$V=\sum_{k=0}^{N}\left[\underline{\hat{y}}(k\Delta t)\right]^{T}\left[\underline{\hat{y}}(k\Delta t)\right]\text{: normalization factor for time domain} \tag{3.2}$$

In this work, $\underline{y}(k\Delta t,\underline{\theta})$ represents the acceleration response predictions at the measured output locations of a structure which are described by the parametric modal model developed in Section 2.5 and $\underline{\hat{y}}(k\Delta t)$ represents the measured accelerations at the same locations. However, the formulation presented is directly applicable to other response time histories such as displacements and velocities.

Using the analysis in Chapter 2, the vector $\underline{y}(t;\underline{\theta})$ of the acceleration responses at the $N_{out}$ measured degrees of freedom, based on the non-classically damped modal models, can be written in the form



Institutional Repository - Library & Information Centre - University of Thessaly
24/04/2024 00:02:26 EEST - 3.141.244.201

$$\underline{y}(t) = \begin{bmatrix} U & U^* \end{bmatrix} \underline{\xi}(t) + D_c \underline{u}(t) \tag{3.3}$$

where $D_c \in \mathbb{R}^{N_{out} \times N_{in}}$, is a real matrix

$$U = \left[\underline{u}_1, \ldots \underline{u}_m\right] \in C^{N_{out} \times m} \tag{3.4}$$

is the matrix of the complex eigenvectors $\underline{u}_r$, $r = 1, \ldots, m$ at $N_{out}$ DOFs, and

$$\underline{\xi}(t) = \begin{Bmatrix} \xi_1(t) \\ \vdots \\ \xi_m(t) \\ \xi_1^*(t) \\ \vdots \\ \xi_m^*(t) \end{Bmatrix} \in C^{2m \times 1} \tag{3.5}$$

is the complex vector of modal coordinates satisfying the complex modal state space equations

$$\begin{aligned} \dot{\xi}_r(t) &= \lambda_r \xi_r(t) + \underline{l}_r^T \underline{u}(t) \\ \dot{\xi}_r^*(t) &= \lambda_r^* \xi_r^*(t) + \underline{l}_r^{*T} \underline{u}(t) \end{aligned} \quad , r = 1, \ldots, m \tag{3.6}$$

where $\underline{l}_r^T \in C^{1 \times N_{in}}$ is the complex vector of the modal participation factors relating the $N_{in}$ inputs to the $r$ mode of the system, and

$$\lambda_r = -\zeta_r \omega_r \pm j\omega_r \sqrt{1 - \zeta_r^2} = -a_r \pm jb_r \quad , r = 1, \ldots, m \tag{3.7}$$

are the complex eigenvalues of the structures. The parameters $\alpha_r = \zeta_r \omega_r$ and $b_r = \omega_r \sqrt{1 - \zeta_r^2}$ are expressed in terms of the modal frequency $\omega_r$ and the modal damping ratio $\zeta_r$. Given $\alpha_r$ and $b_r$, the modal frequency $\omega_r$ and the damping ratio $\zeta_r$ are obtained from the following relationships:

$$\omega_r = \sqrt{a_r^2 + b_r^2} \tag{3.8}$$

$$\zeta_r = \frac{a_r}{\sqrt{a_r^2 + b_r^2}} \tag{3.9}$$

The modal response $\xi_r(t)$ can be obtained by solving (3.6) using the complex-valued initial conditions $\xi_r(0)$.

The parameters set $\underline{\theta}$ in the notation $\underline{y}(t;\underline{\theta})$ contains the parameters that completely define the response vector $\underline{y}(t;\underline{\theta})$ using the modal analysis. From equations (3.3) to (3.7), it is evident that the parameter set $\underline{\theta}$ contains the complex eigenvalue $\lambda_r$ of the $r$ mode, the complex



Institutional Repository - Library & Information Centre - University of Thessaly
24/04/2024 00:02:26 EEST - 3.141.244.201

modeshapes $\underline{u}_r \in C^{N_{out}\times 1}$, the modal participation factor vectors $\underline{l}_r^T \in C^{1\times N_{in}}$, the initial conditions $\xi_r(0) = \xi_r^0$, and the entries of the real matrix $D_c \in \mathbb{R}^{N_{out}\times N_{in}}$, that is

$$\underline{\theta}: \left\{\lambda_r, \underline{u}_r, \underline{l}_r^T, \xi_r^0, r = 1,...,m, D_c\right\} \tag{3.10}$$

where $m$ is the number of contributing modes which is also an unknown in the modal identification process.

It should be noted that in the aforementioned formulation the parameter set $\underline{\theta}$ consist of complex-valued variables, while the response vector $\underline{y}(t;\underline{\theta})$ is also described in terms of complex-valued variables and solutions of modal equations with complex-valued coefficients. From the computer implementation point of view, it is necessary to describe the response vector in terms of real-valued variables, equations and parameters. In what follows, the response vector $\underline{y}(t;\underline{\theta})$ is reformulated in terms of real-valued variables and parameter set $\underline{\theta}$. For this, the complex-valued scalar and vector variables $\underline{u}_r$, $\underline{l}_r$, $\xi_r(t)$ and $\xi_r(0)$ involved in the description of the modal model are expressed in terms of the real and imaginary parts as follows:

$$\underline{u}_r = \underline{\phi}_r + j\underline{\psi}_r \tag{3.11}$$

$$\underline{l}_r^T = \underline{p}_{\mathrm{Re},r}^T + j\underline{p}_{\mathrm{Im},r}^T \tag{3.12}$$

$$\xi_r(t) = n_{\mathrm{Re},r}(t) + jn_{\mathrm{Im},r}(t) \tag{3.13}$$

$$\xi_r^0 = n_{\mathrm{Re},r}^0 + jn_{\mathrm{Im},r}^0 \tag{3.14}$$

Using (3.3), (3.4) and (3.5), the response vector $\underline{y}(t;\underline{\theta}) \equiv \underline{y}(t)$ can be expressed in the form

$$\underline{y}(t) = \sum_{r=1}^{m}\left[\underline{u}_r\xi_r(t) + \underline{u}_r^*\xi_r^*(t)\right] + D_c\underline{u}(t) \tag{3.15}$$

Substituting (3.11) and (3.13) into (3.15), and after rearranging the terms, yields

$$\underline{y}(t) = \sum_{r=1}^{m}\left\{\left(\underline{u}_r + \underline{u}_r^*\right)n_{\mathrm{Re},r}(t) + j\left(\underline{u}_r + \underline{u}_r^*\right)n_{\mathrm{Im},r}(t)\right\} + D_c\underline{u}(t) \tag{3.16}$$

or, equivalently,

$$\underline{y}(t) = \sum_{r=1}^{m}\left\{2\underline{\phi}_r n_{\mathrm{Re},r}(t) - 2\underline{\psi}_r n_{\mathrm{Im},r}(t)\right\} + D_c\underline{u}(t) \tag{3.17}$$

Introducing the two-dimensional real modal vector of real modal coordinates



Institutional Repository - Library & Information Centre - University of Thessaly
24/04/2024 00:02:26 EEST - 3.141.244.201

$$\underline{n}_r(t) = \begin{Bmatrix} n_{\mathrm{Re},r}(t) \\ n_{\mathrm{Im},r}(t) \end{Bmatrix} \in \mathbb{R}^{2\times 1} \tag{3.18}$$

equation (3.17) can be written in the compact matrix form

$$\underline{y}(t) = 2\sum_{r=1}^{m} \left\{ \begin{bmatrix} \underline{\phi}_r & -\underline{\psi}_r \end{bmatrix} \underline{n}_r(t) \right\} + D_c \underline{u}(t) \tag{3.19}$$

The equations for the real and the imaginary parts $n_{\mathrm{Re},r}(t)$ and $n_{\mathrm{Im},r}(t)$, respectively, of the complex modal coordinate $\xi_r(t)$ can be obtained by substituting (3.13), (3.12) and (3.7) into the first of (3.6) to yield

$$\dot{n}_{\mathrm{Re},r}(t) + j\dot{n}_{\mathrm{Im},r}(t) = (-a_r + jb_r)\left(n_{\mathrm{Re},r}(t) + jn_{\mathrm{Im},r}(t)\right) + \left(\underline{p}_{\mathrm{Re},r}^T + j\underline{p}_{\mathrm{Im},r}^T\right)\underline{u}(t) \tag{3.20}$$

Equating the real and the imaginary parts of the above equation, yields the following system of two first-order differential equations that describe the time evolution of $n_{\mathrm{Re},r}(t)$ and $n_{\mathrm{Im},r}(t)$:

$$\dot{n}_{\mathrm{Re},r}(t) = -a_r n_{\mathrm{Re},r}(t) - b_r n_{\mathrm{Im},r}(t) + \underline{p}_{\mathrm{Re},r}^T \underline{u}(t) \tag{3.21}$$

$$\dot{n}_{\mathrm{Im},r}(t) = -a_r n_{\mathrm{Im},r}(t) + b_r n_{\mathrm{Re},r}(t) + \underline{p}_{\mathrm{Im},r}^T \underline{u}(t) \tag{3.22}$$

In matrix form, equations (3.21) and (3.22) become

$$\dot{\underline{n}}_r(t) = \begin{bmatrix} -a_r & -b_r \\ b_r & -a_r \end{bmatrix} \underline{n}_r(t) + \begin{Bmatrix} \underline{p}_{\mathrm{Re},r}^T \\ \underline{p}_{\mathrm{Im},r}^T \end{Bmatrix} \underline{u}(t) \tag{3.23}$$

which can be solved using the initial conditions

$$\underline{n}_r(0) = \begin{Bmatrix} n_{\mathrm{Re},r}^0 \\ n_{\mathrm{Im},r}^0 \end{Bmatrix} \in \mathbb{R}^{2\times 1} \tag{3.24}$$

Summarizing, the response vector $\underline{y}(t)$ is equivalently obtained by the modal expansion expression (3.19), where the real modal vectors $\underline{n}_r(t)$ are given by the first-order differential equations (3.23) that are solved using the initial conditions (3.24). Thus, the response is completely described by the real parameter set $\underline{\theta}$ that contains the modal parameters $\alpha_r = \zeta_r \omega_r$ and $b_r = \omega_r \sqrt{1-\zeta_r^2}$ that are related to the modal frequencies $\omega_r$ and the modal damping ratios $\zeta_r$, the real part $\underline{\phi}_r \in \mathbb{R}^{N_{out}}$ and the imaginary part $\underline{\psi}_r \in \mathbb{R}^{N_{out}}$ of the complex modeshapes $\underline{u}_r \in C^{N_{out}\times 1}$, the real part $\underline{p}_{\mathrm{Re},r}^T \in \mathbb{R}^{N_{in}}$ and the imaginary part $\underline{p}_{\mathrm{Im},r}^T \in \mathbb{R}^{N_{in}}$ of the



Institutional Repository - Library & Information Centre - University of Thessaly
24/04/2024 00:02:26 EEST - 3.141.244.201

modal participation factor vectors $\underline{l}_r^T \in C^{1\times N_{in}}$, the real part $n^0_{\mathrm{Re},r}$ and the imaginary part $n^0_{\mathrm{Im},r}$ of the initial conditions $\xi_r(0) = \xi_r^0$, and the entries of the real matrix $D_c \in \mathbb{R}^{N_{out}\times N_{in}}$, that is,

$$\underline{\theta} = \left\{ a_r,\ b_r,\ \underline{\phi}_r,\ \underline{\psi}_r,\ \underline{p}^T_{\mathrm{Re},r},\ \underline{p}^T_{\mathrm{Im},r},\ n^0_{\mathrm{Re},r},\ n^0_{\mathrm{Im},r},\ r=1,...,m,\ D_c \right\} \tag{3.25}$$

where $m$ is the number of contributing modes which is also an unknown in the identification process. The total number of model parameter involved in the prediction of the response at $N_{out}$ DOFs given $m$ modes and $N_{in}$ base input time histories, is $\left[4m + 2\left(m\times N_{in}\right) + 2\left(N_{out}\times m\right) + \left(N_{out}\times N_{in}\right)\right]$

The previous formulation is an extension to the non-classically damped modes of the time domain formulation developed by Beck (1978) assuming classically damped modes. Basically, the problem being solved is the one of minimizing the cost function $J\left(\underline{\theta}\right)$ in (3.1) with respect to the parameters $\underline{\theta}$. For this case, gradient-based optimization method is implemented that requires initial estimates for the parameters and will be described in detail later on.

## 3.3 Formulation Using Active and Fixed Modes

In order to implement a modal sweep approach similar to one presented in Werner et al. (1987) for classically damped systems, two index sets are introduced, the active index set $I_\alpha$ containing the mode numbers that are active and are optimized during the optimization process and the fixed index set $I_f$ that contains the rest of the $m$ modes that are included in computation of the response vector but their parameter values are kept constant during the optimization process. Consequently, equation (3.19) can be expressed in the form

$$\underline{y}(t) = 2\sum_{r\in I_\alpha}\left\{\left[\underline{\phi}_r \quad -\underline{\psi}_r\right]\underline{n}_r\left(t\right)\right\} + D_c\underline{u}(t) + 2\sum_{f\in I_f}\left\{\left[\underline{\phi}_f \quad -\underline{\psi}_f\right]\underline{n}_f\left(t\right)\right\} \tag{3.26}$$

Introducing the active and the fixed parts of the responses by

$$\underline{x}^r\left(t;\underline{\theta}\right) = 2\sum_{r\in I_\alpha}\left\{\left[\underline{\phi}_r \quad -\underline{\psi}_r\right]\underline{n}_r\left(t\right)\right\} + D_c\underline{u}(t) \tag{3.27}$$

$$\underline{x}^f\left(t\right) = 2\sum_{f\in I_f}\left\{\left[\underline{\phi}_f \quad -\underline{\psi}_f\right]\underline{n}_f\left(t\right)\right\} \tag{3.28}$$

Respectively, the total response $\underline{y}\left(t;\underline{\theta}\right) \equiv \underline{y}\left(t\right)$ due to $m$ contributing modes can be written in the form

$$\underline{y}(t) = \underline{x}^r\left(t;\underline{\theta}\right) + \underline{x}^f\left(t\right) \tag{3.29}$$



Institutional Repository - Library & Information Centre - University of Thessaly
24/04/2024 00:02:26 EEST - 3.141.244.201

which is more appropriate to use when formulating the optimization problem using modal sweeps to identify the modal parameters of the active modes defined in the set $I_\alpha$, holding the parameters of all other fixed modes, defined in the set $I_f$, as constants.

Using active and fixed modes, the objective function (3.1) can be expressed in the form

$$J(\underline{\theta}) = \frac{1}{V}\sum_{k=0}^{N}\left[\underline{x}^r(k\Delta t;\underline{\theta}) + \underline{x}^f(k\Delta t) - \underline{\hat{y}}(k\Delta t)\right]^T\left[\underline{x}^r(k\Delta t;\underline{\theta}) + \underline{x}^f(k\Delta t) - \underline{\hat{y}}(k\Delta t)\right] \quad (3.30)$$

,or equivalently, the final form of the objective function is given by

$$J(\underline{\theta}) = \frac{1}{V}\sum_{k=0}^{N}\left[\underline{x}^r(k\Delta t;\underline{\theta}) - \underline{\hat{e}}(k\Delta t)\right]^T\left[\underline{x}^r(k\Delta t;\underline{\theta}) - \underline{\hat{e}}(k\Delta t)\right] \quad (3.31)$$

where $\underline{x}^r(k\Delta t;\underline{\theta})$, given by (3.27), depends on the parameter set $\underline{\theta}$, while $\underline{\hat{e}}(k\Delta t)$ given by

$$\underline{\hat{e}}(k\Delta t) = \underline{\hat{y}}(k\Delta t) - 2\sum_{f\in I_f}\left\{\left[\underline{\phi}_f \quad -\underline{\psi}_f\right]\underline{n}_f(t)\right\} \quad (3.32)$$

is the constant vector of the measured response minus the response vector that is predicted from the modal model considering only the fixed modes.

## 3.4 Simplifications Explaining Quadratic Dependence on Modal Characteristics

The minimization of the objective function (3.31) can be carried out efficiently, significantly reducing computational cost, by recognizing that the error function in (3.31) is quadratic with respect to the real part $\underline{\phi}_r$ and the imaginary part $\underline{\psi}_r$ of the complex modeshapes $\underline{u}_r$ and the elements in the real matrix $D_c$. This observation is used to develop explicit expressions that relate the parameters $\underline{\phi}_r$, $\underline{\psi}_r$ and $D_c$ to the rest of the model parameters appearing in the parameter set $\underline{\theta}$, such as the real part $\underline{p}_{\mathrm{Re},r}^T$ and the imaginary part $\underline{p}_{\mathrm{Im},r}^T$ of the complex participation factor $\underline{l}_r^{\mathrm{T}}$, as well as the modal parameters $\alpha_r$ and $b_r$ that relate the modal frequencies $\omega_r$ and the modal damping ratios $\zeta_r$, and the initial conditions $n_{\mathrm{Re},r}^0$ and $n_{\mathrm{Im},r}^0$.

For this the parameter set $\underline{\theta}$ in (3.25) is partitioned into parameters sets as follows

$$\underline{\theta} = \left(\underline{\theta}^a, \underline{\theta}^b\right) \quad (3.33)$$

where $\underline{\theta}^b$ is defined by

$$\underline{\theta}^b = \left(\underline{\phi}_r,\ \underline{\psi}_r,\ r = 1,\ldots,m,\ D_c\right) \quad (3.34)$$



Institutional Repository - Library & Information Centre - University of Thessaly
24/04/2024 00:02:26 EEST - 3.141.244.201

and $\underline{\theta}^a$ is defined by

$$\underline{\theta}^a = \left( a_r,\ b_r,\ \underline{p}^T_{\mathrm{Re},r},\ \underline{p}^T_{\mathrm{Im},r},\ n^0_{\mathrm{Re},r},\ n^0_{\mathrm{Im},r},\ r = 1,\ldots,m \right) \tag{3.35}$$

Stationary conditions with respect to the parameters in the set $\underline{\theta}^b$ are used to develop a linear system of equations for solving for the set $\underline{\theta}^b$ given the values of the parameters set $\underline{\theta}^a$.

For convenience in the presentation this linear system can be formulated in the general form

$$\mathrm{A}\left(\underline{\theta}^\alpha\right)\underline{\theta}^b = \underline{b}\left(\underline{\theta}^\alpha\right) \tag{3.36}$$

where $\mathrm{A}\left(\underline{\theta}^\alpha\right)$ and $\underline{b}\left(\underline{\theta}^\alpha\right)$ are functions of the parameter set $\underline{\theta}^a$. Let

$$\underline{\theta}^b = \underline{\theta}^b\left(\underline{\theta}^a\right) \tag{3.37}$$

be the function that gives the relationship between the parameters set $\underline{\theta}^b$ and the parameter set $\underline{\theta}^a$ by solving the system (3.36). Then the objective function $J\left(\underline{\theta}\right)$ takes the form

$$J\left(\underline{\theta}\right) = J\left(\underline{\theta}^a, \underline{\theta}^b\right) = J\left(\underline{\theta}^a, \underline{\theta}^b\left(\underline{\theta}^a\right)\right) \equiv J^*\left(\underline{\theta}^a\right) \tag{3.38}$$

Hence the minimization problem can be stated as follows. Find the values of the parameter set $\underline{\theta}^a$ that minimize the objective function

$$J^*\left(\underline{\theta}\right) = J\left(\underline{\theta}^a, \underline{\theta}^b\left(\underline{\theta}^a\right)\right) \tag{3.39}$$

Once the values of $\underline{\theta}^a$ have been found, the values of $\underline{\theta}^b$ are obtained solving the linear system (3.36). Next our objective is to apply the above concept and first obtain the matrices and vectors that completely define the linear system (3.36).

The linear system for the parameter set $\underline{\theta}^b$ is obtained by setting the derivatives of $J\left(\underline{\theta}\right)$ with respect to each element of $\underline{\theta}^b$ equal to zero, that is,

$$\frac{\partial J\left(\underline{\theta}\right)}{\partial \phi_{l\rho}} = 0 \tag{3.40}$$

$$\frac{\partial J\left(\underline{\theta}\right)}{\partial \psi_{l\rho}} = 0 \tag{3.41}$$

$$\frac{\partial J\left(\underline{\theta}\right)}{\partial D_{c,li}} = 0 \tag{3.42}$$



Institutional Repository - Library & Information Centre - University of Thessaly
24/04/2024 00:02:26 EEST - 3.141.244.201

for $l=1,\ldots,N_{out}$, $r=1,\ldots,m$ and $i=1,\ldots,N_{in}$. Introducing the matrices

$$U=\left[\Phi \quad -\Psi\right]=\left[\underline{\phi}_1,\ldots,\underline{\phi}_m \quad -\underline{\psi}_1,\ldots,-\underline{\psi}_m\right]\in\mathbb{R}^{N_{out}\times 2m} \tag{3.43}$$

and the modal vector

$$\underline{n}\left(t;\underline{\theta}^a\right)=\begin{Bmatrix} n_{\mathrm{Re},1}\left(t;\underline{\theta}^a\right)\\ \vdots \\ n_{\mathrm{Re},m}\left(t;\underline{\theta}^a\right)\\ n_{\mathrm{Im},1}\left(t;\underline{\theta}^a\right)\\ \vdots \\ n_{\mathrm{Im},m}\left(t;\underline{\theta}^a\right)\end{Bmatrix}\in\mathbb{R}^{2m} \tag{3.44}$$

it can be readily shown that the set of linear algebraic equations can be written in the compact matrix form:

$$\begin{bmatrix} 2\cdot\Xi & A\\ 2\cdot A^T & Z\end{bmatrix}\begin{bmatrix} U^{\mathrm{T}}\\ D_c^T\end{bmatrix}=\begin{bmatrix} Y\\ \Lambda\end{bmatrix} \tag{3.45}$$

where

$$\Xi=\Xi\left(\underline{\theta}^a\right)=\sum_{k=0}^{N}\underline{n}\left(k\Delta t;\underline{\theta}^a\right)\underline{n}^{\mathrm{T}}\left(k\Delta t;\underline{\theta}^a\right)\in\mathbb{R}^{2m\times 2m} \tag{3.46}$$

$$A=A\left(\underline{\theta}^a\right)=\sum_{k=0}^{N}\underline{n}\left(k\Delta t;\underline{\theta}^a\right)\underline{u}^{\mathrm{T}}\left(k\Delta t\right)\in\mathbb{R}^{2m\times N_{in}} \tag{3.47}$$

$$Y=Y\left(\underline{\theta}^a\right)=\sum_{k=0}^{N}\underline{n}\left(k\Delta t;\underline{\theta}^a\right)\underline{\hat{e}}^T\left(k\Delta t\right)\in\mathbb{R}^{2m\times N_{out}} \tag{3.48}$$

$$Z=\sum_{k=0}^{N}u\left(k\Delta t\right)\underline{u}^{\mathrm{T}}\left(k\Delta t\right)\in\mathbb{R}^{N_{in}\times N_{in}} \tag{3.49}$$

$$\Lambda=\sum_{k=0}^{N}\underline{u}\left(k\Delta t\right)\underline{\hat{e}}^T\left(k\Delta t\right)\in\mathbb{R}^{N_{in}\times N_{out}} \tag{3.50}$$

Note that the matrices $\Xi$, $A$ and $Y$ depend on $\underline{\theta}^a$, while the matrices $Z$, $\Lambda$ do not depend on $\underline{\theta}^a$. From (3.45) we obtain the matrix $U^{\mathrm{T}}$ that contains the information for the eigenvectors, and the matrix $D_c^T$.



Institutional Repository - Library & Information Centre - University of Thessaly
24/04/2024 00:02:26 EEST - 3.141.244.201

Substituting (3.27) in (3.31), the error function $J^*\left(\underline{\theta}^a\right)$ becomes

$$J^*\left(\underline{\theta}^a\right)=\frac{1}{V}\sum_{k=0}^{N}\left[2\sum_{r\in I_a}\left\{\left[\underline{\phi}_r \quad -\underline{\psi}_r\right]\underline{n}_r\left(k\Delta t;\underline{\theta}^a\right)\right\}+D_c\,\underline{u}(k\Delta t)-\underline{\hat{e}}\left(k\Delta t\right)\right]^{\mathrm{T}}\cdot \left[2\sum_{r\in I_a}\left\{\left[\underline{\phi}_r \quad -\underline{\psi}_r\right]\underline{n}_r\left(k\Delta t;\underline{\theta}^a\right)\right\}+D_c\,\underline{u}(k\Delta t)-\underline{\hat{e}}\left(k\Delta t\right)\right] \tag{3.51}$$

Using the definition of $\begin{bmatrix}U^{\mathrm{T}}\\ D_c^T\end{bmatrix}$ and $\underline{n}$ in (3.45) and (3.44) the latter equation takes the compact form

$$J^*\left(\underline{\theta}^a\right)=\frac{1}{V}\sum_{k=0}^{N}\left[\left[2\underline{n}^T\left(k\Delta t;\underline{\theta}^a\right) \quad \underline{u}^T(k\Delta t)\right]\begin{bmatrix}\Psi^{\mathrm{T}}\\ D^{\mathrm{T}}\end{bmatrix}-\underline{\hat{e}}^{\mathrm{T}}\left(k\Delta t\right)\right]\cdot \left[\begin{bmatrix}\Psi\\ D\end{bmatrix}\left[2\underline{n}\left(k\Delta t;\underline{\theta}^a\right) \quad \underline{u}(k\Delta t)\right]-\underline{\hat{e}}\left(k\Delta t\right)\right] \tag{3.52}$$

The total number of model parameter involved in the prediction of the response at $N_{out}$ DOFs given $m$ modes and $N_{in}$ input time histories, is now reduced from $\left[4m+2\left(m\times N_{in}\right)+2\left(N_{out}\times m\right)+\left(N_{out}\times N_{in}\right)\right]$ to $\left[4m+2\left(m\times N_{in}\right)\right]$.

## 3.5 Analytical Expression of the Gradient of the Objective function

Next, analytically expressions for the gradients and the objective function (3.52) with respect to each parameter in the set $\underline{\theta}^a$ are defined. Differentiating $J^*\left(\underline{\theta}^a\right)$ with respect to a parameter $\theta$ in the parameter set $\underline{\theta}^a$ yields

$$\frac{\partial J^*\left(\underline{\theta}^a\right)}{\partial\theta}=\frac{2}{V}\sum_{k=0}^{N}\left[\left[2\frac{\partial\underline{n}^T\left(k\Delta t;\underline{\theta}^a\right)}{\partial\theta} \quad 0\right]\begin{bmatrix}\Psi^{\mathrm{T}}\\ D_c^T\end{bmatrix}+\left[2\underline{n}\left(k\Delta t;\underline{\theta}^a\right) \quad \underline{u}(k\Delta t)\right]\begin{bmatrix}\frac{\partial\Psi^{\mathrm{T}}}{\partial\theta}\\ \frac{\partial D_c^T}{\partial\theta}\end{bmatrix}\right]\cdot \left[\begin{bmatrix}\Psi\\ D_c\end{bmatrix}\left[2\underline{n}\left(k\Delta t;\underline{\theta}^a\right) \quad \underline{u}(k\Delta t)\right]-\underline{\hat{e}}\left(k\Delta t\right)\right] \tag{3.53}$$

Note that the derivative $\partial U^{\mathrm{T}}/\partial\theta$ and $\partial D_c^T/\partial\theta$ are readily obtained by differentiating with respect to $\theta$ both sides of the system of linear equations (3.45). This yields the following system of linear equation for the derivatives



Institutional Repository - Library & Information Centre - University of Thessaly
24/04/2024 00:02:26 EEST - 3.141.244.201

$$\begin{bmatrix} \Xi & A \\ A^T & Z \end{bmatrix} \begin{bmatrix} \dfrac{\partial U^{\mathrm{T}}}{\partial \theta} \\ \dfrac{\partial D_c^T}{\partial \theta} \end{bmatrix} = \begin{bmatrix} \dfrac{\partial Y}{\partial \theta} \\ \dfrac{\partial \Lambda}{\partial \theta} \end{bmatrix} - \begin{bmatrix} \dfrac{\partial \Xi}{\partial \theta} & \dfrac{\partial A}{\partial \theta} \\ \dfrac{\partial A^T}{\partial \theta} & \dfrac{\partial Z}{\partial \theta} \end{bmatrix} \begin{bmatrix} U^{\mathrm{T}} \\ D_c^T \end{bmatrix} \tag{3.54}$$

Where, using (3.46), (3.47), (3.48), (3.49) and (3.50), it can be readily shown that

$$\frac{\partial \Xi}{\partial \theta} = \sum_{k=0}^{N} \left[ \frac{\partial \underline{n}(k\Delta t)}{\partial \theta} \underline{n}^{\mathrm{T}}(k\Delta t) + \underline{n}(k\Delta t) \frac{\partial \underline{n}^{\mathrm{T}}(k\Delta t)}{\partial \theta} \right] \tag{3.55}$$

$$\frac{\partial \mathrm{A}}{\partial \theta} = \sum_{k=0}^{N} \frac{\partial \underline{n}(k\Delta t)}{\partial \theta} \underline{u}^{T}\left(k\Delta t\right) \tag{3.56}$$

$$\frac{\partial Y}{\partial \theta} = \sum_{k=0}^{N} \frac{\partial \underline{n}(k\Delta t)}{\partial \theta} \underline{\hat{e}}^{T}\left(k\Delta t\right) \tag{3.57}$$

$$\frac{\partial Z}{\partial \theta} = 0 \tag{3.58}$$

$$\frac{\partial \Lambda}{\partial \theta} = 0 \tag{3.59}$$

In order to completely define the gradients of the objective $J^{*}\left(\underline{\theta}^{a}\right)$ one needs to obtain the derivatives $\partial \underline{n}\left(k\Delta t\right)/\partial \theta$. The term $\partial \underline{n}\left(k\Delta t\right)/\partial \theta$ can be evaluated by the modified equation of motion (3.23) for each modal component $\underline{n}_r$. These derivatives depend on the type of the parameter $\theta$ in the set $\underline{\theta}^{a}$. Thus, for each type parameter $\theta$ we define the terms

$$\frac{\partial \underline{n}_r(t)}{\partial a_r} = \underline{n}_{a_r} \tag{3.60}$$

$$\frac{\partial \underline{n}_r(t)}{\partial b_r} = \underline{n}_{b_r} \tag{3.61}$$

$$\frac{\partial \underline{n}_r(t)}{\partial p_{\mathrm{Re},ri}} = \underline{n}_{p_{\mathrm{Re},ri}} \tag{3.62}$$

$$\frac{\partial \underline{n}_r(t)}{\partial p_{\mathrm{Im},ri}} = \underline{n}_{p_{\mathrm{Im},ri}} \tag{3.63}$$

$$\frac{\partial \underline{n}_r(t)}{\partial d_r} = \underline{n}_{d_r} \tag{3.64}$$



Institutional Repository - Library & Information Centre - University of Thessaly
24/04/2024 00:02:26 EEST - 3.141.244.201

$$\frac{\partial \underline{n}_r(t)}{\partial \upsilon_r} = \underline{n}_{\upsilon_r} \tag{3.65}$$

where $d_r = n^0_{\mathrm{Re},r}$ and $\upsilon_r = n^0_{\mathrm{Im},r}$. The above terms are obtained through the derivation of (3.23). These derivatives are with respect to each parameter in $\underline{\theta}^{\alpha}$ thus satisfy the following system of differential equations,

$$\dot{\underline{n}}_{a_r}(t) = \begin{bmatrix} -a_r & -b_r \\ b_r & -a_r \end{bmatrix} \underline{n}_{a_r}(t) + \begin{bmatrix} -1 & 0 \\ 0 & -1 \end{bmatrix} \underline{n}_r(t) \tag{3.66}$$

with initial conditions $\underline{n}_{a_r} = \begin{Bmatrix} 0 \\ 0 \end{Bmatrix}$,

$$\dot{\underline{n}}_{b_r}(t) = \begin{bmatrix} -a_r & -b_r \\ b_r & -a_r \end{bmatrix} \underline{n}_{b_r}(t) + \begin{bmatrix} 0 & -1 \\ 1 & 0 \end{bmatrix} \underline{n}_r(t) \tag{3.67}$$

with initial conditions $\underline{n}_{b_r} = \begin{Bmatrix} 0 \\ 0 \end{Bmatrix}$,

$$\dot{\underline{n}}_{p_{\mathrm{Re},ri}}(t) = \begin{bmatrix} -a_r & -b_r \\ b_r & -a_r \end{bmatrix} \underline{n}_{p_{\mathrm{Re},ri}}(t) + \begin{Bmatrix} 1 \\ 0 \end{Bmatrix} u_i(t) \tag{3.68}$$

with initial conditions $\underline{n}_{p_{\mathrm{Re},ri}} = \begin{Bmatrix} 0 \\ 0 \end{Bmatrix}$,

$$\dot{\underline{n}}_{p_{\mathrm{Im},ri}}(t) = \begin{bmatrix} -a_r & -b_r \\ b_r & -a_r \end{bmatrix} \underline{n}_{p_{\mathrm{Im},ri}}(t) + \begin{Bmatrix} 0 \\ 1 \end{Bmatrix} u_i(t) \tag{3.69}$$

with initial conditions $\underline{n}_{p_{\mathrm{Im},ri}} = \begin{Bmatrix} 0 \\ 0 \end{Bmatrix}$,

$$\dot{\underline{n}}_{d_r}(t) = \begin{bmatrix} -a_r & -b_r \\ b_r & -a_r \end{bmatrix} \underline{n}_{d_r}(t) \tag{3.70}$$

with initial conditions $\underline{n}_{d_r} = \begin{Bmatrix} 1 \\ 0 \end{Bmatrix}$.

$$\dot{\underline{n}}_{\upsilon_r}(t) = \begin{bmatrix} -a_r & -b_r \\ b_r & -a_r \end{bmatrix} \underline{n}_{\upsilon_r}(t) \tag{3.71}$$



Institutional Repository - Library & Information Centre - University of Thessaly
24/04/2024 00:02:26 EEST - 3.141.244.201

with initial conditions $\underline{n}_{0_r} = \begin{Bmatrix} 0 \\ 1 \end{Bmatrix}$.

## 3.6 Special Case: Classically Damped Modal Models

### 3.6.1 Formulation of the Objective Function

Using the analysis in Chapter 2, for the special case of classically damped modal models, the vector $\underline{y}(t;\underline{\theta})$ of the acceleration responses at the $N_{out}$ measured degrees of freedom can be written in the form

$$\underline{y}(t;\underline{\theta}) = \Phi \ddot{\underline{\xi}}(t) + D\underline{u}(t) \tag{3.72}$$

where $D \in \mathbb{R}^{N_{out} \times N_{in}}$ is the pseudostatic matrix,

$$\Phi = \left[ \underline{\phi}_1 \quad \dots \quad \underline{\phi}_m \right] \in \mathbb{R}^{N_{out} \times m} \tag{3.73}$$

is the matrix of the real eigenvectors $\underline{\phi}_r$, $r = 1,\dots,m$ at $N_{out}$ DOFs and

$$\ddot{\underline{\xi}}(t) = \begin{Bmatrix} \ddot{\xi}_1(t) \\ \vdots \\ \ddot{\xi}_m(t) \end{Bmatrix} \in \mathbb{R}^{m \times 1} \tag{3.74}$$

is the real vector of the modal coordinates satisfying the equation of motion for each modal component $\xi_r$

$$\ddot{\xi}_r(t) + a_r \dot{\xi}_r(t) + b_r \xi_r(t) = -[p_{11} \quad \dots \quad p_{ri} \quad \dots \quad p_{mN_{in}}]\,\underline{u}(t) \tag{3.75}$$

where $\underline{p}_r^T \in \mathbb{R}^{1 \times N_{in}}$ is the real vector of the effective participation factors relating the $N_{in}$ inputs to the $r$ mode of the system given by

$$\underline{p}_r^T = \underline{\phi}_r^T L \tag{3.76}$$

where $L$ is a matrix comprised of zeros and ones that maps the $N_{in}$ excited DOFs to the $N_{out}$ output DOFs.

The parameters $a_r = 2\zeta_r\omega_r$ and $b_r = \omega_r^2$ are expressed in terms of the modal frequency $\omega_r$ and the damping ratio $\zeta_r$. Given $\alpha_r$ and $b_r$, the modal frequency $\omega_r$ and the damping ratio $\zeta_r$ are obtained from the following relationships:



Institutional Repository - Library & Information Centre - University of Thessaly
24/04/2024 00:02:26 EEST - 3.141.244.201

$$\omega_r = \sqrt{b_r} \tag{3.77}$$

$$\zeta_r = \frac{a_r}{2\sqrt{b_r}} \tag{3.78}$$

The modal response $\ddot{\xi}_r(t)$ can be obtained by solving (3.75) using the initial conditions $\xi_r^0 = \xi_r(0) = d_r$ and $\dot{\xi}_r^0 = \dot{\xi}_r(0) = \upsilon_r$.

The parameters set $\underline{\theta}$ in the notation $\underline{y}(t;\underline{\theta})$ contains the parameters that completely define the response vector $\underline{y}(t;\underline{\theta})$ using the modal analysis. From equations (3.72) to (3.76), it is evident that the parameter set $\underline{\theta}$ contains the parameters $a_r = 2\zeta_r\omega_r$ and $b_r = \omega_r^2$ which are expressed in terms of the modal frequency $\omega_r$ and the damping ratio $\zeta_r$, the real modeshapes $\underline{\phi}_r \in \mathbb{R}^{N_{out}\times 1}$, the modal participation factor vectors $\underline{p}_r^T \in \mathbb{R}^{1\times N_{in}}$, the initial conditions $\xi_r^0 = \xi_r(0) = d_r$ and $\dot{\xi}_r^0 = \dot{\xi}_r(0) = \upsilon_r$, and the entries of the real pseudostatic matrix $D \in \mathbb{R}^{N_{out}\times N_{in}}$, that is

$$\underline{\theta} = \left\{ a_r, b_r, \underline{\phi}_r, \underline{p}_r^T, d_r, \upsilon_r,\ r = 1,\ldots,m,\ D \right\} \tag{3.79}$$

where $m$ is the number of contributing modes which is also an unknown in the modal identification process. The total number of model parameter involved in the prediction of the response at $N_{out}$ DOFs given $m$ modes and $N_{in}$ base input time histories, is $[4m + (N_{out}\times m) + (m\times N_{in}) + (N_{out}\times N_{in})]$.

In order to implement a modal sweep approach similar to one presented in Section 4.3 for non-classically damped systems, two index sets are introduced, the active index set $I_\alpha$ containing the mode numbers that are active and are optimized during the optimization process and the fixed index set $I_f$ that contains the rest of the $m$ modes that are included in computation of the response vector but their parameter values are kept constant during the optimization process. Consequently, equation (3.72) can be expressed in the form

$$\underline{y}(t;\underline{\theta}) = \sum_{r\in I_\alpha} \left\{ \underline{\phi}_r \ddot{\underline{\xi}}_r(t) \right\} + D\underline{u}(t) + \sum_{f\in I_f} \left\{ \underline{\phi}_f \ddot{\underline{\xi}}_f(t) \right\} \tag{3.80}$$

Introducing the active and the fixed parts of the responses by

$$\underline{x}^r(t;\underline{\theta}) = \sum_{r\in I_\alpha} \left\{ \underline{\phi}_r \ddot{\underline{\xi}}_r(t) \right\} + D\underline{u}(t) \tag{3.81}$$

$$\underline{x}^f(t) = \sum_{f\in I_f} \left\{ \underline{\phi}_f \ddot{\underline{\xi}}_f(t) \right\} \tag{3.82}$$



Institutional Repository - Library & Information Centre - University of Thessaly
24/04/2024 00:02:26 EEST - 3.141.244.201

Respectively, the total response $\underline{y}(t;\underline{\theta}) \equiv \underline{y}(t)$ due to $m$ contributing modes can be written in the form

$$\underline{y}(t) = \underline{x}^r(t;\underline{\theta}) + \underline{x}^f(t) \tag{3.83}$$

which is more appropriate to use when formulating the optimization problem using modal sweeps to identify the modal parameters of the active modes defined in the set $I_\alpha$, holding the parameters of all other fixed modes, defined in the set $I_f$, as constants.

Using active and fixed modes, the objective function (3.1) can be expressed in the form

$$J(\underline{\theta}) = \frac{1}{V}\sum_{k=0}^{N}\left[\underline{x}^r(k\Delta t;\underline{\theta}) + \underline{x}^f(k\Delta t) - \underline{\hat{y}}(k\Delta t)\right]^T\left[\underline{x}^r(k\Delta t;\underline{\theta}) + \underline{x}^f(k\Delta t) - \underline{\hat{y}}(k\Delta t)\right] \tag{3.84}$$

,or equivalently, the final form of the objective function is given by

$$J(\underline{\theta}) = \frac{1}{V}\sum_{k=0}^{N}\left[\underline{x}^r(k\Delta t;\underline{\theta}) - \underline{\hat{e}}(k\Delta t)\right]^T\left[\underline{x}^r(k\Delta t;\underline{\theta}) - \underline{\hat{e}}(k\Delta t)\right] \tag{3.85}$$

where $\underline{x}^r(k\Delta t;\underline{\theta})$, given by (3.81), depends on the parameter set $\underline{\theta}$, while $\underline{\hat{e}}(k\Delta t)$ given by

$$\underline{\hat{e}}(k\Delta t) = \underline{\hat{y}}(k\Delta t) - \sum_{f\in I_f}\left\{\underline{\phi}_f \ddot{\underline{\xi}}_f(t)\right\} \tag{3.86}$$

is the constant vector of the measured response minus the response vector that is predicted from the modal model considering only the fixed modes.

The minimization of the objective function (3.85) can be carried out efficiently, significantly reducing computational cost, by recognizing that the error function in (3.85) is quadratic with respect to the real modeshapes $\underline{\phi}_r$ and the elements in pseudostatic matrix $D$. This observation is used to develop explicit expressions that relate the parameters $\underline{\phi}_r$ and $D$ to the rest of the model parameters appearing in the parameter set $\underline{\theta}$, such as the modal participation factor vectors $\underline{p}_r^T \in \mathbb{R}^{1\times N_{in}}$, as well as the modal parameters $\alpha_r$ and $b_r$ that relate the modal frequencies $\omega_r$ and the modal damping ratios $\zeta_r$, and the initial conditions $\xi_r^0 = \xi_r(0) = d_r$ and $\dot{\xi}_r^0 = \dot{\xi}_r(0) = \upsilon_r$.

For this the parameter set $\underline{\theta}$ in (3.79) is partitioned into parameters sets as follows

$$\underline{\theta} = \left(\underline{\theta}^a, \underline{\theta}^b\right) \tag{3.87}$$

where $\underline{\theta}^b$ is defined by

$$\underline{\theta}^b = \left(\underline{\phi}_r,\ r = 1,\ldots,m,\ D_c\right) \tag{3.88}$$



Institutional Repository - Library & Information Centre - University of Thessaly
24/04/2024 00:02:26 EEST - 3.141.244.201

and $\underline{\theta}^a$ is defined by

$$\underline{\theta}^a = \left( a_r, b_r, \underline{p}_r^T, d_r, \upsilon_r, \ \ r = 1,...,m \right) \tag{3.89}$$

Stationary conditions with respect to the parameters in the set $\underline{\theta}^b$ are used to develop a linear system of equations for solving for the set $\underline{\theta}^b$ given the values of the parameters set $\underline{\theta}^a$.

For convenience in the presentation this linear system can be formulated in the general form

$$\mathrm{A}\left(\underline{\theta}^\alpha\right)\underline{\theta}^b = \underline{b}\left(\underline{\theta}^\alpha\right) \tag{3.90}$$

where $\mathrm{A}\left(\underline{\theta}^\alpha\right)$ and $\underline{b}\left(\underline{\theta}^\alpha\right)$ are functions of the parameter set $\underline{\theta}^a$. Let

$$\underline{\theta}^b = \underline{\theta}^b\left(\underline{\theta}^a\right) \tag{3.91}$$

be the function that gives the relationship between the parameters set $\underline{\theta}^b$ and the parameter set $\underline{\theta}^a$ by solving the system (3.90). Then the objective function $J\left(\underline{\theta}\right)$ takes the form

$$J\left(\underline{\theta}\right) = J\left(\underline{\theta}^a, \underline{\theta}^b\right) = J\left(\underline{\theta}^a, \underline{\theta}^b\left(\underline{\theta}^a\right)\right) \equiv J^*\left(\underline{\theta}^a\right) \tag{3.92}$$

Hence the minimization problem can be stated as follows. Find the values of the parameter set $\underline{\theta}^a$ that minimize the objective function

$$J^*\left(\underline{\theta}\right) = J\left(\underline{\theta}^a, \underline{\theta}^b\left(\underline{\theta}^a\right)\right) \tag{3.93}$$

Once the values of $\underline{\theta}^a$ have been found, the values of $\underline{\theta}^b$ are obtained solving the linear system (3.90). Next our objective is to apply the above concept and first obtain the matrices and vectors that completely define the linear system (3.90).

The linear system for the parameter set $\underline{\theta}^b$ is obtained by setting the derivatives of $J\left(\underline{\theta}\right)$ with respect to each element of $\underline{\theta}^b$ equal to zero, that is,

$$\frac{\partial J\left(\underline{\theta}\right)}{\partial \phi_{lr}} = 0 \tag{3.94}$$

$$\frac{\partial J\left(\underline{\theta}\right)}{\partial D_{,li}} = 0 \tag{3.95}$$

for $l = 1,\ldots,N_{out}$, $r = 1,\ldots,m$ and $i = 1,\ldots,N_{in}$. It can be readily shown that the set of linear algebraic equations can be written in the compact matrix form:



Institutional Repository - Library & Information Centre - University of Thessaly
24/04/2024 00:02:26 EEST - 3.141.244.201

$$\begin{bmatrix} \Xi & A \\ A^T & Z \end{bmatrix} \begin{bmatrix} \Phi^{\mathrm{T}} \\ D^T \end{bmatrix} = \begin{bmatrix} Y \\ \Lambda \end{bmatrix} \tag{3.96}$$

where

$$\Xi = \Xi\left(\underline{\theta}^a\right) = \sum_{k=0}^{N} \left[ \underline{\ddot{\xi}}(k\Delta t;\underline{\theta}^a) \underline{\ddot{\xi}}^{\mathrm{T}}(k\Delta t;\underline{\theta}^a) \right] \in \mathbb{R}^{m\times m} \tag{3.97}$$

$$A = A\left(\underline{\theta}^a\right) = \sum_{k=0}^{N} \underline{\ddot{\xi}}(k\Delta t;\underline{\theta}^a) \underline{u}^T\left(k\Delta t\right) \in \mathbb{R}^{m\times N_{in}} \tag{3.98}$$

$$Y = Y\left(\underline{\theta}^a\right) = \sum_{k=0}^{N} \underline{\ddot{\xi}}(k\Delta t) \underline{\hat{e}}^T\left(k\Delta t\right) \in \mathbb{R}^{m\times N_{out}} \tag{3.99}$$

$$Z = \sum_{k=0}^{N} u\left(k\Delta t\right) \underline{u}^{\mathrm{T}}\left(k\Delta t\right) \in \mathbb{R}^{N_{in}\times N_{in}} \tag{3.100}$$

$$\Lambda = \sum_{k=0}^{N} \underline{u}\left(k\Delta t\right) \underline{\hat{e}}^T\left(k\Delta t\right) \in \mathbb{R}^{N_{in}\times N_{out}} \tag{3.101}$$

Note that the matrices $\Xi$, $A$ and $Y$ depend on $\underline{\theta}^a$, while the matrices $Z$, $\Lambda$ do not depend on $\underline{\theta}^a$. From (3.96) we obtain the matrix $\Phi^{\mathrm{T}}$ that contains the information for the eigenvectors, and the matrix $D^T$.

Substituting (3.81) in (3.85), the error function $J^*\left(\underline{\theta}^a\right)$ becomes

$$J^*\left(\underline{\theta}^a\right) = \frac{1}{V} \sum_{k=0}^{N} \left[ \sum_{r\in I_a} \left\{ \underline{\phi}_r \underline{\ddot{\xi}}_r(t) \right\} + D\underline{u}\left(t\right) + D\underline{u}(k\Delta t) - \underline{\hat{e}}\left(k\Delta t\right) \right]^{\mathrm{T}} \cdot \left[ \sum_{r\in I_a} \left\{ \underline{\phi}_r \underline{\ddot{\xi}}_r(t) \right\} + D\underline{u}\left(t\right) + D\underline{u}(k\Delta t) - \underline{\hat{e}}\left(k\Delta t\right) \right] \tag{3.102}$$

Using the definition of $\begin{bmatrix} \Phi^{\mathrm{T}} \\ D^T \end{bmatrix}$ in (3.96) the latter equation takes the compact form

$$J^*\left(\underline{\theta}^a\right) = \frac{1}{V} \sum_{k=0}^{N} \left[ \left[ \underline{\ddot{\xi}}^{\mathrm{T}}(k\Delta t;\underline{\theta}^a) \quad \underline{u}^T(k\Delta t) \right] \begin{bmatrix} \Psi^{\mathrm{T}} \\ D^{\mathrm{T}} \end{bmatrix} - \underline{\hat{e}}^{\mathrm{T}}\left(k\Delta t\right) \right] \cdot \left[ \begin{bmatrix} \Psi \\ D \end{bmatrix} \left[ \underline{\ddot{\xi}}(k\Delta t;\underline{\theta}^a) \quad \underline{u}(k\Delta t) \right] - \underline{\hat{e}}\left(k\Delta t\right) \right] \tag{3.103}$$



Institutional Repository - Library & Information Centre - University of Thessaly
24/04/2024 00:02:26 EEST - 3.141.244.201

The total number of model parameter involved in the prediction of the response at $N_{out}$ DOFs given $m$ modes and $N_{in}$ input time histories, is now reduced from $\left[4m+\left(m\times N_{in}\right)+\left(N_{out}\times m\right)+\left(N_{out}\times N_{in}\right)\right]$ to $\left[4m+\left(m\times N_{in}\right)\right]$.

### 3.6.2 Analytical Expression of the Gradient of the Objective function

Next, analytically expressions for the gradients and the objective function (3.103) with respect to each parameter in the set $\underline{\theta}^a$ are defined. Differentiating $J^*\left(\underline{\theta}^a\right)$ with respect to a parameter $\theta$ in the parameter set $\underline{\theta}^a$ yields

$$\frac{\partial J^*\left(\underline{\theta}^a\right)}{\partial\theta}=\frac{2}{V}\sum_{k=0}^{N}\left[\left[\frac{\partial\ddot{\underline{\xi}}^{\mathrm{T}}(k\Delta t;\underline{\theta}^a)}{\partial\theta}\quad 0\right]\begin{bmatrix}\Phi^{\mathrm{T}}\\ D^{\mathrm{T}}\end{bmatrix}+\left[\ddot{\underline{\xi}}(k\Delta t;\underline{\theta}^a)\quad \underline{u}(k\Delta t)\right]\begin{bmatrix}\frac{\partial\Phi^{\mathrm{T}}}{\partial\theta}\\ \frac{\partial D^{\mathrm{T}}}{\partial\theta}\end{bmatrix}\right]\cdot \left[\begin{bmatrix}\Psi\\ D\end{bmatrix}\left[\ddot{\underline{\xi}}(k\Delta t;\underline{\theta}^a)\quad \underline{u}(k\Delta t)\right]-\underline{\hat{e}}\left(k\Delta t\right)\right] \tag{3.104}$$

Note that the derivative $\partial\Phi^{\mathrm{T}}/\partial\theta$ and $\partial D^{\mathrm{T}}/\partial\theta$ are readily obtained by differentiating with respect to $\theta$ both sides of the system of linear equations (3.96). This yields the following system of linear equation for the derivatives

$$\begin{bmatrix}\Xi & A\\ A^T & Z\end{bmatrix}\begin{bmatrix}\frac{\partial\Phi^{\mathrm{T}}}{\partial\theta}\\ \frac{\partial D^T}{\partial\theta}\end{bmatrix}=\begin{bmatrix}\frac{\partial Y}{\partial\theta}\\ \frac{\partial\Lambda}{\partial\theta}\end{bmatrix}-\begin{bmatrix}\frac{\partial\Xi}{\partial\theta} & \frac{\partial A}{\partial\theta}\\ \frac{\partial A^T}{\partial\theta} & \frac{\partial Z}{\partial\theta}\end{bmatrix}\begin{bmatrix}\Phi^{\mathrm{T}}\\ D^T\end{bmatrix} \tag{3.105}$$

Where, using (3.97), (3.98), (3.99), (3.100) and (3.101), it can be readily shown that

$$\frac{\partial\Xi}{\partial\theta}=\sum_{k=0}^{N}\left[\frac{\partial\ddot{\underline{\xi}}(k\Delta t)}{\partial\theta}\ddot{\underline{\xi}}^{\mathrm{T}}(k\Delta t)+\ddot{\underline{\xi}}(k\Delta t)\frac{\partial\ddot{\underline{\xi}}^{\mathrm{T}}(k\Delta t)}{\partial\theta}\right] \tag{3.106}$$

$$\frac{\partial\mathrm{A}}{\partial\theta}=\sum_{k=0}^{N}\frac{\partial\ddot{\underline{\xi}}(k\Delta t)}{\partial\theta}\underline{u}^T\left(k\Delta t\right) \tag{3.107}$$

$$\frac{\partial Y}{\partial\theta}=\sum_{k=0}^{N}\frac{\partial\ddot{\underline{\xi}}(k\Delta t)}{\partial\theta}\underline{\hat{e}}^T\left(k\Delta t\right) \tag{3.108}$$

$$\frac{\partial Z}{\partial\theta}=0 \tag{3.109}$$



Institutional Repository - Library & Information Centre - University of Thessaly
24/04/2024 00:02:26 EEST - 3.141.244.201

$$\frac{\partial \Lambda}{\partial \theta} = 0 \tag{3.110}$$

In order to completely define the gradients of the objective $J^*\left(\underline{\theta}^a\right)$ one needs to obtain the derivatives $\partial \underline{\ddot{\xi}}(k\Delta t)/\partial\theta$. The term $\partial \underline{\ddot{\xi}}(k\Delta t)/\partial\theta$ can be evaluated by the equation of motion for classically damped modal models (3.75) for each modal component $\xi_r$. These derivatives depend on the type of the parameter $\theta$ in the set $\underline{\theta}^a$. Thus, for each type parameter $\theta$ we define the terms

$$\frac{\partial \xi_r(t)}{\partial a_r} = n_{a_r} \tag{3.111}$$

$$\frac{\partial \xi_r(t)}{\partial b_r} = n_{b_r} \tag{3.112}$$

$$\frac{\partial \xi_r(t)}{\partial p_{ri}} = n_{p_{ri}} \tag{3.113}$$

$$\frac{\partial \xi_r(t)}{\partial d_r} = n_{d_r} \tag{3.114}$$

$$\frac{\partial \xi_r(t)}{\partial \upsilon_r} = n_{\upsilon_r} \tag{3.115}$$

The above terms are obtained through the derivation of (3.75) with respect to each parameter $\underline{\theta}$. These derivatives are with respect to each parameter in $\underline{\theta}^\alpha$ thus satisfy the following system of differential equations,

$$\Rightarrow \ddot{n}_{a_r} + a_r \dot{n}_{a_r} + b_r n_{a_r} = -\dot{\xi}_r \tag{3.116}$$

with initial conditions $n_{a_r} = 0$ and $\dot{n}_{a_r} = 0$,

$$\Rightarrow \ddot{n}_{b_r} + a_r \dot{n}_{b_r} + b_r n_{b_r} = -\xi_r \tag{3.117}$$

with initial conditions $n_{b_r} = 0$ and $\dot{n}_{b_r} = 0$,

$$\Rightarrow \ddot{n}_{p_{ri}} + a_r \dot{n}_{p_{ri}} + b_r n_{p_{ri}} = -u_i(t) \tag{3.118}$$

with initial conditions $n_{p_{ri}} = 0$ and $\dot{n}_{p_{ri}} = 0$,

$$\Rightarrow \ddot{n}_{d_r} + a_r \dot{n}_{d_r} + b_r n_{d_r} = 0 \tag{3.119}$$



Institutional Repository - Library & Information Centre - University of Thessaly
24/04/2024 00:02:26 EEST - 3.141.244.201

with initial conditions $n_{d_r} = 1$ and $\dot{n}_{d_r} = 0$,

$$\Rightarrow \ddot{n}_{v_r} + a_r \dot{n}_{v_r} + b_r n_{v_r} = 0 \tag{3.120}$$

with initial conditions $n_{v_r} = 0$ and $\dot{n}_{v_r} = 1$.

## 3.7 Modal Sweep Approach

In modal identification procedure appears the need of determining the optimal parameter set $\underline{\theta}$ that fully characterizes the model under consideration, by minimizing the relevant error objective function $J(\underline{\theta})$ given by (3.1) with respect to the model parameters. The implemented optimization routine follows the lines of a modal-minimization method developed by Werner et al. (1987). This algorithm consists of a series of modal sweeps in which, during each sweep, the estimates of the parameters of each mode $r$ are successively updated by a series of single-mode minimization of $J(\underline{\theta})$, while holding the values of the parameters for the rest of the modes equal to their latest calculated values. This minimization of each mode actually corresponds to least-squares matching of the measured response to the predicted response from a modal model for which the parameters of a single mode are successively updated while the other modes are computed using the latest optimal values of the parameter estimates already obtained from previous minimizations. For the first sweep, the contribution from the modes that have not yet been treated in the sweep is neglected, since good estimates of the corresponding modal parameters are not available. A single sweep is completed when all the significant modes have been treated in this manner. Successive modal sweeps are performed until the fractional decrease in $J(\underline{\theta})$ is less than a prescribed value, given by the user, or until a prescribed maximum number of modal sweeps has been completed.

Specifically, gradient-based method is used to optimize the error function $J(\underline{\theta})$ for each mode $r$. In the first sweep, for the $r = 1,\ldots,m$ mode, the gradient-based optimization algorithm concludes in a set of optimal values, using the optimal estimates computed for the last $1,\ldots,r-1$ modes and neglecting the rest $r+1,\ldots,m$ modes. After the first sweep, a second sweep follows where the optimal values of all $m$ desired modes are used as initial estimates in order to obtain better estimates of the these modes. In this sweep, for the $s = 1,\ldots,m$ mode, the gradient-based optimization algorithm concludes in a set of optimal values, using the optimal estimates computed for the $1,\ldots,s-1,s+1,\ldots,m$ modes in the first sweep.



Institutional Repository - Library & Information Centre - University of Thessaly
24/04/2024 00:02:26 EEST - 3.141.244.201

# Chapter 4

# Frequency Domain Methods for Identification of Non-classically Damped Modal Models

## 4.1 Introduction

In this chapter, a frequency domain methodology is presented for identifying the modal parameters of non-classically damped modal models used to describe the response of linear structures subjected to multiple base excitations. The modal parameters to be identified include the modal frequencies, the modal damping ratios, the modeshapes and the participation factors. The proposed structural modal identification methodology is applicable to civil engineering structures such as buildings, towers, bridges, offshore structures, etc., subjected to earthquake excitations. The identification methodology uses the Fourier transforms of the measured input accelerations at the base degrees of freedom and the Fourier transforms of the output accelerations at the model degrees of freedom of the structure. An output error formulation is presented, in which the selected modal parameters are identified through least-squares matching between the Fourier transform of the output measured acceleration and the Fourier transform of the acceleration predicted by a modal model of the structure, over a specified frequency band, subjected to the measured base input accelerations.

In particular, the proposed frequency domain methodology uses a three step approach to solve the error optimization problem. The first step provides estimates of the modal frequencies and modal damping ratios by solving a system of linear algebraic equations using the common denominator model. Stabilization diagrams are used to distinguish between physical and mathematical modes. This method (first step) is an extension of the PolyMAX or polyreference least-squares complex frequency domain method, developed by Peeters et al. (2004), in order to treat non-classically damped modal models describing a system's response characteristics based on earthquake-induced vibration data. The second step provides estimates of the modeshapes and the participation factors by solving a system of linear algebraic equations. It should be noted that two different approaches have been developed for the computation of the modeshapes and participation factors in this second step. In the first approach the modal properties derive directly by the Singular Value Decomposition (SVD) of the resulting numerator matrix. In the second approach the advantage that the error function is quadratic with respect to the modeshapes is used, so the modeshapes are computed by taking stationary conditions in order to develop a linear system of equations from which the modeshapes are derived. The first two steps usually give accurate estimates of the modal characteristics. However, a third step is often recommended to improve these estimates, especially for closely spaced and overlapping modes, by efficiently solving the full nonlinear optimization problem with initial estimates of the modal parameters those obtained from the first and second steps.



Institutional Repository - Library & Information Centre - University of Thessaly
24/04/2024 00:02:26 EEST - 3.141.244.201

This chapter is divided into the following sections. Section 4.2 presents the formulation of the modal observation equations for the general case of a non-classically damped model in the frequency domain. In Section 4.3 the formulation of a system of linear algebraic equations using the common denominator model is presented, which is used to set up Stabilization Diagrams in order to distinguish the physical from the mathematical modes. In Section 4.4 an output error formulation is presented as a weighted least squares optimization problem in the frequency domain and in Sections 4.5, 4.6 and 4.7 the formulation of the frequency domain methodology which uses a three step approach is presented. In particular, in Section 4.5 the first approach of the second step of the proposed frequency domain methodology is presented, in Section 4.6 the second approach of the second step is presented and finally in Section 4.7 the third step is presented. For Sections 4.5, 4.6 and 4.7 the formulation of the minimization of the error function and the parameter set $\underline{\theta}$ which is optimized for each step are presented and also simplifications are given explaining the quadratic dependence of the objective function on the modal characteristics. In addition, analytical expressions of the gradient of the objective function for each step are presented. Finally, in the appendices (Section 4.8), details are given for the computation of some derivatives of the objective function.

## 4.2 Modal model – Frequency domain

Generally, a function $f(t)$ can be analyzed using Fourier components

$$f(t) = \frac{1}{2\pi} \int_{-\infty}^{\infty} \hat{f}(\omega) e^{j\omega t} d\omega \tag{4.1}$$

where $\hat{f}(\omega)$ is the Fourier coefficient given by

$$\hat{f}(\omega) = \int_{-\infty}^{\infty} f(t) e^{-j\omega t} dt \tag{4.2}$$

Applying the Fourier transform to equation (2.1) in the frequency domain yields

$$\underline{\hat{x}}(\omega) = H(j\omega) L \underline{\hat{u}}(\omega) \tag{4.3}$$

where $\underline{\hat{u}}(\omega)$ is the Fourier transform of the applied force and

$$H(j\omega) = \left[ M(j\omega)^2 + C(j\omega) + K \right]^{-1} \tag{4.4}$$

The matrix $H(j\omega)$ is called transfer function matrix. The modal observation equations (2.55)can be written in the form



Institutional Repository - Library & Information Centre - University of Thessaly
24/04/2024 00:02:26 EEST - 3.141.244.201

$$\underline{y}(t) = \sum_{r=1}^{n} (\underline{u}_r \underline{\xi}_r(t) + \underline{u}_r^* \underline{\xi}_r^*(t)) + D_c \underline{u}(t) \tag{4.5}$$

where

$$\dot{\underline{\xi}}_r(t) = \lambda_r \underline{\xi}_r(t) + \underline{l}_r^T \underline{u}(t) \tag{4.6}$$

$$\dot{\underline{\xi}}_r^*(t) = \lambda_r^* \underline{\xi}_r^*(t) + \underline{l}_r^{*T} \underline{u}(t) \tag{4.7}$$

$$\lambda_r = -\zeta_r \omega_r \pm j\omega_r \sqrt{1-\zeta^2} \tag{4.8}$$

Using the Fourier Transform for the modal coordinates $\xi_r(t)$ and assuming the boundary conditions to be zero, yields

$$\dot{\underline{\xi}}_r(\omega) = \int_{-\infty}^{\infty} \dot{\underline{\xi}}_r(t) e^{-j\omega t} dt = \int_0^T \frac{\partial \underline{\xi}_r(t)}{\partial t} e^{-j\omega t} dt = e^{-j\omega t}\, \underline{\xi}_r(t)\Big|_0^T + (j\omega) \underbrace{\int_0^T \underline{\xi}_r(t) e^{-j\omega t} dt}_{\underline{\xi}_r(\omega)} = (j\omega) \underline{\xi}_r(\omega) \tag{4.9}$$

Substituting (4.9) in (4.6)

$$(j\omega) \underline{\xi}_r(\omega) = \lambda_r \underline{\xi}_r(\omega) + \underline{l}_r^T \hat{\underline{u}}(\omega) \Rightarrow \underline{\xi}_r(\omega) = \frac{\underline{l}_r^T \hat{\underline{u}}(\omega)}{j\omega - \lambda_r} \tag{4.10}$$

Thus, substituting (4.10) in (4.5) the relation between the response $\underline{y}(\omega)$ and the excitation $\hat{\underline{u}}(\omega)$ in the frequency domain is given by

$$\underline{y}(\omega) = H(j\omega) \hat{\underline{u}}(\omega) \tag{4.11}$$

where

$$H(j\omega) = \sum_{r=1}^{n} \left[ \frac{\underline{u}_r \underline{l}_r^T}{(j\omega) - \lambda_r} + \frac{\underline{u}_r^* \underline{l}_r^{*T}}{(j\omega) - \lambda_r^*} \right] + D_c \tag{4.12}$$

## 4.3 Stabilization Diagrams (First Step)

### 4.3.1 Common Denominator Model

The common denominator model consider all input-output measurements simultaneously by the following model

$$\left[ H(\omega) \right] = \left[ B(\omega) \right] \left[ A(\omega) \right]^{-1} \tag{4.13}$$



Institutional Repository - Library & Information Centre - University of Thessaly
24/04/2024 00:02:26 EEST - 3.141.244.201

with $A(\omega)$ a polynomial and $B(\omega)$ a matrix polynomial with square $N_{out} \times N_{in}$ matrix coefficients. Every line of RMFD can be expressed in the form:

$$\left\langle H_o(\omega) \right\rangle = \left\langle \underline{B}_o^T(\omega) \right\rangle \left[ A(\omega) \right]^{-1} , \forall O = 1, 2, \cdots, N_{out} \tag{4.14}$$

where

$$\left\langle \underline{B}_o^T(\omega) \right\rangle = \sum_{r=0}^{p} \Omega_r(\omega) \left\langle \underline{\beta}_{or}^T \right\rangle \tag{4.15}$$

$$\left[ A(\omega) \right] = \sum_{r=0}^{p} \Omega_r(\omega) \left[ \alpha_r \right] \tag{4.16}$$

where $\Omega_r(\omega)$ are the polynomial basis functions and $p$ is the order of the polynomial. Using method LSCF (least squares-complex frequency domain) the polynomial basis functions are:

$$\Omega_r(\omega) = e^{j\omega\Delta t_r} \tag{4.17}$$

where $\Delta t_r$ is the time band. Polynomial coefficients $\underline{\beta}_{or} \in \mathbb{R}^{N_{in} \times 1}$ and $a_r \in \mathbb{R}^{1 \times 1}$ are assembled in following matrices:

$$\underline{\beta}_o = \begin{pmatrix} \underline{\beta}_{o0} \\ \underline{\beta}_{o1} \\ \cdots \\ \underline{\beta}_{op} \end{pmatrix} \in \mathbb{R}^{\left(N_{in}(p+1)\right) \times 1} \quad , \forall O = 1, 2, \cdots, N_{out} \tag{4.18}$$

$$\underline{\alpha} = \begin{pmatrix} \alpha_0 \\ \alpha_1 \\ \cdots \\ \alpha_p \end{pmatrix} \in \mathbb{R}^{(p+1) \times 1} \tag{4.19}$$

$$\underline{\theta} = \begin{bmatrix} \underline{\beta}_1 \\ \vdots \\ \underline{\beta}_{N_{out}} \\ \underline{a} \end{bmatrix} \in \mathbb{R}^{\left((N_{out}N_{in}+1)(p+1)\right) \times 1} \tag{4.20}$$



Institutional Repository - Library & Information Centre - University of Thessaly
24/04/2024 00:02:26 EEST - 3.141.244.201

### 4.3.2 Error Function

Coefficients $\underline{\theta}$ can be evaluated by minimizing the following non linear least squares error function $\varepsilon_o^{NLS}(\omega_k,\theta)\in C^{o\times 1}$:

$$\varepsilon_o^{NLS}(\omega_k,\underline{\theta}) = \underline{y}_o(\omega_k,\underline{\theta}) - \hat{y}_o(\omega_k) \tag{4.21}$$

where

$\omega_k,\ k=1,2,\ldots,N$: The discrete frequencies at which the FRF (Frequency Response Functions) are evaluated

$\hat{y}_o(\omega_k,\underline{\theta})$: Fourier Transform of the acceleration at the measured DOF predicted by the modal model

$\hat{y}_o(\omega_k)$: Fourier Transform of the acceleration at the measured DOF predicted by the modal model

Using the relation between the response $\underline{y}(\omega)$ and the excitation $\hat{\underline{u}}(\omega)$ in the frequency domain (equation (4.11)) and substituting (4.13) in (4.21) yields

$$\varepsilon_o^{NLS}(\omega_k,\theta) = \underline{B}_o^T(\omega_k,\beta_o)\hat{\underline{u}}(\omega_k)A^{-1}(\omega_k,a) - \underline{\hat{y}}_o(\omega_k) \tag{4.22}$$

Thus, the cost function is

$$l^{NLS}(\theta) = \sum_{o=1}^{l}\sum_{k=1}^{N} tr\left\{\left(\varepsilon_o^{NLS}(\omega_k,\underline{\theta})\right)^{*T}\varepsilon_o^{NLS}(\omega_k,\underline{\theta})\right\} \tag{4.23}$$

where $^{*T}$ is the complex conjugate conversion (Hermittian) of a matrix and $tr\{\bullet\}$ is the trace of a matrix. The cost function can be minimized by setting the derivatives of (4.23) under $\theta$ equal to zeros. It is obvious that it leads to a non linear system of equations when equation (4.22) is used in this form. Premultiplying (4.22) with $A(\omega_k,a)$ yields

$$\varepsilon_o^{LS}(\omega_k,\theta) = \underline{B}_o^T(\omega_k,\beta_o)\hat{\underline{u}}(\omega_k) - \underline{\hat{y}}_o(\omega_k)A(\omega_k,a) = \sum_{r=0}^{p}\left(\Omega_r(\omega_k)\underline{\beta}_{or}^T\hat{\underline{u}}(\omega_k) - \Omega_r(\omega_k)\underline{\hat{y}}_o(\omega_k)\alpha_r\right) \tag{4.24}$$

Error functions for each $\omega_k$ can be written as a vector $\underline{E}_o^{LS}(\theta)\in C^{N\times 1}$, of the form

$$\underline{E}_o^{LS}(\underline{\theta}) = \begin{pmatrix}\varepsilon_o^{LS}(\omega_1,\underline{\theta})\\ \varepsilon_o^{LS}(\omega_2,\underline{\theta})\\ \cdots\\ \varepsilon_o^{LS}(\omega_N,\underline{\theta})\end{pmatrix} = \begin{bmatrix}X & Y_o\end{bmatrix}\begin{Bmatrix}\underline{\beta}_o\\ \underline{a}\end{Bmatrix} \tag{4.25}$$

where



Institutional Repository - Library & Information Centre - University of Thessaly
24/04/2024 00:02:26 EEST - 3.141.244.201

$$X = \begin{bmatrix} \underline{\hat{u}}^T(\omega_1) \otimes \left[\Omega_1(\omega_1) \cdots \Omega_p(\omega_1)\right] \\ \cdots \\ \underline{\hat{u}}^T(\omega_N) \otimes \left[\Omega_1(\omega_N) \cdots \Omega_p(\omega_N)\right] \end{bmatrix} \in C^{N \times (N_{in}(p+1))} \tag{4.26}$$

$$Y_o = \begin{bmatrix} -\left[\Omega_1(\omega_1) \cdots \Omega_p(\omega_1)\right] \otimes \hat{y}_o(\omega_1) \\ \cdots \\ -\left[\Omega_1(\omega_N) \cdots \Omega_p(\omega_N)\right] \otimes \hat{y}_o(\omega_N) \end{bmatrix} \in C^{N \times (p+1)} \tag{4.27}$$

### 4.3.3 Reduced Normal Equations

Similar to (4.23) the following cost function can be written according to the error function (4.24):

$$l^{LS}(\underline{\theta}) = \sum_{o=1}^{i} \sum_{k=1}^{N_f} tr\left\{ \left(\varepsilon_o^{LS}(\omega_k, \underline{\theta})\right)^H \left(\varepsilon_o^{LS}(\omega_k, \underline{\theta})\right) \right\} \tag{4.28}$$

The minimization of the cost function leads to a Weighted Least-Squares Problem. Substituting equations (4.25), (4.26) and (4.27) in (4.28) yields

$$l^{LS}(\underline{\theta}) = \sum_{o=1}^{N_{out}} tr\left\{ \left(E_o^{LS}(\underline{\theta})\right)^{*T} \left(E_o^{LS}(\underline{\theta})\right) \right\} = \sum_{o=1}^{N_{out}} tr\left\{ \begin{pmatrix} \underline{\beta}_o^T & \underline{\alpha}^T \end{pmatrix} \begin{pmatrix} X^{*T} \\ Y_o^{*T} \end{pmatrix} \begin{pmatrix} X & Y_o \end{pmatrix} \begin{pmatrix} \underline{\beta}_o \\ \underline{\alpha} \end{pmatrix} \right\} = \sum_{o=1}^{N_{out}} tr\left\{ \underline{\theta}^T J_o^{*T} J_o \underline{\theta} \right\} \tag{4.29}$$

where $J \in C^{N \times (N_{in}+1)(p+1)}$ is the Jacobian matrix

$$J_o = \begin{pmatrix} X & Y_o \end{pmatrix} \tag{4.30}$$

In case of real-valued coefficients $\theta$, it can be shown that the expression $J_o^{*T} J_o$ can be substituted by its real part. Hence, the cost function (4.29) becomes

$$l^{LS}(\underline{\theta}) = \sum_{o=1}^{N_{out}} tr\left\{ \underline{\theta}^T \, \mathrm{Re}\left(J_o^{*T} J_o\right) \underline{\theta} \right\} \tag{4.31}$$

where

$$\mathrm{Re}(J_o^{*T} J_o) = \begin{pmatrix} R & S_o \\ S_o^T & T_o \end{pmatrix} \in \mathbb{R}^{(N_{in}+1)(p+1) \times (N_{in}+1)(p+1)} \tag{4.32}$$

with

$$R = \mathrm{Re}(X^{*T} X) \in \mathbb{R}^{N_{in}(p+1) \times N_{in}(p+1)} \tag{4.33}$$



Institutional Repository - Library & Information Centre - University of Thessaly
24/04/2024 00:02:26 EEST - 3.141.244.201

$$S_o = \mathrm{Re}(X^{*T} Y_o) \in \mathbb{R}^{N_{in}(p+1)\times(p+1)} \tag{4.34}$$

$$T_o = \mathrm{Re}(Y_o^{*T} Y_o) \in \mathbb{R}^{(p+1)\times(p+1)} \tag{4.35}$$

The cost function is minimized by setting the derivatives of (4.31) with respect to the unknown polynomial coefficients $\theta$ equal to zero:

$$\frac{\partial l^{LS}(\underline{\theta})}{\partial \underline{\beta}_o} = 2(R\underline{\beta}_o + S_o\underline{\alpha}) = 0 \qquad \forall o = 1,\cdots,N_{out} \tag{4.36}$$

$$\frac{\partial l^{LS}(\underline{\theta})}{\partial \underline{\alpha}} = 2\sum_{o=1}^{l}(S_o^T\underline{\beta}_o + T_o\underline{\alpha}) = 0 \qquad \forall o = 1,\cdots,N_{out} \tag{4.37}$$

These equations are the so - called normal equations which can be written (using equations (4.32) - (4.35)) in the form:

$$2\,\mathrm{Re}(J_o^{*T} J_o)\underline{\theta} = 0 \tag{4.38}$$

We focus on the polynomial denominator $\underline{\alpha}$ from which result the poles and the modal coefficients in order to set up a stabilization diagram. Consequently, least-squares problem can be simplified by substituting the coefficients $\underline{\beta}_o$, which result from (4.36)

$$\beta_o = -R^{-1}S_o\alpha \tag{4.39}$$

in to (4.37). Thus, equation (4.37) becomes:

$$\left\{2\sum_{o=1}^{l}\left(\mathrm{T_o} - \mathrm{S_o^T R^{-1} S_o}\right)\right\}\underline{\alpha} = 0$$
$$\mathrm{M}\underline{\alpha} = 0 \tag{4.40}$$

where $M \in \mathbb{R}^{(p+1)\times(p+1)}$ is defined in above equation and can be computed from the measured FRF data. This equation can be solved for the denominator polynomial $\alpha$ in a least-squares sense. To avoid finding the trivial solution $\alpha = 0$, a constraint is imposed on the parameters. Such a constraint also removes the parameter redundancy that exists in the common denominator model (multiplying numerator and denominator with the same matrix yields different numerator and denominator polynomials, but the same transfer function matrix).

This first step can also be used for the time domain analysis where the modal frequency $\omega_r$ and the fraction of critical viscous damping $\zeta_r$ will be the initial values for parameters $\alpha_r = \zeta_r\omega_r$ and $b_r = \omega_r\sqrt{1-\zeta_r^2}$ in the optimization problem.



Institutional Repository - Library & Information Centre - University of Thessaly
24/04/2024 00:02:26 EEST - 3.141.244.201

## 4.4 Formulation as a Weighted Least-Squares Optimization Problem

In the frequency domain, the optimal values of $\underline{\theta}$ result from the minimization of the measure of fit between the Fourier Transform of the measured acceleration $\underline{\hat{y}}(k\Delta\omega)$ and the Fourier Transform of the acceleration $\underline{y}(k\Delta\omega,\underline{\theta})$ predicted from the model. The variable $\Delta\omega$ denotes the frequency discretization step and $k=\{1,2,\ldots,N\}$ is an index set. The parameters in $\underline{\theta}$ include the modal characteristics such as modal frequencies, modal damping ratios, and modeshape components at the measured locations, modal participation factors, and other parameters that completely define the response vector $\underline{y}(k\Delta\omega,\underline{\theta})$.

A modal model output-error identification approach seeks the optimal values of the parameter set $\underline{\theta}$ that minimize a measure of fit between the Fourier Transform of the acceleration predicted by the modal model of the structure and the Fourier Transform of the corresponding response acceleration $\underline{\hat{y}}(k\Delta\omega)$ estimated from the measured data . Thus, the error measure $J(\underline{\theta})$ between measurement data and model predictions that correspond to a certain value of $\underline{\theta}$, is described similar to (3.1) by

$$J(\underline{\theta})=\frac{1}{V}\sum_{k=0}^{N}\left[\underline{y}(k\Delta\omega,\underline{\theta})-\underline{\hat{y}}(k\Delta\omega)\right]^{*T}\left[\underline{y}(k\Delta\omega,\underline{\theta})-\underline{\hat{y}}(k\Delta\omega)\right] \tag{4.41}$$

$\underline{\hat{y}}$: Fourier transform of the measured response acceleration at the $N_{in}$ measured DOF

$\underline{y}$: Fourier transform of the response acceleration at the measured $N_{out}$ DOF predicted by the modal model

$\Delta\omega$: sampling frequency interval of the Fourier transform of the acceleration

$N$: total number of sample data over the duration $T$ of the Fourier transform of the response acceleration

$k$: the time index set at time $\omega=k\Delta\omega$

$$V=\sum_{k=0}^{N}\left[\underline{\hat{y}}(k\Delta\omega)\right]^{*T}\left[\underline{\hat{y}}(k\Delta\omega)\right]: \text{normalization factor for frequency domain} \tag{4.42}$$

Using the Fourier transform for the modal observation equations (2.55), expressed in the form of (4.5), the vector $\underline{y}(\omega;\underline{\theta})$ of the Fourier transform of the acceleration responses at the $N_{out}$ measured degrees of freedom, based on the non-classically damped modal models, is written in the form

$$\underline{y}(\omega)=\sum_{r=1}^{m}(\underline{u}_r\xi_r(\omega)+\underline{u}_r^{*}\xi_r^{*}(\omega))+D_c\underline{\hat{u}}(\omega) \tag{4.43}$$

Considering the boundary conditions not equal to zero and using the Fourier transform over the duration $T$ for the first part of the first complex modal state space equation (3.6) yields



Institutional Repository - Library & Information Centre - University of Thessaly
24/04/2024 00:02:26 EEST - 3.141.244.201

$$\dot{\xi}_r(\omega) = \int_{-\infty}^{\infty} \dot{\xi}_r(t) e^{-j\omega t} dt = \int_0^T \frac{\partial \xi_r(t)}{dt} e^{-j\omega t} dt = e^{-j\omega t}\, \xi_r(t)\Big|_0^T + (j\omega) \underbrace{\int_0^T \xi_r(t) e^{-j\omega t} dt}_{\xi_r(\omega)} \tag{4.44}$$

Consequently,

$$\dot{\xi}_r(\omega) = e^{-j\omega t} \xi_r(\mathrm{T}) - e^{-j\omega t} \xi_r(0) + (j\omega) \xi_r(\omega) \tag{4.45}$$

Equalizing (4.45) with the first of the complex state space equations (3.6) yields

$$\dot{\xi}_r(t) = \lambda_r \xi_r(t) + \underline{l}_r^T \underline{u}(t) \Rightarrow e^{-j\omega t} \xi_r(\mathrm{T}) - e^{-j\omega t} \xi_r(0) + (j\omega) \xi_r(\omega) = \lambda_r \xi_r(\omega) + \underline{l}_r^T \hat{\underline{u}}(\omega) \tag{4.46}$$

The above equation can be expressed in the form

$$\xi_r(\omega) = \frac{\underline{l}_r^T \hat{\underline{u}}(\omega)}{j\omega - \lambda_r} + \frac{e^{-j\omega t} \xi_r(\mathrm{T})}{j\omega - \lambda_r} - \frac{\xi_r(0)}{j\omega - \lambda_r} \tag{4.47}$$

Thus, substituting (4.47) in to (4.43) the relation between the response $\underline{y}(\omega)$ and the excitation $\hat{\underline{u}}(\omega)$ in the frequency domain is given by

$$\begin{aligned} \underline{y}(\omega) = & \sum_{r=1}^{m} \left[ \frac{\underline{u}_r \underline{l}_r^T}{(j\omega) - \lambda_r} + \frac{\underline{u}_r^* \underline{l}_r^{*T}}{(j\omega) - \lambda_r^*} \right] \hat{\underline{u}}(\omega) + \sum_{r=1}^{m} \left[ \underline{u}_r \frac{e^{-j\omega T}}{(j\omega) - \lambda_r} \xi_r(\mathrm{T}) + \underline{u}_r^* \frac{e^{-j\omega T}}{(j\omega) - \lambda_r^*} \xi_r(\mathrm{T}) \right] - \\ & \sum_{r=1}^{m} \left[ \frac{\underline{u}_r}{(j\omega) - \lambda_r} \xi_r(0) + \frac{\underline{u}_r^*}{(j\omega) - \lambda_r^*} \xi_r(0) \right] + D_c \hat{\underline{u}}(\omega) + \end{aligned} \tag{4.48}$$

where $D_c \in \mathbb{R}^{N_{out} \times N_{in}}$, is a real matrix, $\underline{u}_r$, $r = 1, \ldots, m$ are the complex eigenvectors at $N_{out}$ DOFs, $\underline{l}_r^T \in C^{1 \times N_{in}}$ is the complex vector of the modal participation factors relating the $N_{in}$ inputs to the $r$ mode of the system, $\xi_r(0)$ and $\xi_r(\mathrm{T})$ are the boundary conditions of the modal response $\xi_r(t)$ and

$$\lambda_r = -\zeta_r \omega_r \pm j\omega_r \sqrt{1 - \zeta_r^2} = -a_r \pm j b_r \qquad , r = 1, \ldots, m \tag{4.49}$$

are the complex eigenvalues of the structures. The parameters $\alpha_r = \zeta_r \omega_r$ and $b_r = \omega_r \sqrt{1 - \zeta_r^2}$ are expressed in terms of the modal frequency $\omega_r$ and the modal damping ratio $\zeta_r$. Given $\alpha_r$ and $b_r$, the modal frequency $\omega_r$ and the damping ratio $\zeta_r$ are obtained from the following relationships:

$$\omega_r = \sqrt{a_r^2 + b_r^2} \tag{4.50}$$



Institutional Repository - Library & Information Centre - University of Thessaly
24/04/2024 00:02:26 EEST - 3.141.244.201

$$\zeta_r = \frac{a_r}{\sqrt{a_r^2 + b_r^2}} \tag{4.51}$$

The parameters set $\underline{\theta}$ in the notation $\underline{y}(\omega;\underline{\theta})$ contains the parameters that completely define the response vector $\underline{y}(\omega;\underline{\theta})$ using the modal analysis. From equations (4.43) to (4.49), it is evident that the parameter set $\underline{\theta}$ contains the complex eigenvalue $\lambda_r$ of the $r$ mode, the complex modeshapes $\underline{u}_r \in C^{N_{out}\times 1}$, the modal participation factor vectors $\underline{l}_r^T \in C^{1\times N_{in}}$, the initial conditions $\xi_r(0)$ and $\xi_r(\mathrm{T})$, and the entries of the real matrix $D_c \in \mathbb{R}^{N_{out}\times N_{in}}$, that is

$$\underline{\theta}: \left\{\lambda_r, \underline{u}_r, \underline{l}_r^T, \xi_r(0), \xi_r(T), r = 1,...,m, D_c\right\} \tag{4.52}$$

where $m$ is the number of contributing modes which is also an unknown in the modal identification process.

## 4.5 Second Step (First Approach)

In this section, the first approach of the second step is presented which provides an estimate of the modeshapes and the participation factors by solving a system of linear algebraic equations. In particular, the modeshapes and the participation factors derive through the Singular Value Decomposition (SVD) of the complex matrix $R_r \in C^{N_{out}\times N_{in}}$ presented further down. Hence, setting

$$R_r = \underline{u}_r \underline{l}_r^T \in C^{N_{out}\times N_{in}} \tag{4.53}$$

$$\underline{\alpha}_r = \underline{u}_r \xi_r(\mathrm{T}) \in C^{N_{out}\times 1} \tag{4.54}$$

$$\underline{\beta}_r = \underline{u}_r \xi_r(0) \in C^{N_{out}\times 1} \tag{4.55}$$

equation (4.48) becomes

$$\begin{aligned}\underline{y}(\omega) = &\sum_{r=1}^{m}\left[\frac{R_r}{(j\omega)-\lambda_r} + \frac{R_r^*}{(j\omega)-\lambda_r^*}\right]\hat{\underline{u}}(\omega) + \sum_{r=1}^{m}\left[\frac{\underline{\alpha}_r}{(j\omega)-\lambda_r} + \frac{\underline{\alpha}_r^*}{(j\omega)-\lambda_r^*}\right]e^{-j\omega T} - \\ &-\sum_{r=1}^{m}\left[\frac{\underline{\beta}_r}{(j\omega)-\lambda_r} + \frac{\underline{\beta}_r^*}{(j\omega)-\lambda_r^*}\right] + D_c\hat{\underline{u}}(\omega)\end{aligned} \tag{4.56}$$

It should be noted that in the aforementioned formulation the parameter set $\underline{\theta}$ consist of complex-valued variables, while the response vector $\underline{y}(\omega;\underline{\theta})$ is also described in terms of complex-valued variables and solutions of modal equations with complex-valued coefficients. From the computer implementation point of view, it is necessary to describe the response vector in terms of real-valued variables, equations and parameters. In what follows, the response vector



Institutional Repository - Library & Information Centre - University of Thessaly
24/04/2024 00:02:26 EEST - 3.141.244.201

$\underline{y}(\omega;\underline{\theta})$ is reformulated in terms of real-valued variables and parameter set $\underline{\theta}$. For this, the complex-valued matrix and vector variables $R_r$, $\underline{\alpha}_r$ and $\underline{\beta}_r$ involved in the description of the modal model are expressed in terms of the real and imaginary parts as follows:

$$R_r = L_r + jG_r \tag{4.57}$$

$$\underline{\alpha}_r = \underline{c}_r + j\underline{d}_r \tag{4.58}$$

$$\underline{\beta}_r = \underline{p}_r + j\underline{q}_r \tag{4.59}$$

and equation (4.56) becomes

$$\begin{aligned}\underline{y}(\omega) = &\sum_{r=1}^{m}\left[L_r\mu_r^+ + G_r\mu_r^-\right]\underline{\hat{u}}(\omega) + \sum_{r=1}^{m}\left[\underline{c}_r\mu_r^+ + \underline{d}_r\mu_r^-\right]e^{-j\omega T} - \\ &-\sum_{r=1}^{m}\left[\underline{p}_r\mu_r^+ + \underline{q}_r\mu_r^-\right] + D_c\underline{\hat{u}}(\omega)\end{aligned} \tag{4.60}$$

where

$$\underline{\mu}^+ = \begin{Bmatrix} \dfrac{1}{(j\omega)-\lambda_1} + \dfrac{1}{(j\omega)-\lambda_1^*} \\ \vdots \\ \dfrac{1}{(j\omega)-\lambda_m} + \dfrac{1}{(j\omega)-\lambda_m^*} \end{Bmatrix} \in C^m \tag{4.61}$$

$$\underline{\mu}^- = j\begin{Bmatrix} \dfrac{1}{(j\omega)-\lambda_1} - \dfrac{1}{(j\omega)-\lambda_1^*} \\ \\ \dfrac{1}{(j\omega)-\lambda_m} - \dfrac{1}{(j\omega)-\lambda_m^*} \end{Bmatrix} \in C^m \tag{4.62}$$

In order to implement a modal sweep approach similar to one presented in Werner et al. (1987) for classically damped systems, two index sets are introduced, the active index set $I_\alpha$ containing the mode numbers that are active and are optimized during the optimization process and the fixed index set $I_f$ that contains the rest of the $m$ modes that are included in computation of the response vector but their parameter values are kept constant during the optimization process. Thus, introducing the active and the fixed parts of the responses by



Institutional Repository - Library & Information Centre - University of Thessaly
24/04/2024 00:02:26 EEST - 3.141.244.201

$$\underline{x}^r(\omega;\underline{\theta}) = \sum_{r\in I_\alpha}\left[L_r\mu_r^+ + G_r\mu_r^-\right]\hat{\underline{u}}(\omega) + \sum_{r\in I_\alpha}\left[\underline{c}_r\mu_r^+ + \underline{d}_r\mu_r^-\right]e^{-j\omega T} - \\ -\sum_{r\in I_\alpha}\left[\underline{p}_r\mu_r^+ + \underline{q}_r\mu_r^-\right] + D_c\hat{\underline{u}}(\omega) \tag{4.63}$$

$$\underline{x}^f(\omega) = \sum_{f\in I_f}\left[L_f\mu_f^+ + G_f\mu_f^-\right]\hat{\underline{u}}(\omega) + \sum_{f\in I_f}\left[\underline{c}_f\mu_f^+ + \underline{d}_f\mu_f^-\right]e^{-j\omega T} - \\ -\sum_{f\in I_f}\left[\underline{p}_f\mu_f^+ + \underline{q}_f\mu_f^-\right] \tag{4.64}$$

the total response $\underline{y}(\omega;\underline{\theta}) \equiv \underline{y}(\omega)$ due to $m$ contributing modes can be written in the form

$$\underline{y}(\omega) = \underline{x}^r(\omega;\underline{\theta}) + \underline{x}^f(\omega) \tag{4.65}$$

which is more appropriate to use when formulating the optimization problem using modal sweeps to identify the modal parameters of the active modes defined in the set $I_\alpha$, holding the parameters of all other fixed modes, defined in the set $I_f$, as constants.

Using active and fixed modes, the objective function (4.41) can be expressed in the form

$$J(\underline{\theta}) = \frac{1}{V}\sum_{k=0}^{N}\left\{\begin{array}{l}\left[\underline{x}^r(k\Delta\omega;\underline{\theta}) + \underline{x}^f(k\Delta\omega) - \underline{\hat{y}}(k\Delta\omega)\right]^{*T}\cdot \\ \cdot\left[\underline{x}^r(k\Delta\omega;\underline{\theta}) + \underline{x}^f(k\Delta\omega) - \underline{\hat{y}}(k\Delta\omega)\right]\end{array}\right\} \tag{4.66}$$

,or equivalently, the final form of the objective function is given by

$$J(\underline{\theta}) = \frac{1}{V}\sum_{k=0}^{N}\left[\underline{x}^r(k\Delta\omega;\underline{\theta}) - \underline{\hat{e}}(k\Delta\omega)\right]^{*T}\left[\underline{x}^r(k\Delta\omega;\underline{\theta}) - \underline{\hat{e}}(k\Delta\omega)\right] \tag{4.67}$$

where $\underline{x}^r(k\Delta\omega;\underline{\theta})$, given by (4.63), depends on the parameter set $\underline{\theta}$, while $\underline{\hat{e}}(k\Delta\omega)$ given by

$$\underline{\hat{e}}(k\Delta\omega) = \underline{\hat{y}}(k\Delta\omega) - \left(\begin{array}{c}\sum_{r\in I_f}\left[L_f\mu_f^+ + G_f\mu_f^-\right]\hat{\underline{u}}(k\Delta\omega) + \sum_{r\in I_f}\left[\underline{c}_f\mu_f^+ + \underline{d}_f\mu_f^-\right]e^{-jk\Delta\omega T} - \\ -\sum_{r\in I_f}\left[\underline{p}_f\mu_f^+ + \underline{q}_f\mu_f^-\right]\end{array}\right) \tag{4.68}$$

is the constant vector of the measured response minus the response vector that is predicted from the modal model considering only the fixed modes.

Summarizing, the response is completely described by the real parameter set $\underline{\theta}$ that contains the modal parameters $\alpha_r = \zeta_r\omega_r$ and $b_r = \omega_r\sqrt{1-\zeta_r^2}$ that are related to the modal



Institutional Repository - Library & Information Centre - University of Thessaly
24/04/2024 00:02:26 EEST - 3.141.244.201

frequencies $\omega_r$ and the modal damping ratios $\zeta_r$, the real part $L_r$ and the imaginary part $G_r$ of the complex matrix $R_r$, the real part $\underline{c}_r$ and the imaginary part $\underline{d}_r$ of the complex vector $\underline{\alpha}_r$, the real part $\underline{p}_r$ and the imaginary part $\underline{q}_r$ of the complex vector $\underline{\beta}_r$ and the elements in the real matrix $D_c$, that is,

$$\underline{\theta}: \left\{\alpha_r, b_r, D_c, L_r, G_r, \underline{c}_r, \underline{d}_r, \underline{p}_r, \underline{q}_r,\ r=1,...,m\right\} \tag{4.69}$$

The total number of model parameter involved in the prediction of the response is $[4m+3(N_{out}\times N_{in})+4(N_{out}\times m)]$.

### 4.5.1 Simplifications Explaining Quadratic Dependence on Modal Characteristics

The minimization of the objective function (4.67) can be carried out efficiently, significantly reducing computational cost, by recognizing that the error function in (4.67) is quadratic with respect to the real part $L_r$ and the imaginary part $G_r$ of the complex matrix $R_r$, the real part $\underline{c}_r$ and the imaginary part $\underline{d}_r$ of the complex vector $\underline{\alpha}_r$, the real part $\underline{p}_r$ and the imaginary part $\underline{q}_r$ of the complex vector $\underline{\beta}_r$ and the elements in the real matrix $D_c$. This observation is used to develop explicit expressions that relate the parameters $L_r, G_r$, $\underline{c}_r$, $\underline{d}_r$, $\underline{p}_r$, $\underline{q}_r$ and $D_c$ to the rest of the model parameters appearing in the parameter set $\underline{\theta}$, such as the modal parameters $\alpha_r$ and $b_r$ that relate the modal frequencies $\omega_r$ and the modal damping ratios $\zeta_r$.

For this the parameter set $\underline{\theta}$ in (4.69) is partitioned into parameters sets as follows

$$\underline{\theta} = \left(\underline{\theta}^a, \underline{\theta}^b\right) \tag{4.70}$$

where $\underline{\theta}^b$ is defined by

$$\underline{\theta}^b = \left(\ D_c, L_r, G_r, \underline{c}_r, \underline{d}_r, \underline{p}_r, \underline{q}_r,\ r=1,...,m\right) \tag{4.71}$$

and $\underline{\theta}^a$ is defined by

$$\underline{\theta}^a = \left(\ a_r,\ b_r,\ r=1,...,m\right) \tag{4.72}$$

Stationary conditions with respect to the parameters in the set $\underline{\theta}^b$ are used to develop a linear system of equations for solving for the set $\underline{\theta}^b$ given the values of the parameters set $\underline{\theta}^a$.

For convenience in the presentation this linear system can be formulated in the general form

$$\mathrm{A}\left(\underline{\theta}^\alpha\right)\underline{\theta}^b = \underline{b}\left(\underline{\theta}^\alpha\right) \tag{4.73}$$



Institutional Repository - Library & Information Centre - University of Thessaly
24/04/2024 00:02:26 EEST - 3.141.244.201

where $\underline{A}\left(\underline{\theta}^{\alpha}\right)$ and $\underline{b}\left(\underline{\theta}^{\alpha}\right)$ are functions of the parameter set $\underline{\theta}^{a}$. Let

$$\underline{\theta}^{b} = \underline{\theta}^{b}\left(\underline{\theta}^{a}\right) \tag{4.74}$$

be the function that gives the relationship between the parameters set $\underline{\theta}^{b}$ and the parameter set $\underline{\theta}^{a}$ by solving the system (4.73). Then the objective function $J\left(\underline{\theta}\right)$ takes the form

$$J\left(\underline{\theta}\right) = J\left(\underline{\theta}^{a}, \underline{\theta}^{b}\right) = J\left(\underline{\theta}^{a}, \underline{\theta}^{b}\left(\underline{\theta}^{a}\right)\right) \equiv J^{*}\left(\underline{\theta}^{a}\right) \tag{4.75}$$

Hence the minimization problem can be stated as follows. Find the values of the parameter set $\underline{\theta}^{a}$ that minimize the objective function

$$J^{*}\left(\underline{\theta}\right) = J\left(\underline{\theta}^{a}, \underline{\theta}^{b}\left(\underline{\theta}^{a}\right)\right) \tag{4.76}$$

Once the values of $\underline{\theta}^{a}$ have been found, the values of $\underline{\theta}^{b}$ are obtained solving the linear system (4.73). Next our objective is to apply the above concept and first obtain the matrices and vectors that completely define the linear system (4.73).

The linear system for the parameter set $\underline{\theta}^{b}$ is obtained by setting the derivatives of $J\left(\underline{\theta}\right)$ with respect to each element of $\underline{\theta}^{b}$ equal to zero, that is,

$$\frac{\partial J\left(\underline{\theta}\right)}{\partial L_{r,li}} = 0 \tag{4.77}$$

$$\frac{\partial J\left(\underline{\theta}\right)}{\partial G_{r,li}} = 0 \tag{4.78}$$

$$\frac{\partial J\left(\underline{\theta}\right)}{\partial D_{c,li}} = 0 \tag{4.79}$$

$$\frac{\partial J\left(\underline{\theta}\right)}{\partial c_{r,l}} = 0 \tag{4.80}$$

$$\frac{\partial J\left(\underline{\theta}\right)}{\partial d_{r,l}} = 0 \tag{4.81}$$

$$\frac{\partial J\left(\underline{\theta}\right)}{\partial p_{r,l}} = 0 \tag{4.82}$$



Institutional Repository - Library & Information Centre - University of Thessaly
24/04/2024 00:02:26 EEST - 3.141.244.201

$$\frac{\partial J(\underline{\theta})}{\partial q_{r,l}} = 0 \tag{4.83}$$

for $l = 1,\ldots,N_{out}$, $r = 1,\ldots,m$ and $i = 1,\ldots,N_{in}$. The analytical computation of these derivatives is shown in the appendices. It can be readily shown that the set of linear algebraic equations can be written in the compact matrix form:

$$\left[\sum_{k=1}^{N}\left(A\left(\underline{\theta}^a\right)+A^{*T}\left(\underline{\theta}^a\right)\right)\right]X=\left[\sum_{k=1}^{N}\left(B\left(\underline{\theta}^a\right)+B^{*T}\left(\underline{\theta}^a\right)\right)\right] \tag{4.84}$$

where

$$A\left(\underline{\theta}^a\right)=\begin{bmatrix} \left(\underline{\mu}\otimes\underline{u}(\omega_k)\right)^*\left(\underline{\mu}\otimes\underline{u}(\omega_k)\right)^T & \left(\underline{\mu}\otimes\underline{u}(\omega_k)\right)^*\underline{u}^T(\omega_k) & \left(\underline{\mu}\otimes\underline{u}(\omega_k)\right)^*\underline{\mu}^T e^{-j\omega_k T} & -\left(\underline{\mu}\otimes\underline{u}(\omega_k)\right)^*\underline{\mu}^T \\ \underline{u}^*(\omega_k)\left(\underline{\mu}\otimes\underline{u}(\omega_k)\right)^T & \underline{u}^*(\omega_k)\underline{u}^T(\omega_k) & \underline{u}^*(\omega_k)\underline{\mu}^T e^{-j\omega_k T} & -\underline{u}^*(\omega_k)\underline{\mu}^T \\ \underline{\mu}^*\left(\underline{\mu}\otimes\underline{u}(\omega_k)\right)^T e^{j\omega_k T} & \underline{\mu}^*\underline{u}^T(\omega_k)e^{j\omega_k T} & \underline{\mu}^*\underline{\mu}^T & -\underline{\mu}^*\underline{\mu}^T e^{j\omega_k T} \\ \underline{\mu}^*\left(\underline{\mu}\otimes\underline{u}(\omega_k)\right)^T & \underline{\mu}^*\underline{u}^T(\omega_k) & \underline{\mu}^*\underline{\mu}^T e^{-j\omega_k T} & -\underline{\mu}^*\underline{\mu}^T \end{bmatrix} \tag{4.85}$$

$$B\left(\underline{\theta}^a\right)=\begin{bmatrix} \left(\underline{\mu}\otimes\underline{u}(\omega_k)\right)^*\hat{\underline{e}}^T(\omega_k) \\ \underline{u}^*(\omega_k)\hat{\underline{e}}^T(\omega_k) \\ \underline{\mu}^* e^{j\omega_k T}\hat{\underline{e}}^T(\omega_k) \\ \underline{\mu}^*\hat{\underline{e}}^T(\omega_k) \end{bmatrix} \tag{4.86}$$

$$X=\begin{Bmatrix} L_1^T \\ \vdots \\ L_m^T \\ G_1^T \\ \vdots \\ G_m^T \\ D_c^T \\ c^T \\ d^T \\ p^T \\ q^T \end{Bmatrix} \tag{4.87}$$

and $\omega_k = k\Delta\omega$, $k = 1,\ldots,N$,



Institutional Repository - Library & Information Centre - University of Thessaly
24/04/2024 00:02:26 EEST - 3.141.244.201

$$c^T = \begin{Bmatrix} c_1^T \\ \vdots \\ c_m^T \end{Bmatrix},\ d = \begin{Bmatrix} d_1^T \\ \vdots \\ d_m^T \end{Bmatrix},\ p = \begin{Bmatrix} p_1^T \\ \vdots \\ p_m^T \end{Bmatrix},\ q = \begin{Bmatrix} q_1^T \\ \vdots \\ q_m^T \end{Bmatrix} \text{ and } \underline{\mu} = \begin{Bmatrix} \underline{\mu}^+ \\ \underline{\mu}^- \end{Bmatrix}.$$

The system of equations (4.84) can be expressed in the form

$$\mathrm{Re}\left\{\sum_{k=1}^{N}\left(A\left(\underline{\theta}^a\right)\right)\right\} X = \mathrm{Re}\left\{\sum_{k=1}^{N}\left(B\left(\underline{\theta}^a\right)\right)\right\} \tag{4.88}$$

From (4.88) we obtain the matrices $L_r$ and $G_r$ that contains the information for the eigenvectors $\underline{u}_r$ and the participation factors $\underline{l}_r^T$. Hence, the modeshapes and the participation factors derive through the Singular Value Decomposition (SVD) of the complex matrix $R_r \in C^{N_{out} \times N_{in}}$.

Substituting (4.63) in (4.67), the error function $J^*\left(\underline{\theta}^a\right)$ becomes

$$J^*\left(\underline{\theta}^a\right) = \frac{1}{V}\sum_{k=0}^{N} \left[\begin{array}{l} \left[\sum_{r\in l_u}\left[L_r\mu_r^+\left(\underline{\theta}^a\right)+G_r\mu_r^-\left(\underline{\theta}^a\right)\right]\hat{\underline{u}}(k\Delta\omega)+\sum_{r\in l_u}\left[\underline{c}_r\mu_r^+\left(\underline{\theta}^a\right)+\underline{d}_r\mu_r^-\left(\underline{\theta}^a\right)\right]e^{-jk\Delta\omega\bar{t}}-\right. \\ \left.-\sum_{r\in l_u}\left[\underline{p}_r\mu_r^+\left(\underline{\theta}^a\right)+\underline{q}_r\mu_r^-\left(\underline{\theta}^a\right)\right]+D_c\hat{\underline{u}}(k\Delta\omega)-\hat{\underline{e}}\left(k\Delta\omega\right)\right]^T \\ \left[\sum_{r\in l_u}\left[L_r\mu_r^+\left(\underline{\theta}^a\right)+G_r\mu_r^-\left(\underline{\theta}^a\right)\right]\hat{\underline{u}}(k\Delta\omega)+\sum_{r\in l_u}\left[\underline{c}_r\mu_r^+\left(\underline{\theta}^a\right)+\underline{d}_r\mu_r^-\left(\underline{\theta}^a\right)\right]e^{-jk\Delta\omega\bar{t}}-\right. \\ \left.-\sum_{r\in l_u}\left[\underline{p}_r\mu_r^+\left(\underline{\theta}^a\right)+\underline{q}_r\mu_r^-\left(\underline{\theta}^a\right)\right]+D_c\hat{\underline{u}}(k\Delta\omega)-\hat{\underline{e}}\left(k\Delta\omega\right)\right] \end{array} \tag{4.89}$$

or in compact form

$$J^*\left(\underline{\theta}^a\right) = \frac{1}{V}\sum_{k=0}^{N}\left[\underline{x}^r\left(k\Delta\omega;\underline{\theta}^a\right)-\hat{\underline{e}}\left(k\Delta\omega\right)\right]^T\left[\underline{x}^r\left(k\Delta\omega;\underline{\theta}^a\right)-\hat{\underline{e}}\left(k\Delta\omega\right)\right] \tag{4.90}$$

where

$$\begin{aligned} \underline{x}^r\left(k\Delta\omega;\underline{\theta}^a\right) = &\sum_{r\in l_u}\left[L_r\mu_r^+\left(\underline{\theta}^a\right)+G_r\mu_r^-\left(\underline{\theta}^a\right)\right]\hat{\underline{u}}(k\Delta\omega)+\sum_{r\in l_u}\left[\underline{c}_r\mu_r^+\left(\underline{\theta}^a\right)+\underline{d}_r\mu_r^-\left(\underline{\theta}^a\right)\right]e^{-jk\Delta\omega\bar{t}}- \\ &-\sum_{r\in l_u}\left[\underline{p}_r\mu_r^+\left(\underline{\theta}^a\right)+\underline{q}_r\mu_r^-\left(\underline{\theta}^a\right)\right]+D_c\hat{\underline{u}}(k\Delta\omega) \end{aligned} \tag{4.91}$$

The total number of model parameter involved in the prediction of the response at $N_{out}$ DOFs given $m$ modes and $N_{in}$ input time histories, is now reduced from $[4m+3(N_{out}\times N_{in})+4(N_{out}\times m)]$ to $[2m]$.



Institutional Repository - Library & Information Centre - University of Thessaly
24/04/2024 00:02:26 EEST - 3.141.244.201

It should be noted that in this section the general case of the second step has been presented where the parameters $\alpha_r$ and $b_r$ that relate the modal frequencies $\omega_r$ and the modal damping ratios $\zeta_r$ are used for the minimization of the error function (4.90). In the special case of the second step the parameters $\alpha_r$ and $b_r$ are obtained from the first step (Stabilization Diagrams) and second step becomes a problem of solving linear algebraic equations for the parameter set $\underline{\theta}^b$.

### 4.5.2 Analytical Expression of the Gradient of the Objective function

Next, analytically expressions for the gradients and the objective function (4.90) with respect to each parameter in the set $\underline{\theta}^a$ are defined. Differentiating $J^*\left(\underline{\theta}^a\right)$ with respect to a parameter $\theta$ in the parameter set $\underline{\theta}^a$ yields

$$\frac{\partial J^*\left(\underline{\theta}^a\right)}{\partial \theta}=\frac{1}{V}\sum_{k=0}^{N}\left\{\frac{\partial \underline{x}^{r*T}\left(k\Delta\omega;\underline{\theta}^a\right)}{\partial \theta}\left[\underline{x}^r\left(k\Delta\omega;\underline{\theta}^a\right)-\underline{\hat{e}}\left(k\Delta\omega\right)\right]+CT\right\} \tag{4.92}$$

where $CT$ is the conjugate transpose of the term $\frac{\partial \underline{x}^{r*T}\left(k\Delta\omega;\underline{\theta}^a\right)}{\partial \theta}\left[\underline{x}^r\left(k\Delta\omega;\underline{\theta}^a\right)-\underline{\hat{e}}\left(k\Delta\omega\right)\right]$, and

$$\begin{aligned}\frac{\partial \underline{x}^{r*T}\left(k\Delta\omega;\underline{\theta}^a\right)}{\partial \theta}=\underline{\hat{u}}^{*T}(k\Delta\omega)\sum_{r\in I_a}\left[L_r^T\frac{\partial\left(\mu_r^+\right)^*}{\partial\theta}+G_r^T\frac{\partial\left(\mu_r^-\right)^*}{\partial\theta}+\frac{\partial\left(L_r\right)^{*T}}{\partial\theta}\left(\mu_r^+\right)^*+\frac{\partial\left(G_r\right)^{*T}}{\partial\theta}\left(\mu_r^-\right)^*\right]+\\ e^{jk\Delta\omega T}\sum_{r\in I_a}\left[\underline{c}_r^T\frac{\partial\left(\mu_r^+\right)^*}{\partial\theta}+\underline{d}_r^T\frac{\partial\left(\mu_r^-\right)^*}{\partial\theta}+\frac{\partial\left(\underline{c}_r\right)^{*T}}{\partial\theta}\left(\mu_r^+\right)^*+\frac{\partial\left(\underline{d}_r\right)^{*T}}{\partial\theta}\left(\mu_r^-\right)^*\right]-\\ \sum_{r\in I_a}\left[\underline{p}_r^T\frac{\partial\left(\mu_r^+\right)^*}{\partial\theta}+\underline{q}_r^T\frac{\partial\left(\mu_r^-\right)^*}{\partial\theta}+\frac{\partial\left(\underline{p}_r\right)^{*T}}{\partial\theta}\left(\mu_r^+\right)^*+\frac{\partial\left(\underline{q}_r\right)^{*T}}{\partial\theta}\left(\mu_r^-\right)^*\right]+\\ +\underline{\hat{u}}^{*T}(k\Delta\omega)\frac{\partial\left(D_c\right)^{*T}}{\partial\theta}+\end{aligned} \tag{4.93}$$

and the derivatives $\frac{\partial\left(\mu_r^+\right)^*}{\partial\theta}$ and $\frac{\partial\left(\mu_r^-\right)^*}{\partial\theta}$ with respect to each parameter $\theta$ are given by

$$\frac{\partial\left(\mu_r^+\right)^*}{\partial a_r}=-\left(\frac{1}{\left((jk\Delta\omega)-\lambda_r\right)^2}+\frac{1}{\left((j\omega)-\lambda_r^*\right)^2}\right)^* \tag{4.94}$$



Institutional Repository - Library & Information Centre - University of Thessaly
24/04/2024 00:02:26 EEST - 3.141.244.201

$$\frac{\partial\left(\mu_r^-\right)^*}{\partial a_r}=\left(-\frac{j}{\left((jk\Delta\omega)-\lambda_r\right)^2}+\frac{j}{\left((j\omega)-\lambda_r^*\right)^2}\right)^* \tag{4.95}$$

$$\frac{\partial\left(\mu_r^+\right)^*}{\partial b_r}=\left(\frac{j}{\left((jk\Delta\omega)-\lambda_r\right)^2}-\frac{j}{\left((j\omega)-\lambda_r^*\right)^2}\right)^* \tag{4.96}$$

$$\frac{\partial\left(\mu_r^-\right)^*}{\partial b_r}=-\left(\frac{1}{\left((jk\Delta\omega)-\lambda_r\right)^2}+\frac{1}{\left((j\omega)-\lambda_r^*\right)^2}\right)^* \tag{4.97}$$

Note that the derivatives $\partial\left(L_r\right)^{*T}/\partial\theta,\partial\left(G_r\right)^{*T}/\partial\theta,\partial\left(\underline{c}_r\right)^{*T}/\partial\theta,\partial\left(\underline{d}_r\right)^{*T}/\partial\theta$ and $\partial\left(\underline{p}_r\right)^{*T}/\partial\theta,\partial\left(\underline{q}_r\right)^{*T}/\partial\theta$ are readily obtained by differentiating with respect to $\theta$ both sides of the system of linear equations (4.88). This yields the following system of linear equation for the derivatives

$$\mathrm{Re}\left\{\sum_{k=1}^{N}A\left(\underline{\theta}^a\right)\right\}\frac{\partial X}{\partial\theta}=\mathrm{Re}\left\{\frac{\sum_{k=1}^{N}\partial\left(B\left(\underline{\theta}^a\right)\right)}{\partial\theta}\right\}-\mathrm{Re}\left\{\frac{\sum_{k=1}^{N}\partial\left(A\left(\underline{\theta}^a\right)\right)}{\partial\theta}\right\}X \tag{4.98}$$

where, using (4.85) and (4.86), it can be readily shown that

$$\frac{\partial\left(A\left(\underline{\theta}^a\right)\right)}{\partial\theta}=$$



Institutional Repository - Library & Information Centre - University of Thessaly
24/04/2024 00:02:26 EEST - 3.141.244.201

$$\begin{bmatrix} \left[\left(\frac{\partial \underline{\underline{\mu}}}{\partial \theta}\otimes \underline{u}(\omega_k)\right)^{*}\left(\underline{\mu}\otimes \underline{u}(\omega_k)\right)^{T}+\left(\underline{\mu}\otimes \underline{u}(\omega_k)\right)^{*}\left(\frac{\partial \underline{\underline{\mu}}}{\partial \theta}\otimes \underline{u}(\omega_k)\right)^{T}\right] & \left(\frac{\partial \underline{\underline{\mu}}}{\partial \theta}\otimes \underline{u}(\omega_k)\right)^{*}\underline{u}^{T}(\omega_k) & \left[\left(\frac{\partial \underline{\underline{\mu}}}{\partial \theta}\otimes \underline{u}(\omega_k)\right)^{*}\underline{\mu}^{T}+\left(\underline{\mu}\otimes \underline{u}(\omega_k)\right)^{*}\frac{\partial \underline{\mu}^{T}}{\partial \theta}\right]e^{-j\omega_k T} & -\left[\left(\frac{\partial \underline{\underline{\mu}}}{\partial \theta}\otimes \underline{u}(\omega_k)\right)^{*}\underline{\mu}^{T}+\left(\underline{\mu}\otimes \underline{u}(\omega_k)\right)^{*}\frac{\partial \underline{\mu}^{T}}{\partial \theta}\right] \\ \underline{u}^{*}(\omega_k)\left(\frac{\partial \underline{\mu}_r}{\partial \theta_r}\otimes \underline{u}(\omega_k)\right)^{T} & 0 & \underline{u}^{*}(\omega_k)\frac{\partial \underline{\mu}^{T}}{\partial \theta}e^{-j\omega_k T} & -\underline{u}^{*}(\omega_k)\frac{\partial \underline{\mu}^{T}}{\partial \theta} \\ \left[\frac{\partial \underline{\mu}^{*}}{\partial \theta}\left(\underline{\mu}\otimes \underline{u}(\omega_k)\right)^{T}+\underline{\mu}^{*}\left(\frac{\partial \underline{\underline{\mu}}}{\partial \theta}\otimes \underline{u}(\omega_k)\right)^{T}\right]e^{j\omega_k T} & \frac{\partial \underline{\mu}^{*}}{\partial \theta}\underline{u}^{T}(\omega_k)e^{j\omega_k T} & \frac{\partial \underline{\mu}^{*}}{\partial \theta}\underline{\mu}^{T}+\underline{\mu}^{*}\frac{\partial \underline{\mu}^{T}}{\partial \theta} & -\left[\frac{\partial \underline{\mu}^{*}}{\partial \theta}\underline{\mu}^{T}+\underline{\mu}^{*}\frac{\partial \underline{\mu}^{T}}{\partial \theta}\right]e^{j\omega_k T} \\ \left[\frac{\partial \underline{\mu}^{*}}{\partial \theta}\left(\underline{\mu}\otimes \underline{u}(\omega_k)\right)^{T}+\underline{\mu}^{*}\left(\frac{\partial \underline{\underline{\mu}}}{\partial \theta}\otimes \underline{u}(\omega_k)\right)^{T}\right] & \frac{\partial \underline{\mu}^{*}}{\partial \theta}\underline{u}^{T}(\omega_k) & \left[\frac{\partial \underline{\mu}^{*}}{\partial \theta}\underline{\mu}^{T}+\underline{\mu}^{*}\frac{\partial \underline{\mu}^{T}}{\partial \theta}\right]e^{-j\omega_k T} & -\left[\frac{\partial \underline{\mu}^{*}}{\partial \theta}\underline{\mu}^{T}+\underline{\mu}^{*}\frac{\partial \underline{\mu}^{T}}{\partial \theta}\right] \end{bmatrix} \tag{4.99}$$

$$\frac{\partial(B)}{\partial \theta}=\sum_{k=1}^{N}\begin{bmatrix} \left(\frac{\partial \underline{\underline{\mu}}}{\partial \theta}\otimes \underline{u}(\omega_k)\right)^{*}\hat{e}^{\mathrm{T}}(\omega_k) \\ 0 \\ \frac{\partial \underline{\mu}^{*}}{\partial \theta}\hat{e}^{\mathrm{T}}(\omega_k)e^{j\omega_k T} \\ \frac{\partial \underline{\mu}^{*}}{\partial \theta}\hat{e}^{\mathrm{T}}(\omega_k) \end{bmatrix} \tag{4.100}$$

where $\omega_k = k\Delta\omega$, $k=1,\ldots,N$, and the derivative $\partial\underline{\mu}/\partial\theta$ is given by

$$\frac{\partial \underline{\mu}}{\partial \theta}=\begin{Bmatrix} \frac{\partial \underline{\mu}^{+}}{\partial \theta} \\ \frac{\partial \underline{\mu}^{-}}{\partial \theta} \end{Bmatrix} \tag{4.101}$$

## 4.6 Second Step (Second Approach)

In this section, the second approach of the second step is presented which provides an estimate of the modeshapes by solving a system of linear algebraic equations. In particular, this part takes advantage of that the error function is quadratic with respect to the modeshapes, thus stationary conditions are used in order to develop a linear system of equations from which the modeshapes are derived.



Institutional Repository - Library & Information Centre - University of Thessaly
24/04/2024 00:02:26 EEST - 3.141.244.201

It should be noted that in the aforementioned formulation the parameter set $\underline{\theta}$ consist of complex-valued variables, while the response vector $\underline{y}(\omega;\underline{\theta})$ in (4.48) is also described in terms of complex-valued variables. From the computer implementation point of view, it is necessary to describe the response vector in terms of real-valued variables, equations and parameters. In what follows, the response vector $\underline{y}(\omega;\underline{\theta})$ is reformulated in terms of real-valued variables and parameter set $\underline{\theta}$. For this, the complex-valued scalar and vector variables $\underline{u}_r$, $\underline{l}_r$, $\xi_r(0)$ and $\xi_r(\mathrm{T})$ involved in the description of the modal model are expressed in terms of the real and imaginary parts as follows:

$$\underline{u}_r = \underline{\phi}_r + j\underline{\psi}_r \tag{4.102}$$

$$\underline{l}_r^{\mathrm{T}} = \underline{p}_{\mathrm{Re},r}^T + j\underline{p}_{\mathrm{Im},r}^T \tag{4.103}$$

$$\xi_r(0) = n_{\mathrm{Re},r}^0 + jn_{\mathrm{Im},r}^0 \tag{4.104}$$

$$\xi_r(T) = n_{\mathrm{Re},r}^\tau + jn_{\mathrm{Im},r}^\tau \tag{4.105}$$

Substituting (4.102), (4.103), (4.104) and (4.105) in (4.48) yields

$$\begin{aligned}
\underline{y}(\omega) = &\sum_{r=1}^{m}\left[\begin{array}{l}\left(\left(\underline{p}_{\mathrm{Re},r}^T + j\underline{p}_{\mathrm{Im},r}^T\right)\dfrac{\hat{\underline{u}}(\omega)}{(j\omega_k)-\lambda_r} + \left(\underline{p}_{\mathrm{Re},r}^T - j\underline{p}_{\mathrm{Im},r}^T\right)\dfrac{\hat{\underline{u}}(\omega)}{(j\omega)-\lambda_r^*}\right)\underline{\phi}_r + \\ j\left(\left(\underline{p}_{\mathrm{Re},r}^T + j\underline{p}_{\mathrm{Im},r}^T\right)\dfrac{\hat{\underline{u}}(\omega)}{(j\omega_k)-\lambda_r} - \left(\underline{p}_{\mathrm{Re},r}^T - j\underline{p}_{\mathrm{Im},r}^T\right)\dfrac{\hat{\underline{u}}(\omega)}{(j\omega)-\lambda_r^*}\right)\underline{\psi}_r\end{array}\right] + \\
&\sum_{r=1}^{m}\left[\begin{array}{l}\left(\dfrac{e^{-j\omega T}}{(j\omega)-\lambda_r} + \dfrac{e^{-j\omega T}}{(j\omega)-\lambda_r^*}\right)\left(n_{\mathrm{Re},r}^\tau + jn_{\mathrm{Im},r}^\tau\right)\underline{\phi}_r + \\ j\left(\dfrac{e^{-j\omega T}}{(j\omega)-\lambda_r} - \dfrac{e^{-j\omega T}}{(j\omega)-\lambda_r^*}\right)\left(n_{\mathrm{Re},r}^\tau + jn_{\mathrm{Im},r}^\tau\right)\underline{\psi}_r\end{array}\right] - \\
&\sum_{r=1}^{m}\left[\begin{array}{l}\left(\dfrac{1}{(j\omega)-\lambda_r} + \dfrac{1}{(j\omega)-\lambda_r^*}\right)\left(n_{\mathrm{Re},r}^0 + jn_{\mathrm{Im},r}^0\right)\underline{\phi}_r + \\ j\left(\dfrac{1}{(j\omega)-\lambda_r} - \dfrac{1}{(j\omega)-\lambda_r^*}\right)\left(n_{\mathrm{Re},r}^0 + jn_{\mathrm{Im},r}^0\right)\underline{\psi}_r\end{array}\right] + D_c\hat{\underline{u}}(\omega)
\end{aligned} \tag{4.106}$$

Two index sets are introduced, the active index set $I_\alpha$ containing the mode numbers that are active and are optimized during the optimization process and the fixed index set $I_f$ that contains the rest of the $m$ modes that are included in computation of the response vector but their parameter values are kept constant during the optimization process. Hence, the active and the fixed parts of the responses are given by



Institutional Repository - Library & Information Centre - University of Thessaly
24/04/2024 00:02:26 EEST - 3.141.244.201

$$\underline{x}^{r}(\omega;\underline{\theta}) = \sum_{r\in I_\alpha}\left[\begin{array}{l}\left(\left(\underline{p}^{T}_{\mathrm{Re},r}+j\underline{p}^{T}_{\mathrm{Im},r}\right)\dfrac{\hat{\underline{u}}(\omega)}{(j\omega)-\lambda_r}+\left(\underline{p}^{T}_{\mathrm{Re},r}-j\underline{p}^{T}_{\mathrm{Im},r}\right)\dfrac{\hat{\underline{u}}(\omega)}{(j\omega)-\lambda_r^{*}}\right)\underline{\phi}_r+\\ j\left(\left(\underline{p}^{T}_{\mathrm{Re},r}+j\underline{p}^{T}_{\mathrm{Im},r}\right)\dfrac{\hat{\underline{u}}(\omega)}{(j\omega)-\lambda_r}-\left(\underline{p}^{T}_{\mathrm{Re},r}-j\underline{p}^{T}_{\mathrm{Im},r}\right)\dfrac{\hat{\underline{u}}(\omega)}{(j\omega)-\lambda_r^{*}}\right)\underline{\psi}_r\end{array}\right]+$$
$$\sum_{r\in I_\alpha}\left[\begin{array}{l}\left(\dfrac{e^{-j\omega T}}{(j\omega)-\lambda_r}+\dfrac{e^{-j\omega T}}{(j\omega)-\lambda_r^{*}}\right)\left(n^{\tau}_{\mathrm{Re},r}+jn^{\tau}_{\mathrm{Im},r}\right)\underline{\phi}_r+\\ j\left(\dfrac{e^{-j\omega T}}{(j\omega)-\lambda_r}-\dfrac{e^{-j\omega T}}{(j\omega)-\lambda_r^{*}}\right)\left(n^{\tau}_{\mathrm{Re},r}+jn^{\tau}_{\mathrm{Im},r}\right)\underline{\psi}_r\end{array}\right]-$$
$$\sum_{r\in I_\alpha}\left[\begin{array}{l}\left(\dfrac{1}{(j\omega)-\lambda_r}+\dfrac{1}{(j\omega)-\lambda_r^{*}}\right)\left(n^{0}_{\mathrm{Re},r}+jn^{0}_{\mathrm{Im},r}\right)\underline{\phi}_r+\\ j\left(\dfrac{1}{(j\omega)-\lambda_r}-\dfrac{1}{(j\omega)-\lambda_r^{*}}\right)\left(n^{0}_{\mathrm{Re},r}+jn^{0}_{\mathrm{Im},r}\right)\underline{\psi}_r\end{array}\right]+D_c\,\hat{\underline{u}}(\omega) \tag{4.107}$$

$$\underline{x}^{f}(\omega) = \sum_{f\in I_f}\left[\begin{array}{l}\left(\left(\underline{p}^{T}_{\mathrm{Re},f}+j\underline{p}^{T}_{\mathrm{Im},f}\right)\dfrac{\hat{\underline{u}}(\omega)}{(j\omega)-\lambda_f}+\left(\underline{p}^{T}_{\mathrm{Re},f}-j\underline{p}^{T}_{\mathrm{Im},f}\right)\dfrac{\hat{\underline{u}}(\omega)}{(j\omega)-\lambda_f^{*}}\right)\underline{\phi}_f+\\ j\left(\left(\underline{p}^{T}_{\mathrm{Re},f}+j\underline{p}^{T}_{\mathrm{Im},f}\right)\dfrac{\hat{\underline{u}}(\omega)}{(j\omega)-\lambda_f}-\left(\underline{p}^{T}_{\mathrm{Re},f}-j\underline{p}^{T}_{\mathrm{Im},f}\right)\dfrac{\hat{\underline{u}}(\omega)}{(j\omega)-\lambda_f^{*}}\right)\underline{\psi}_f\end{array}\right]+$$
$$\sum_{f\in I_f}\left[\begin{array}{l}\left(\dfrac{e^{-j\omega T}}{(j\omega)-\lambda_f}+\dfrac{e^{-j\omega T}}{(j\omega)-\lambda_f^{*}}\right)\left(n^{\tau}_{\mathrm{Re},f}+jn^{\tau}_{\mathrm{Im},f}\right)\underline{\phi}_f+\\ j\left(\dfrac{e^{-j\omega T}}{(j\omega)-\lambda_f}-\dfrac{e^{-j\omega T}}{(j\omega)-\lambda_f^{*}}\right)\left(n^{\tau}_{\mathrm{Re},f}+jn^{\tau}_{\mathrm{Im},f}\right)\underline{\psi}_f\end{array}\right]-$$
$$\sum_{f\in I_f}\left[\begin{array}{l}\left(\dfrac{1}{(j\omega)-\lambda_f}+\dfrac{1}{(j\omega)-\lambda_f^{*}}\right)\left(n^{0}_{\mathrm{Re},f}+jn^{0}_{\mathrm{Im},f}\right)\underline{\phi}_f+\\ j\left(\dfrac{1}{(j\omega)-\lambda_f}-\dfrac{1}{(j\omega)-\lambda_f^{*}}\right)\left(n^{0}_{\mathrm{Re},f}+jn^{0}_{\mathrm{Im},f}\right)\underline{\psi}_f\end{array}\right] \tag{4.108}$$

the total response $\underline{y}(\omega;\underline{\theta}) \equiv \underline{y}(\omega)$ due to $m$ contributing modes can be written in the form

$$\underline{y}(\omega) = \underline{x}^{r}(\omega;\underline{\theta}) + \underline{x}^{f}(\omega) \tag{4.109}$$

which is more appropriate to use when formulating the optimization problem using modal sweeps to identify the modal parameters of the active modes defined in the set $I_\alpha$, holding the parameters of all other fixed modes, defined in the set $I_f$, as constants.



Institutional Repository - Library & Information Centre - University of Thessaly
24/04/2024 00:02:26 EEST - 3.141.244.201

Using active and fixed modes, the objective function (4.41) can be expressed in the form

$$J(\underline{\theta}) = \frac{1}{V}\sum_{k=0}^{N}\left\{\begin{array}{l}\left[\underline{x}^{r}(k\Delta\omega;\underline{\theta}) + \underline{x}^{f}(k\Delta\omega) - \underline{\hat{y}}(k\Delta\omega)\right]^{*T}\cdot \\ \cdot\left[\underline{x}^{r}(k\Delta\omega;\underline{\theta}) + \underline{x}^{f}(k\Delta\omega) - \underline{\hat{y}}(k\Delta\omega)\right]\end{array}\right\} \tag{4.110}$$

,or equivalently, the final form of the objective function is given by

$$J(\underline{\theta}) = \frac{1}{V}\sum_{k=0}^{N}\left[\underline{x}^{r}(k\Delta\omega;\underline{\theta}) - \underline{\hat{e}}(k\Delta\omega)\right]^{*T}\left[\underline{x}^{r}(k\Delta\omega;\underline{\theta}) - \underline{\hat{e}}(k\Delta\omega)\right] \tag{4.111}$$

where $\underline{x}^{r}(k\Delta\omega;\underline{\theta})$, given by (4.107), depends on the parameter set $\underline{\theta}$, while $\underline{\hat{e}}(k\Delta\omega)$ given by

$$\underline{\hat{e}}(k\Delta\omega) = \underline{\hat{y}}(k\Delta\omega) -$$

$$-\left(\begin{array}{l}\displaystyle\sum_{f\in I_f}\left[\begin{array}{l}\left(\left(\underline{p}_{\mathrm{Re},f}^{T} + j\underline{p}_{\mathrm{Im},f}^{T}\right)\frac{\underline{\hat{u}}(k\Delta\omega)}{(jk\Delta\omega)-\lambda_f} + \left(\underline{p}_{\mathrm{Re},f}^{T} - j\underline{p}_{\mathrm{Im},f}^{T}\right)\frac{\underline{\hat{u}}(k\Delta\omega)}{(jk\Delta\omega)-\lambda_f^{*}}\right)\underline{\phi}_f + \\ j\left(\left(\underline{p}_{\mathrm{Re},f}^{T} + j\underline{p}_{\mathrm{Im},f}^{T}\right)\frac{\underline{\hat{u}}(k\Delta\omega)}{(jk\Delta\omega)-\lambda_f} - \left(\underline{p}_{\mathrm{Re},f}^{T} - j\underline{p}_{\mathrm{Im},f}^{T}\right)\frac{\underline{\hat{u}}(k\Delta\omega)}{(jk\Delta\omega)-\lambda_f^{*}}\right)\underline{\psi}_f\end{array}\right] + \\ \displaystyle\sum_{f\in I_f}\left[\begin{array}{l}\left(\frac{e^{-jk\Delta\omega T}}{(jk\Delta\omega)-\lambda_f} + \frac{e^{-jk\Delta\omega T}}{(jk\Delta\omega)-\lambda_f^{*}}\right)\left(n_{\mathrm{Re},f}^{r} + jn_{\mathrm{Im},f}^{r}\right)\underline{\phi}_f + \\ j\left(\frac{e^{-jk\Delta\omega T}}{(jk\Delta\omega)-\lambda_f} - \frac{e^{-jk\Delta\omega T}}{(jk\Delta\omega)-\lambda_f^{*}}\right)\left(n_{\mathrm{Re},f}^{r} + jn_{\mathrm{Im},f}^{r}\right)\underline{\psi}_f\end{array}\right] - \\ \displaystyle\sum_{f\in I_f}\left[\begin{array}{l}\left(\frac{1}{(jk\Delta\omega)-\lambda_f} + \frac{1}{(jk\Delta\omega)-\lambda_f^{*}}\right)\left(n_{\mathrm{Re},f}^{0} + jn_{\mathrm{Im},f}^{0}\right)\underline{\phi}_f + \\ j\left(\frac{1}{(jk\Delta\omega)-\lambda_f} - \frac{1}{(jk\Delta\omega)-\lambda_f^{*}}\right)\left(n_{\mathrm{Re},f}^{0} + jn_{\mathrm{Im},f}^{0}\right)\underline{\psi}_f\end{array}\right]\end{array}\right) \tag{4.112}$$

is the constant vector of the measured response minus the response vector that is predicted from the modal model considering only the fixed modes.

Summarizing, the response is completely described by the real parameter set $\underline{\theta}$ that contains the real part $\underline{\phi}_r \in \mathbb{R}^{N_{out}}$ and the imaginary part $\underline{\psi}_r \in \mathbb{R}^{N_{out}}$ of the complex modeshapes $\underline{u}_r \in C^{N_{out}\times 1}$, the real part $\underline{p}_{\mathrm{Re},r}^{T} \in \mathbb{R}^{N_{in}}$ and the imaginary part $\underline{p}_{\mathrm{Im},r}^{T} \in \mathbb{R}^{N_{in}}$ of the modal participation factor vectors $\underline{l}_r^{T} \in C^{1\times N_{in}}$, the real part $n_{\mathrm{Re},r}^{0}$ and the imaginary part $n_{\mathrm{Im},r}^{0}$ of the



Institutional Repository - Library & Information Centre - University of Thessaly
24/04/2024 00:02:26 EEST - 3.141.244.201

initial conditions $\xi_r(0)$, the real part $n^{\tau}_{\mathrm{Re},r}$ and the imaginary part $n^{\tau}_{\mathrm{Im},r}$ of the initial conditions $\xi_r(T)$, and the entries of the real matrix $D_c \in \mathbb{R}^{N_{out}\times N_{in}}$, that is,

$$\underline{\theta} = \left\{ \underline{\phi}_r,\ \underline{\psi}_r,\ \underline{p}^T_{\mathrm{Re},r},\ \underline{p}^T_{\mathrm{Im},r},\ n^0_{\mathrm{Re},r},\ n^0_{\mathrm{Im},r},\ n^{\tau}_{\mathrm{Re},r}, n^{\tau}_{\mathrm{Im},r}, r=1,\ldots,m,\ D_c \right\} \tag{4.113}$$

where $m$ is the number of contributing modes which is also an unknown in the identification process. The total number of model parameter involved in the prediction of the response at $N_{out}$ DOFs given $m$ modes and $N_{in}$ base input time histories, is $\left[4m + 2\left(m\times N_{in}\right) + 2\left(N_{out}\times m\right) + \left(N_{out}\times N_{in}\right)\right]$.

It should be noted that the parameters $\alpha_r$ and $b_r$ that relate the modal frequencies $\omega_r$ and the modal damping ratios $\zeta_r$ are excluded during the optimization process because their optimal values are obtained either from Step1 (Stabilization Diagrams) or Step 2A.

### 4.6.1 Simplifications Explaining Quadratic Dependence on Modal Characteristics

The minimization of the objective function (4.67) can be carried out efficiently, significantly reducing computational cost, by recognizing that the error function in (4.67) is quadratic with respect to the real part $\underline{\phi}_r$ and the imaginary part $\underline{\psi}_r$ of the complex modeshapes $\underline{u}_r$, and the elements in the real matrix $D_c$. This observation is used to develop explicit expressions that relate the parameters $\underline{\phi}_r$, $\underline{\psi}_r$ and $D_c$ to the rest of the model parameters appearing in the parameter set $\underline{\theta}$, such as the real part $\underline{p}^T_{\mathrm{Re},r}$ and the imaginary part $\underline{p}^T_{\mathrm{Im},r}$ of the complex participation factor $\underline{l}^{\mathrm{T}}_r$, the real part $n^0_{\mathrm{Re},r}$ and the imaginary part $n^0_{\mathrm{Im},r}$ of the initial conditions $\xi_r(0)$ and the real part $n^{\tau}_{\mathrm{Re},r}$ and the imaginary part $n^{\tau}_{\mathrm{Im},r}$ of the initial conditions $\xi_r(T)$.

For this the parameter set $\underline{\theta}$ in (4.113) is partitioned into parameters sets as follows

$$\underline{\theta} = \left(\underline{\theta}^a, \underline{\theta}^b\right) \tag{4.114}$$

where $\underline{\theta}^b$ is defined by

$$\underline{\theta}^b = \left(\ \underline{\phi}_r,\ \underline{\psi}_r,\ r=1,\ldots,m,\ D_c\right) \tag{4.115}$$

and $\underline{\theta}^a$ is defined by

$$\underline{\theta}^a = \left(\underline{p}^T_{\mathrm{Re},r},\ \underline{p}^T_{\mathrm{Im},r},\ n^0_{\mathrm{Re},r},\ n^0_{\mathrm{Im},r},\ n^{\tau}_{\mathrm{Re},r},\ n^{\tau}_{\mathrm{Im},r},\ r=1,\ldots,m\ \right) \tag{4.116}$$



Institutional Repository - Library & Information Centre - University of Thessaly
24/04/2024 00:02:26 EEST - 3.141.244.201

Stationary conditions with respect to the parameters in the set $\underline{\theta}^b$ are used to develop a linear system of equations for solving for the set $\underline{\theta}^b$ given the values of the parameters set $\underline{\theta}^a$.

For convenience in the presentation this linear system can be formulated in the general form

$$\mathrm{A}\left(\underline{\theta}^{\alpha}\right)\underline{\theta}^{b} = \underline{b}\left(\underline{\theta}^{\alpha}\right) \tag{4.117}$$

where $\mathrm{A}\left(\underline{\theta}^{\alpha}\right)$ and $\underline{b}\left(\underline{\theta}^{\alpha}\right)$ are functions of the parameter set $\underline{\theta}^a$. Let

$$\underline{\theta}^{b} = \underline{\theta}^{b}\left(\underline{\theta}^{a}\right) \tag{4.118}$$

be the function that gives the relationship between the parameters set $\underline{\theta}^b$ and the parameter set $\underline{\theta}^a$ by solving the system (4.117). Then the objective function $J\left(\underline{\theta}\right)$ takes the form

$$J\left(\underline{\theta}\right) = J\left(\underline{\theta}^{a}, \underline{\theta}^{b}\right) = J\left(\underline{\theta}^{a}, \underline{\theta}^{b}\left(\underline{\theta}^{a}\right)\right) \equiv J^{*}\left(\underline{\theta}^{a}\right) \tag{4.119}$$

Hence the minimization problem can be stated as follows. Find the values of the parameter set $\underline{\theta}^a$ that minimize the objective function

$$J^{*}\left(\underline{\theta}\right) = J\left(\underline{\theta}^{a}, \underline{\theta}^{b}\left(\underline{\theta}^{a}\right)\right) \tag{4.120}$$

Once the values of $\underline{\theta}^a$ have been found, the values of $\underline{\theta}^b$ are obtained solving the linear system (4.117). Next our objective is to apply the above concept and first obtain the matrices and vectors that completely define the linear system (4.117).

The linear system for the parameter set $\underline{\theta}^b$ is obtained by setting the derivatives of $J\left(\underline{\theta}\right)$ with respect to each element of $\underline{\theta}^b$ equal to zero, that is,

$$\frac{\partial J\left(\underline{\theta}\right)}{\partial \phi_{lr}} = 0 \tag{4.121}$$

$$\frac{\partial J\left(\underline{\theta}\right)}{\partial \psi_{lr}} = 0 \tag{4.122}$$

$$\frac{\partial J\left(\underline{\theta}\right)}{\partial D_{c,li}} = 0 \tag{4.123}$$

for $l = 1, \ldots, N_{out}$, $r = 1, \ldots, m$ and $i = 1, \ldots, N_{in}$. The analytical computation of these derivatives is shown in the appendices. It can be readily shown that the set of linear algebraic equations can be written in the compact matrix form:



Institutional Repository - Library & Information Centre - University of Thessaly
24/04/2024 00:02:26 EEST - 3.141.244.201

$$\left[\sum_{k=1}^{N}\left(AA\left(\underline{\theta}^{a}\right)+AA^{*T}\left(\underline{\theta}^{a}\right)\right)\right]X=\left[\sum_{k=1}^{N}\left(BB\left(\underline{\theta}^{a}\right)+BB^{*T}\left(\underline{\theta}^{a}\right)\right)\right] \tag{4.124}$$

where

$$AA\left(\underline{\theta}^{a}\right)=\begin{bmatrix}\underline{A}(\omega_k)\left[\underline{term}_1^T+\underline{term}_2^T+\underline{term}_3^T-\underline{term}_5^T\right] & \underline{A}(\omega_k)\left[j\left(\underline{term}_1^T-\underline{term}_2^T\right)+j\underline{term}_4^T-\underline{term}_6^T\right] & \underline{A}(\omega_k)\hat{\underline{u}}^T(\omega_k)\\ \underline{B}(\omega_k)\left[\underline{term}_1^T+\underline{term}_2^T+\underline{term}_3^T-\underline{term}_5^T\right] & \underline{B}(\omega_k)\left[j\left(\underline{term}_1^T-\underline{term}_2^T\right)+j\underline{term}_4^T-\underline{term}_6^T\right] & \underline{B}(\omega_k)\hat{\underline{u}}^T(\omega_k)\\ \hat{\underline{u}}^*(\omega_k)\left[\underline{term}_1^T+\underline{term}_2^T+\underline{term}_3^T-\underline{term}_5^T\right] & \hat{\underline{u}}^*(\omega_k)\left[j\left(\underline{term}_1^T-\underline{term}_2^T\right)+j\underline{term}_4^T-\underline{term}_6^T\right] & \hat{\underline{u}}^*(\omega_k)\hat{\underline{u}}^T(\omega_k)\end{bmatrix} \tag{4.125}$$

$$BB\left(\underline{\theta}^{a}\right)=\begin{bmatrix}\underline{A}(\omega_k)\hat{\underline{e}}^T(\omega_k)\\ \underline{B}(\omega_k)\hat{\underline{e}}^T(\omega_k)\\ \hat{\underline{u}}^*(\omega_k)\hat{\underline{e}}^T(\omega_k)\end{bmatrix} \tag{4.126}$$

$$X=\begin{Bmatrix}\underline{\phi}^T\\ \underline{\psi}^T\\ D_c^T\end{Bmatrix}\in\mathbb{R}^{(2m+N_{in})\times N_{out}} \tag{4.127}$$

and $\omega_k=k\Delta\omega$, $k=1,\ldots,N$. The system of equations (4.124) can be expressed in the form

$$\mathrm{Re}\left\{\sum_{k=1}^{N}\left(AA\left(\underline{\theta}^{a}\right)\right)\right\}X=\mathrm{Re}\left\{\sum_{k=1}^{N}\left(BB\left(\underline{\theta}^{a}\right)\right)\right\} \tag{4.128}$$

where

$$\underline{A}(\omega_k)=\begin{Bmatrix}\left[\left(\frac{1}{\left((j\omega_k)-\lambda_1^*\right)^*}\right)\left(\hat{\underline{u}}^{*T}(\omega_k)\underline{l}_1^*+e^{j\omega_k T}\xi_1^*(\mathrm{T})-\xi_1^*(0)\right)+\right.\\ \left.\left(\frac{1}{\left((j\omega_k)-\lambda_1^*\right)^*}\right)\left(\hat{\underline{u}}^{*T}(\omega_k)\underline{l}_1+e^{j\omega_k T}\xi_1^*(\mathrm{T})-\xi_1^*(0)\right)\right]\\ \vdots\\ \left[\left(\frac{1}{\left((j\omega_k)-\lambda_m^*\right)^*}\right)\left(\hat{\underline{u}}^{*T}(\omega_k)\underline{l}_m^*+e^{j\omega_k T}\xi_m^*(\mathrm{T})-\xi_m^*(0)\right)+\right.\\ \left.\left(\frac{1}{\left((j\omega_k)-\lambda_m^*\right)^*}\right)\left(\hat{\underline{u}}^{*T}(\omega_k)\underline{l}_m+e^{j\omega_k T}\xi_m^*(\mathrm{T})-\xi_m^*(0)\right)\right]\end{Bmatrix} \tag{4.129}$$



Institutional Repository - Library & Information Centre - University of Thessaly
24/04/2024 00:02:26 EEST - 3.141.244.201

$$\underline{B}(\omega_k)=\begin{Bmatrix}\left[\left(\frac{-j}{(j\omega_k)-\lambda_1^*}\right)\left(\underline{\hat{u}}^{*T}(\omega_k)\underline{l}_1^*+e^{j\omega_k T}\xi_1^*(\mathrm{T})-\xi_1^*(0)\right)+\right.\\ \left.\left[\left(\frac{j}{\left((j\omega_k)-\lambda_1^*\right)^*}\right)\left(\underline{\hat{u}}^{*T}(\omega_k)\underline{l}_1+e^{j\omega_k T}\xi_1^*(\mathrm{T})-\xi_1^*(0)\right)\right.\right.\\ \vdots\\ \left.\left[\left(\frac{-j}{(j\omega_k)-\lambda_m^*}\right)\left(\underline{\hat{u}}^{*T}(\omega_k)\underline{l}_m^*+e^{j\omega_k T}\xi_m^*(\mathrm{T})-\xi_m^*(0)\right)+\right.\right.\\ \left.\left.\left[\left(\frac{j}{\left((j\omega_k)-\lambda_m^*\right)^*}\right)\left(\underline{\hat{u}}^{*T}(\omega_k)\underline{l}_m+e^{j\omega_k T}\xi_m^*(\mathrm{T})-\xi_m^*(0)\right)\right.\right.\end{Bmatrix} \tag{4.130}$$

$$\underline{term}_1^T\equiv\left[\frac{\underline{l}_1^T\underline{\hat{u}}(\omega_k)}{(j\omega_k)-\lambda_1}\quad\cdots\quad\frac{\underline{l}_m^T\underline{\hat{u}}(\omega_k)}{(j\omega_k)-\lambda_m}\right] \tag{4.131}$$

$$\underline{term}_2^T=\left[\frac{\underline{l}_1^{*T}\underline{\hat{u}}(\omega_k)}{(j\omega_k)-\lambda_1^*}\quad\cdots\quad\frac{\underline{l}_m^{*T}\underline{\hat{u}}(\omega_k)}{(j\omega_k)-\lambda_m^*}\right] \tag{4.132}$$

$$\underline{term}_3^T=\left[\left(\frac{e^{-j\omega_k T}}{(j\omega_k)-\lambda_1}+\frac{e^{-j\omega_k T}}{(j\omega_k)-\lambda_1^*}\right)\xi_1(\mathrm{T})\quad\cdots\quad\left(\frac{e^{-j\omega_k T}}{(j\omega_k)-\lambda_m}+\frac{e^{-j\omega_k T}}{(j\omega_k)-\lambda_m^*}\right)\xi_m(\mathrm{T})\right] \tag{4.133}$$

$$\underline{term}_4^T=\left[\left(\frac{e^{-j\omega_k T}}{(j\omega_k)-\lambda_1}-\frac{e^{-j\omega_k T}}{(j\omega_k)-\lambda_r^*}\right)\xi_1(\mathrm{T})\quad\cdots\quad\left(\frac{e^{-j\omega_k T}}{(j\omega_k)-\lambda_m}-\frac{e^{-j\omega_k T}}{(j\omega_k)-\lambda_m^*}\right)\xi_m(\mathrm{T})\right] \tag{4.134}$$

$$\underline{term}_5^T=\left[\left(\frac{1}{(j\omega_k)-\lambda_1}+\frac{1}{(j\omega_k)-\lambda_1^*}\right)\xi_1(0)\quad\cdots\quad\left(\frac{1}{(j\omega_k)-\lambda_m}+\frac{1}{(j\omega_k)-\lambda_m^*}\right)\xi_m(0)\right] \tag{4.135}$$

$$\underline{term}_6^T=\left[\left(\frac{1}{(j\omega_k)-\lambda_1}-\frac{1}{(j\omega_k)-\lambda_1^*}\right)\xi_1(0)\quad\cdots\quad\left(\frac{1}{(j\omega_k)-\lambda_m}-\frac{1}{(j\omega_k)-\lambda_m^*}\right)\xi_m(0)\right] \tag{4.136}$$

From (4.128) we obtain the real part $\underline{\phi}_r$ and the imaginary part $\underline{\psi}_r$ of the complex modeshapes. Substituting (4.107) in (4.111), the error function $J^*\left(\underline{\theta}^a\right)$ becomes

$$J^*\left(\underline{\theta}^a\right)=\frac{1}{V}\sum_{k=0}^{N}\left[\underline{x}^r\left(k\Delta\omega;\underline{\theta}^a\right)-\underline{\hat{e}}\left(k\Delta\omega\right)\right]^T\left[\underline{x}^r\left(k\Delta\omega;\underline{\theta}^a\right)-\underline{\hat{e}}\left(k\Delta\omega\right)\right] \tag{4.137}$$

where



Institutional Repository - Library & Information Centre - University of Thessaly
24/04/2024 00:02:26 EEST - 3.141.244.201

$$\underline{x}^r\left(k\Delta\omega;\underline{\theta}_a\right)=\sum_{r\in I_u}\left[\begin{array}{l}\left(\left(\underline{p}_{\mathrm{Re},r}^T+j\underline{p}_{\mathrm{Im},r}^T\right)\dfrac{\hat{\underline{u}}(k\Delta\omega)}{(jk\Delta\omega)-\lambda_r}+\left(\underline{p}_{\mathrm{Re},r}^T-j\underline{p}_{\mathrm{Im},r}^T\right)\dfrac{\hat{\underline{u}}(k\Delta\omega)}{(jk\Delta\omega)-\lambda_r^*}\right)\underline{\phi}_r+\\ j\left(\left(\underline{p}_{\mathrm{Re},r}^T+j\underline{p}_{\mathrm{Im},r}^T\right)\dfrac{\hat{\underline{u}}(k\Delta\omega)}{(jk\Delta\omega)-\lambda_r}-\left(\underline{p}_{\mathrm{Re},r}^T-j\underline{p}_{\mathrm{Im},r}^T\right)\dfrac{\hat{\underline{u}}(k\Delta\omega)}{(jk\Delta\omega)-\lambda_r^*}\right)\underline{\psi}_r\end{array}\right]+$$
$$\sum_{r\in I_u}\left[\begin{array}{l}\left(\dfrac{e^{-jk\Delta\omega T}}{(jk\Delta\omega)-\lambda_r}+\dfrac{e^{-jk\Delta\omega T}}{(jk\Delta\omega)-\lambda_r^*}\right)\left(n_{\mathrm{Re},r}^\tau+jn_{\mathrm{Im},r}^\tau\right)\underline{\phi}_r+\\ j\left(\dfrac{e^{-jk\Delta\omega T}}{(jk\Delta\omega)-\lambda_r}-\dfrac{e^{-jk\Delta\omega T}}{(jk\Delta\omega)-\lambda_r^*}\right)\left(n_{\mathrm{Re},r}^\tau+jn_{\mathrm{Im},r}^\tau\right)\underline{\psi}_r\end{array}\right]- \tag{4.138}$$
$$\sum_{r\in I_u}\left[\begin{array}{l}\left(\dfrac{1}{(jk\Delta\omega)-\lambda_r}+\dfrac{1}{(jk\Delta\omega)-\lambda_r^*}\right)\left(n_{\mathrm{Re},r}^0+jn_{\mathrm{Im},r}^0\right)\underline{\phi}_r+\\ j\left(\dfrac{1}{(jk\Delta\omega)-\lambda_r}-\dfrac{1}{(jk\Delta\omega)-\lambda_r^*}\right)\left(n_{\mathrm{Re},r}^0+jn_{\mathrm{Im},r}^0\right)\underline{\psi}_r\end{array}\right]+D_c\hat{\underline{u}}(k\Delta\omega)$$

The total number of model parameter involved in the prediction of the response at $N_{out}$ DOFs given $m$ modes and $N_{in}$ input time histories, is now reduced from $\left[4m+2\left(m\times N_{in}\right)+2\left(N_{out}\times m\right)+\left(N_{out}\times N_{in}\right)\right]$ to $\left[4m+2\left(m\times N_{in}\right)\right]$.

### 4.6.2 Analytical Expression of the Gradient of the Objective function

Next, analytically expressions for the gradients and the objective function (4.137) with respect to each parameter in the set $\underline{\theta}^a$ are defined. Differentiating $J^*\left(\underline{\theta}^a\right)$ with respect to a parameter $\theta$ in the parameter set $\underline{\theta}^a$ yields

$$\frac{\partial J^*\left(\underline{\theta}^a\right)}{\partial\theta}=\frac{1}{V}\sum_{k=0}^{N}\left\{\frac{\partial\underline{x}^{r*T}\left(k\Delta\omega;\underline{\theta}^a\right)}{\partial\theta}\left[\underline{x}^r\left(k\Delta\omega;\underline{\theta}^a\right)-\hat{\underline{e}}\left(k\Delta\omega\right)\right]+CT\right\} \tag{4.139}$$

where



Institutional Repository - Library & Information Centre - University of Thessaly
24/04/2024 00:02:26 EEST - 3.141.244.201

$$\frac{\partial \underline{x}^{r*T}\left(k\Delta\omega;\underline{\theta}^{a}\right)}{\partial p_{\mathrm{Re},ri}} = \hat{u}_i^{*}(k\Delta\omega)\underline{\phi}_r^{*T}\left(\frac{1}{\left((jk\Delta\omega)-\lambda_r\right)^{*}}+\frac{1}{\left((jk\Delta\omega)-\lambda_r^{*}\right)^{*}}\right)+$$
$$\frac{\partial \underline{\phi}_r^{*T}}{\partial p_{\mathrm{Re},ri}}\left[\frac{\hat{u}_i^{*}(k\Delta\omega)l_{ri}^{*}}{\left((jk\Delta\omega)-\lambda_r\right)^{*}}+\frac{\hat{u}_i^{*}(k\Delta\omega)l_{ri}}{\left((jk\Delta\omega)-\lambda_r\right)^{*}}\right]+$$
$$\hat{u}_i^{*}(k\Delta\omega)\underline{\psi}_r^{*T}\left(\frac{1}{\left((jk\Delta\omega)-\lambda_r\right)^{*}}-\frac{1}{\left((jk\Delta\omega)-\lambda_r^{*}\right)^{*}}\right)+ \tag{4.140}$$
$$\frac{\partial \underline{\psi}_r^{*T}}{\partial p_{\mathrm{Re},ri}}\left[\frac{\hat{u}_i^{*}(k\Delta\omega)l_{ri}^{*}}{\left((jk\Delta\omega)-\lambda_r\right)^{*}}-\frac{\hat{u}_i^{*}(k\Delta\omega)l_{ri}}{\left((jk\Delta\omega)-\lambda_r\right)^{*}}\right]+\hat{u}_i^{*}(k\Delta\omega)\frac{\partial D_c^{T}}{\partial p_{\mathrm{Re},ri}}$$

$$\frac{\partial \underline{x}^{r*T}\left(k\Delta\omega;\underline{\theta}^{a}\right)}{\partial p_{\mathrm{Im},ri}} = -\hat{u}_i^{*}(k\Delta\omega)\underline{\phi}_r^{*T}j\left(\frac{1}{\left((jk\Delta\omega)-\lambda_r\right)^{*}}-\frac{1}{\left((jk\Delta\omega)-\lambda_r^{*}\right)^{*}}\right)+$$
$$\frac{\partial \underline{\phi}_r^{*T}}{\partial p_{\mathrm{Re},ri}}\left[\frac{\hat{u}_i^{*}(k\Delta\omega)l_{ri}^{*}}{\left((jk\Delta\omega)-\lambda_r\right)^{*}}+\frac{\hat{u}_i^{*}(k\Delta\omega)l_{ri}}{\left((jk\Delta\omega)-\lambda_r\right)^{*}}\right]-$$
$$\hat{u}_i^{*}(\omega_k)\underline{\psi}_r^{*T}j\left(\frac{1}{\left((jk\Delta\omega)-\lambda_r\right)^{*}}-\frac{1}{\left((jk\Delta\omega)-\lambda_r^{*}\right)^{*}}\right)+ \tag{4.141}$$
$$\frac{\partial \underline{\psi}_r^{*T}}{\partial p_{\mathrm{Re},ri}}\left[\frac{\hat{u}_i^{*}(k\Delta\omega)l_{ri}^{*}}{\left((jk\Delta\omega)-\lambda_r\right)^{*}}-\frac{\hat{u}_i^{*}(k\Delta\omega)l_{ri}}{\left((jk\Delta\omega)-\lambda_r\right)^{*}}\right]+\hat{u}_i^{*}(k\Delta\omega)\frac{\partial D_c^{T}}{\partial p_{\mathrm{Im},ri}}$$

$$\frac{\partial \underline{x}^{r*T}\left(k\Delta\omega;\underline{\theta}^{a}\right)}{\partial n_{\mathrm{Re},r}} = -\left(\frac{1}{\left((jk\Delta\omega)-\lambda_r\right)^{*}}+\frac{1}{\left((jk\Delta\omega)-\lambda_r^{*}\right)^{*}}\right)\underline{\phi}_r^{*T}-$$
$$\left(\frac{1}{\left((jk\Delta\omega)-\lambda_r\right)^{*}}+\frac{1}{\left((jk\Delta\omega)-\lambda_r^{*}\right)^{*}}\right)\xi_r^{*}(0)\frac{\partial \underline{\phi}_r^{*T}}{\partial n_{\mathrm{Re},r}}-$$
$$\left(\left(\frac{j}{(jk\Delta\omega)-\lambda_r}\right)^{*}-\left(\frac{j}{(jk\Delta\omega)-\lambda_r^{*}}\right)^{*}\right)\underline{\psi}_r^{*T}- \tag{4.142}$$
$$\left(\left(\frac{j}{(jk\Delta\omega)-\lambda_r}\right)^{*}-\left(\frac{j}{(jk\Delta\omega)-\lambda_r^{*}}\right)^{*}\right)\xi_r^{*}(0)\frac{\partial \underline{\psi}_r^{*T}}{\partial n_{\mathrm{Re},r}}+$$
$$\underline{\hat{u}}^{*}(k\Delta\omega)\frac{\partial D_c^{T}}{\partial n_{\mathrm{Re},r}}$$



Institutional Repository - Library & Information Centre - University of Thessaly
24/04/2024 00:02:26 EEST - 3.141.244.201

$$\frac{\partial \underline{x}^{r*T}\left(k\Delta\omega;\underline{\theta}^{a}\right)}{\partial n_{\mathrm{Im},r}} = j\left(\frac{1}{\left((jk\Delta\omega)-\lambda_r\right)^{*}}+\frac{1}{\left((jk\Delta\omega)-\lambda_r^{*}\right)^{*}}\right)\underline{\phi}_r^{*T} -$$
$$\left(\frac{1}{\left((jk\Delta\omega)-\lambda_r\right)^{*}}+\frac{1}{\left((jk\Delta\omega)-\lambda_r^{*}\right)^{*}}\right)\xi_r^{*}(0)\frac{\partial \underline{\phi}_r^{*T}}{\partial n_{\mathrm{Im},r}}+$$
$$\left(\left(\frac{1}{(jk\Delta\omega)-\lambda_r}\right)^{*}-\left(\frac{1}{(jk\Delta\omega)-\lambda_r^{*}}\right)^{*}\right)\underline{\psi}_r^{*T} - \qquad (4.143)$$
$$\left(\left(\frac{j}{(jk\Delta\omega)-\lambda_r}\right)^{*}-\left(\frac{j}{(jk\Delta\omega)-\lambda_r^{*}}\right)^{*}\right)\xi_r^{*}(0)\frac{\partial \underline{\psi}_r^{*T}}{\partial n_{\mathrm{Im},r}}+$$
$$\underline{\hat{u}}^{*}(k\Delta\omega)\frac{\partial D_c^{T}}{\partial n_{\mathrm{Im},r}}$$

$$\frac{\partial \underline{x}^{r*T}\left(k\Delta\omega;\underline{\theta}^{a}\right)}{\partial n_{\mathrm{Re},r}^{\tau}} = \left(\frac{e^{jk\Delta\omega\mathrm{T}}}{\left((jk\Delta\omega)-\lambda_r\right)^{*}}+\frac{e^{jk\Delta\omega\mathrm{T}}}{\left((jk\Delta\omega)-\lambda_r^{*}\right)^{*}}\right)\underline{\phi}_r^{*T} +$$
$$\left(\frac{e^{jk\Delta\omega\mathrm{T}}}{\left((jk\Delta\omega)-\lambda_r\right)^{*}}+\frac{e^{jk\Delta\omega\mathrm{T}}}{\left((jk\Delta\omega)-\lambda_r^{*}\right)^{*}}\right)\xi_r^{*}(\mathrm{T})\frac{\partial \underline{\phi}_r^{*T}}{\partial n_{\mathrm{Re},r}^{\tau}} -$$
$$j\left(\frac{e^{jk\Delta\omega\mathrm{T}}}{\left((jk\Delta\omega)-\lambda_r\right)^{*}}-\frac{e^{jk\Delta\omega\mathrm{T}}}{\left((jk\Delta\omega)-\lambda_r^{*}\right)^{*}}\right)\underline{\psi}_r^{*T} - \qquad (4.144)$$
$$j\left(\frac{e^{jk\Delta\omega\mathrm{T}}}{\left((jk\Delta\omega)-\lambda_r\right)^{*}}-\frac{e^{jk\Delta\omega\mathrm{T}}}{\left((jk\Delta\omega)-\lambda_r^{*}\right)^{*}}\right)\xi_r^{*}(\mathrm{T})\frac{\partial \underline{\psi}_r^{*T}}{\partial n_{\mathrm{Re},r}^{\tau}}+$$
$$\underline{\hat{u}}^{*}(k\Delta\omega)\frac{\partial D_c^{\mathrm{T}}}{\partial n_{\mathrm{Re},r}^{\tau}}$$



Institutional Repository - Library & Information Centre - University of Thessaly
24/04/2024 00:02:26 EEST - 3.141.244.201

$$\frac{\partial \underline{x}^{r*T}\left(k\Delta\omega;\underline{\theta}^{a}\right)}{\partial n_{\mathrm{lm},r}^{\tau}} = -j\left(\frac{e^{jk\Delta\omega \mathrm{T}}}{\left((jk\Delta\omega)-\lambda_r\right)^{*}}+\frac{e^{jk\Delta\omega \mathrm{T}}}{\left((jk\Delta\omega)-\lambda_r^{*}\right)^{*}}\right)\underline{\phi}_r^{*T}+$$
$$\left(\frac{e^{jk\Delta\omega \mathrm{T}}}{\left((jk\Delta\omega)-\lambda_r\right)^{*}}+\frac{e^{jk\Delta\omega \mathrm{T}}}{\left((jk\Delta\omega)-\lambda_r^{*}\right)^{*}}\right)\xi_r^{*}(\mathrm{T})\frac{\partial \underline{\phi}_r^{*T}}{\partial n_{\mathrm{lm},r}^{\tau}}-$$
$$\left(\frac{e^{jk\Delta\omega \mathrm{T}}}{\left((jk\Delta\omega)-\lambda_r\right)^{*}}-\frac{e^{jk\Delta\omega \mathrm{T}}}{\left((jk\Delta\omega)-\lambda_r^{*}\right)^{*}}\right)\underline{\psi}_r^{*T}- \qquad (4.145)$$
$$j\left(\frac{e^{jk\Delta\omega \mathrm{T}}}{\left((jk\Delta\omega)-\lambda_r\right)^{*}}-\frac{e^{jk\Delta\omega \mathrm{T}}}{\left((jk\Delta\omega)-\lambda_r^{*}\right)^{*}}\right)\xi_r^{*}(\mathrm{T})\frac{\partial \underline{\psi}_r^{*T}}{\partial n_{\mathrm{lm},r}^{\tau}}+$$
$$\hat{\underline{u}}^{*}(k\Delta\omega)\frac{\partial D_c^{T}}{\partial n_{\mathrm{lm},r}^{\tau}}$$

Note that the derivatives $\partial\underline{\phi}_r^{*T}/\partial\theta$, $\partial\underline{\psi}_r^{*T}/\partial\theta$ and $\partial D_c^{T}/\partial\theta$ are readily obtained by differentiating with respect to $\theta$ both sides of the system of linear equations (4.128). This yields the following system of linear equation for the derivatives

$$\mathrm{Re}\left\{\sum_{k=1}^{N}A\left(\underline{\theta}^{a}\right)\right\}\frac{\partial X}{\partial\theta}=\mathrm{Re}\left\{\frac{\sum_{k=1}^{N}\partial\left(BB\left(\underline{\theta}^{a}\right)\right)}{\partial\theta}\right\}-\mathrm{Re}\left\{\frac{\sum_{k=1}^{N}\partial\left(AA\left(\underline{\theta}^{a}\right)\right)}{\partial\theta}\right\}X \qquad (4.146)$$

where using (4.125) and (4.126), it can be readily shown that

$$\frac{\partial\left(AA\left(\underline{\theta}^{a}\right)\right)}{\partial\theta}=$$



Institutional Repository - Library & Information Centre - University of Thessaly
24/04/2024 00:02:26 EEST - 3.141.244.201

$$\begin{bmatrix} \left(\frac{\partial \underline{A}(\omega_k)}{\partial\theta}\left[\underline{term}_1^T+\underline{term}_2^T+\underline{term}_3^T-\underline{term}_5^T\right]+ \underline{A}(\omega_k)\frac{\partial\left[\underline{term}_1^T+\underline{term}_2^T+\underline{term}_3^T-\underline{term}_5^T\right]}{\partial\theta}\right) & \left(\frac{\partial \underline{A}(\omega_k)}{\partial\theta}\left[\Im\left(\underline{term}_1^T-\underline{term}_2^T\right)+\Im\underline{term}_4^T-\underline{term}_6^T\right]+ \underline{A}(\omega_k)\frac{\partial\left[\Im\left(\underline{term}_1^T-\underline{term}_2^T\right)+\Im\underline{term}_4^T-\underline{term}_6^T\right]}{\partial\theta}\right) & \frac{\partial \underline{A}(\omega_k)}{\partial\theta}\underline{\hat{u}}^T(\omega_k) \\ \left(\frac{\partial \underline{B}(\omega_k)}{\partial\theta}\left[\underline{term}_1^T+\underline{term}_2^T+\underline{term}_3^T-\underline{term}_5^T\right]+ \underline{B}(\omega_k)\frac{\partial\left[\underline{term}_1^T+\underline{term}_2^T+\underline{term}_3^T-\underline{term}_5^T\right]}{\partial\theta}\right) & \left(\frac{\partial \underline{B}(\omega_k)}{\partial\theta}\left[\Im\left(\underline{term}_1^T-\underline{term}_2^T\right)+\Im\underline{term}_4^T-\underline{term}_6^T\right]+ \underline{B}(\omega_k)\frac{\partial\left[\Im\left(\underline{term}_1^T-\underline{term}_2^T\right)+\Im\underline{term}_4^T-\underline{term}_6^T\right]}{\partial\theta}\right) & \frac{\partial \underline{B}(\omega_k)}{\partial\theta}\underline{\hat{u}}^T(\omega_k) \\ \underline{\hat{u}}^*(\omega_k)\frac{\partial\left[\underline{term}_1^T+\underline{term}_2^T+\underline{term}_3^T-\underline{term}_5^T\right]}{\partial\theta} & \underline{\hat{u}}^*(\omega_k)\frac{\partial\left[\Im\left(\underline{term}_1^T-\underline{term}_2^T\right)+\Im\underline{term}_4^T-\underline{term}_6^T\right]}{\partial\theta} & 0 \end{bmatrix} \tag{4.147}$$

$$\frac{\partial(BB)}{\partial\theta}=\sum_{k=1}^{N}\begin{bmatrix} \frac{\partial \underline{A}(\omega_k)}{\partial\theta}\underline{\hat{e}}^T(\omega_k) \\ \frac{\partial \underline{B}(\omega_k)}{\partial\theta}\underline{\hat{e}}^T(\omega_k) \\ 0 \end{bmatrix} \tag{4.148}$$

where $\omega_k = k\Delta\omega$, $k=1,\ldots,N$, and

$$\frac{\partial \underline{A}(\omega_k)}{\partial p_{\mathrm{Re},ri}}=\left(\frac{1}{\left((j\omega_k)-\lambda_r\right)^*}+\frac{1}{\left((j\omega_k)-\lambda_r^*\right)^*}\right)\hat{u}_i^*(\omega_k) \tag{4.149}$$

$$\frac{\partial \underline{A}(\omega_k)}{\partial p_{\mathrm{Im},ri}}=j\left(-\frac{1}{\left((j\omega_k)-\lambda_r\right)^*}+\frac{1}{\left((j\omega_k)-\lambda_r^*\right)^*}\right)\hat{u}_i^*(\omega_k) \tag{4.150}$$

$$\frac{\partial \underline{A}(\omega_k)}{\partial n_{\mathrm{Re},r}}=-j\left(\frac{1}{\left((j\omega_k)-\lambda_r\right)^*}+\frac{1}{\left((j\omega_k)-\lambda_r^*\right)^*}\right) \tag{4.151}$$

$$\frac{\partial \underline{A}(\omega_k)}{\partial n_{\mathrm{Im},r}}=j\left(\frac{1}{\left((j\omega_k)-\lambda_r\right)^*}+\frac{1}{\left((j\omega_k)-\lambda_r^*\right)^*}\right) \tag{4.152}$$

$$\frac{\partial \underline{A}(\omega_k)}{\partial n_{\mathrm{Re},r}^{\tau}}=\left(\frac{1}{\left((j\omega_k)-\lambda_r\right)^*}+\frac{1}{\left((j\omega_k)-\lambda_r^*\right)^*}\right)e^{j\omega_k T} \tag{4.153}$$



Institutional Repository - Library & Information Centre - University of Thessaly
24/04/2024 00:02:26 EEST - 3.141.244.201

$$\frac{\partial \underline{A}(\omega_k)}{\partial n^{\tau}_{\mathrm{Im},r}} = -j\left(\frac{1}{\left((j\omega_k)-\lambda_r\right)^*}+\frac{1}{\left((j\omega_k)-\lambda_r^*\right)^*}\right)e^{j\omega_k T} \tag{4.154}$$

$$\frac{\partial \underline{B}(\omega_k)}{\partial p_{\mathrm{Re},ri}} = j\left(-\frac{1}{\left((j\omega_k)-\lambda_r\right)^*}+\frac{1}{\left((j\omega_k)-\lambda_r^*\right)^*}\right)\hat{u}_i^*(\omega_k) \tag{4.155}$$

$$\frac{\partial \underline{B}(\omega_k)}{\partial p_{\mathrm{Im},ri}} = \left(-\frac{1}{\left((j\omega_k)-\lambda_r\right)^*}-\frac{1}{\left((j\omega_k)-\lambda_r^*\right)^*}\right)\hat{u}_i^*(\omega_k) \tag{4.156}$$

$$\frac{\partial \underline{B}(\omega_k)}{\partial n_{\mathrm{Re},r}} = j\left(\frac{1}{\left((j\omega_k)-\lambda_r\right)^*}-\frac{1}{\left((j\omega_k)-\lambda_r^*\right)^*}\right) \tag{4.157}$$

$$\frac{\partial \underline{B}(\omega_k)}{\partial n_{\mathrm{Im},r}} = \left(\frac{1}{\left((j\omega_k)-\lambda_r\right)^*}-\frac{1}{\left((j\omega_k)-\lambda_r^*\right)^*}\right) \tag{4.158}$$

$$\frac{\partial \underline{B}(\omega_k)}{\partial n^{\tau}_{\mathrm{Re},r}} = j\left(-\frac{1}{\left((j\omega_k)-\lambda_r\right)^*}+\frac{1}{\left((j\omega_k)-\lambda_r^*\right)^*}\right)e^{j\omega_k T} \tag{4.159}$$

$$\frac{\partial \underline{B}(\omega_k)}{\partial n^{\tau}_{\mathrm{Im},r}} = \left(-\frac{1}{\left((j\omega_k)-\lambda_r\right)^*}+\frac{1}{\left((j\omega_k)-\lambda_r^*\right)^*}\right)e^{j\omega_k T} \tag{4.160}$$

$$\frac{\partial \underline{term}_1^T}{\partial p_{\mathrm{Re},ri}} = \left(\frac{1}{(j\omega_k)-\lambda_r}\right)\hat{u}_i^*(\omega_k) \tag{4.161}$$

$$\frac{\partial \underline{term}_1^T}{\partial p_{\mathrm{Im},ri}} = \left(\frac{j}{(j\omega_k)-\lambda_r}\right)\hat{u}_i^*(\omega_k) \tag{4.162}$$

$$\frac{\partial \underline{term}_2^T}{\partial p_{\mathrm{Re},ri}} = \left(\frac{1}{(j\omega_k)-\lambda_r^*}\right)\hat{u}_i^*(\omega_k) \tag{4.163}$$

$$\frac{\partial \underline{term}_2^T}{\partial p_{\mathrm{Im},ri}} = -\left(\frac{\mathfrak{I}}{(j\omega_k)-\lambda_r^*}\right)\hat{u}_i^*(\omega_k) \tag{4.164}$$



Institutional Repository - Library & Information Centre - University of Thessaly
24/04/2024 00:02:26 EEST - 3.141.244.201

$$\frac{\partial \underline{term}_3^T}{\partial n_{\mathrm{Re},r}^{\tau}} = \left( \frac{e^{-j\omega T}}{(j\omega)-\lambda_r} + \frac{e^{-j\omega T}}{(j\omega)-\lambda_r^*} \right) \tag{4.165}$$

$$\frac{\partial \underline{term}_3^T}{\partial n_{\mathrm{Im},r}^{\tau}} = j\left( \frac{e^{-j\omega T}}{(j\omega)-\lambda_r} + \frac{e^{-j\omega T}}{(j\omega)-\lambda_r^*} \right) \tag{4.166}$$

$$\frac{\partial \underline{term}_4^T}{\partial n_{\mathrm{Re},r}^{\tau}} = \left( \frac{e^{-j\omega T}}{(j\omega)-\lambda_r} - \frac{e^{-j\omega T}}{(j\omega)-\lambda_r^*} \right) \tag{4.167}$$

$$\frac{\partial \underline{term}_4^T}{\partial n_{\mathrm{Im},r}^{\tau}} = j\left( \frac{e^{-j\omega T}}{(j\omega)-\lambda_r} - \frac{e^{-j\omega T}}{(j\omega)-\lambda_r^*} \right) \tag{4.168}$$

$$\frac{\partial \underline{term}_5^T}{\partial n_{\mathrm{Re},r}} = \left( \frac{1}{(j\omega)-\lambda_r} + \frac{1}{(j\omega)-\lambda_r^*} \right) \tag{4.169}$$

$$\frac{\partial \underline{term}_5^T}{\partial n_{\mathrm{Im},r}} = j\left( \frac{1}{(j\omega)-\lambda_r} + \frac{1}{(j\omega)-\lambda_r^*} \right) \tag{4.170}$$

$$\frac{\partial \underline{term}_6^T}{\partial p_{\mathrm{Re},ri}} = \left( \frac{1}{(j\omega_k)-\lambda_r} \right) \hat{u}_i^*(\omega_k) \tag{4.171}$$

$$\frac{\partial \underline{term}_6^T}{\partial p_{\mathrm{Im},ri}} = \left( \frac{j}{(j\omega_k)-\lambda_r^*} \right) \hat{u}_i^*(\omega_k) \tag{4.172}$$

$$\frac{\partial \underline{term}_6^T}{\partial n_{\mathrm{Re},r}} = \left( \frac{1}{(j\omega)-\lambda_r} - \frac{1}{(j\omega)-\lambda_r^*} \right) \tag{4.173}$$

$$\frac{\partial \underline{term}_6^T}{\partial n_{\mathrm{Im},r}} = j\left( \frac{1}{(j\omega)-\lambda_r} - \frac{1}{(j\omega)-\lambda_r^*} \right) \tag{4.174}$$

The derivatives:

$$\frac{\partial \underline{term}_1^T}{\partial n_{\mathrm{Re},r}}, \frac{\partial \underline{term}_1^T}{\partial n_{\mathrm{Im},r}}, \frac{\partial \underline{term}_1^T}{\partial n_{\mathrm{Re},r}^{\tau}}, \frac{\partial \underline{term}_1^T}{\partial n_{\mathrm{Im},r}^{\tau}}, \frac{\partial \underline{term}_2^T}{\partial n_{\mathrm{Re},r}}, \frac{\partial \underline{term}_2^T}{\partial n_{\mathrm{Im},r}}, \frac{\partial \underline{term}_2^T}{\partial n_{\mathrm{Re},r}^{\tau}}, \frac{\partial \underline{term}_2^T}{\partial n_{\mathrm{Im},r}^{\tau}}, \frac{\partial \underline{term}_3^T}{\partial p_{\mathrm{Re},ri}}, \frac{\partial \underline{term}_3^T}{\partial p_{\mathrm{Im},ri}},$$
$$\frac{\partial \underline{term}_3^T}{\partial n_{\mathrm{Re},r}}, \frac{\partial \underline{term}_3^T}{\partial n_{\mathrm{Im},r}}, \frac{\partial \underline{term}_4^T}{\partial p_{\mathrm{Re},ri}}, \frac{\partial \underline{term}_4^T}{\partial p_{\mathrm{Im},ri}}, \frac{\partial \underline{term}_4^T}{\partial n_{\mathrm{Re},r}}, \frac{\partial \underline{term}_4^T}{\partial n_{\mathrm{Im},r}}, \frac{\partial \underline{term}_5^T}{\partial p_{\mathrm{Re},ri}}, \frac{\partial \underline{term}_5^T}{\partial p_{\mathrm{Im},ri}}, \frac{\partial \underline{term}_5^T}{\partial n_{\mathrm{Re},r}^{\tau}}, \frac{\partial \underline{term}_5^T}{\partial n_{\mathrm{Im},r}^{\tau}},$$
$$\frac{\partial \underline{term}_6^T}{\partial n_{\mathrm{Re},r}^{\tau}}, \frac{\partial \underline{term}_6^T}{\partial n_{\mathrm{Im},r}^{\tau}}, \text{ are equal to zero.}$$



Institutional Repository - Library & Information Centre - University of Thessaly
24/04/2024 00:02:26 EEST - 3.141.244.201

## 4.7 Third Step (Nonlinear Optimization)

In this section, the third step is presented in which the formulation of the Section 4.6 is used. In particular, the response is completely described by the real parameter set $\underline{\theta}$ that contains the real part $\underline{\phi}_r \in \mathbb{R}^{N_{out}}$ and the imaginary part $\underline{\psi}_r \in \mathbb{R}^{N_{out}}$ of the complex modeshapes $\underline{u}_r \in C^{N_{out}\times 1}$, the real part $\underline{p}^T_{\mathrm{Re},r} \in \mathbb{R}^{N_{in}}$ and the imaginary part $\underline{p}^T_{\mathrm{Im},r} \in \mathbb{R}^{N_{in}}$ of the modal participation factor vectors $\underline{l}^T_r \in C^{1\times N_{in}}$, the real part $n^0_{\mathrm{Re},r}$ and the imaginary part $n^0_{\mathrm{Im},r}$ of the initial conditions $\xi_r(0)$, the real part $n^\tau_{\mathrm{Re},r}$ and the imaginary part $n^\tau_{\mathrm{Im},r}$ of the initial conditions $\xi_r(T)$, and the entries of the real matrix $D_c \in \mathbb{R}^{N_{out}\times N_{in}}$. In addition, in the real parameter set $\underline{\theta}$ are also include the modal parameters $\alpha_r = \zeta_r\omega_r$ and $b_r = \omega_r\sqrt{1-\zeta_r^2}$ that are related to the modal frequencies $\omega_r$ and the modal damping ratios $\zeta_r$, that is

$$\underline{\theta} = \left\{\alpha_r, b_r, \underline{\phi}_r,\ \underline{\psi}_r,\ \underline{p}^T_{\mathrm{Re},r},\ \underline{p}^T_{\mathrm{Im},r},\ n^0_{\mathrm{Re},r},\ n^0_{\mathrm{Im},r},\ n^\tau_{\mathrm{Re},r},\ n^\tau_{\mathrm{Im},r}, r=1,\ldots,m,\ D_c\right\} \tag{4.175}$$

where $m$ is the number of contributing modes which is also an unknown in the identification process. The total number of model parameter involved in the prediction of the response at $N_{out}$ DOFs given $m$ modes and $N_{in}$ base input time histories, is $\left[6m + 2\left(m\times N_{in}\right) + 2\left(N_{out}\times m\right) + \left(N_{out}\times N_{in}\right)\right]$

For this the parameter set $\underline{\theta}$ in (4.175) is partitioned into parameters sets as follows

$$\underline{\theta} = \left(\underline{\theta}^a, \underline{\theta}^b\right) \tag{4.176}$$

where $\underline{\theta}^b$ is defined by

$$\underline{\theta}^b = \left(\ \underline{\phi}_r,\ \underline{\psi}_r,\ r=1,\ldots,m,\ D_c\right) \tag{4.177}$$

and $\underline{\theta}^a$ is defined by

$$\underline{\theta}^a = \left(\alpha_r,\ b_r,\ \underline{p}^T_{\mathrm{Re},r},\ \underline{p}^T_{\mathrm{Im},r},\ n^0_{\mathrm{Re},r},\ n^0_{\mathrm{Im},r},\ n^\tau_{\mathrm{Re},r},\ n^\tau_{\mathrm{Im},r},\ r=1,\ldots,m\ \right) \tag{4.178}$$

The same analysis with this in Section 4.6 is used. The nonlinear optimization process is based on the minimization of the error function $J^*\left(\underline{\theta}^a\right)$ given by (4.137) with respect to the parameter set $\underline{\theta}$ which is defined in (4.175). In particular, the parameter set $\underline{\theta}$ in (4.175) is partitioned into the two sets $\underline{\theta}^a$ and $\underline{\theta}^b$. Hence, the optimization process is based on the parameter set $\underline{\theta}^b$ using as initial conditions the optimal values of the set $\underline{\theta}^b$ resulted from the first and second approach of the second step.



Institutional Repository - Library & Information Centre - University of Thessaly
24/04/2024 00:02:26 EEST - 3.141.244.201

## 4.8 Appendix

### 4.8.1 System Of Linear Algebraic Equations (First Approach of Second Step)

Taking the stationary condition

$$\frac{1}{V}\sum_{k=0}^{N}\left\{\frac{\partial \underline{x}^{r*T}\left(k\Delta\omega;\underline{\theta}\right)}{\partial\theta}\left[\underline{x}^{r}\left(k\Delta\omega;\underline{\theta}\right)-\underline{\hat{e}}\left(k\Delta\omega\right)\right]+CT\right\}=0 \tag{4.179}$$

Thus $\dfrac{\partial \underline{x}^{r*T}\left(k\Delta\omega;\underline{\theta}\right)}{\partial\theta}$ must be evaluated

For $\theta = L_{r,li}$

$$\frac{\partial \underline{x}^{r}\left(k\Delta\omega;\underline{\theta}\right)}{\partial L_{r,li}}=\underline{\delta}_l\underline{\delta}_i^{T}\mu_r^{+}\hat{\underline{u}}(k\Delta\omega)\Rightarrow\frac{\partial \underline{x}^{r*T}\left(k\Delta\omega;\underline{\theta}\right)}{\partial L_{r,li}}=\hat{\underline{u}}^{*T}(k\Delta\omega)\underline{\delta}_l\underline{\delta}_i^{T}\left(\mu_r^{+}\right)^{*} \tag{4.180}$$

Substituting (4.180) in (4.179)yields

$$\frac{\partial J(\underline{\theta})}{\partial L_{r,li}}=0\Rightarrow$$

$$\sum_{k=0}^{N}\left\{\left(\mu_r^{+}\right)^{*}\hat{\underline{u}}^{*T}(k\Delta\omega)\underline{\delta}_i\underline{\delta}_l^{T}\left[\underline{x}^{r}\left(k\Delta\omega;\underline{\theta}\right)-\underline{\hat{e}}\left(k\Delta\omega\right)\right]+CT\right\}=0\;\Rightarrow\sum_{k=0}^{N}\left\{\left(\mu_r^{+}\right)^{*}\hat{u}_i^{*}(k\Delta\omega)\left[x_l^{r}\left(k\Delta\omega;\underline{\theta}\right)-\hat{e}_l\left(k\Delta\omega\right)\right]+CT\right\}=0\Rightarrow$$

$$\sum_{k=0}^{N}\left\{\underbrace{\left(\mu_r^{+}\right)^{*}\hat{u}_i^{*}(k\Delta\omega)}_{\left(\mu^{+}\otimes\hat{u}_i\right)^{*}}\left[\begin{array}{l}\sum_{r=1}^{m}\left[\underline{L}_{r,l}^{T}\mu_r^{+}+\underline{G}_{r,l}^{T}\mu_r^{-}\right]\hat{\underline{u}}(k\Delta\omega)+\underline{D}_{e,l}^{T}\hat{\underline{u}}(k\Delta\omega)\\ +\sum_{r=1}^{m}\left[c_{r,l}\mu_r^{+}+d_{r,l}\mu_r^{-}\right]e^{-jk\Delta\omega T}-\sum_{r=1}^{m}\left[p_{r,l}\mu_r^{+}+q_{r,l}\mu_r^{-}\right]\end{array}\right]+CT\right\}=\sum_{k=1}^{N}\left\{\left(\mu_r^{+}\right)^{*}\hat{u}_i^{*}(k\Delta\omega)\left[\hat{e}_l\left(k\Delta\omega\right)\right]+CT\right\}\Rightarrow$$

$$\sum_{k=0}^{N}\left\{\left(\underline{\mu}^{+}\otimes\hat{\underline{u}}(k\Delta\omega)\right)^{*}\left[\begin{array}{l}\underbrace{\left[\hat{\underline{u}}^{T}(k\Delta\omega)\mu_1^{+}\cdots\;\hat{\underline{u}}^{T}(k\Delta\omega)\mu_m^{+}\right]}_{\mu^{+T}\otimes\hat{u}^{T}(\omega)}\left\{\begin{array}{c}\underline{L}_{1,l}^{T}\\ \vdots\\ \underline{L}_{m,l}^{T}\end{array}\right\}+\\ \underbrace{\left[\hat{\underline{u}}^{T}(k\Delta\omega)\mu_1^{-}\cdots\;\hat{\underline{u}}^{T}(k\Delta\omega)\mu_m^{-}\right]}_{\mu^{-T}\otimes\hat{u}^{T}(\omega)}\left\{\begin{array}{c}\underline{G}_{1,l}^{T}\\ \vdots\\ \underline{G}_{m,l}^{T}\end{array}\right\}+\\ +\underline{D}_{e,l}^{T}\hat{\underline{u}}(k\Delta\omega)+\left(\underline{c}_l^{T}\underline{\mu}^{+}+\underline{d}_l^{T}\underline{\mu}^{-}\right)e^{-jn\delta T}-\left(\underline{p}_l^{T}\underline{\mu}^{+}+\underline{q}_l^{T}\underline{\mu}^{-}\right)\end{array}\right]+CT\right\}=\sum_{k=0}^{N}\left\{\left(\underline{\mu}^{+}\otimes\hat{\underline{u}}(k\Delta\omega)\right)^{*}\left[\hat{e}_l\left(k\Delta\omega\right)\right]+CT\right\}\Rightarrow \tag{4.181}$$

$$\sum_{k=0}^{N}\left\{\left(\underline{\mu}^{+}\otimes\hat{\underline{u}}(k\Delta\omega)\right)^{*}\left[\begin{array}{l}\left(\underline{\mu}^{*T}\otimes\hat{\underline{u}}^{T}(k\Delta\omega)\right)\left\{\begin{array}{c}\underline{L}_{1,l}^{T}\\ \vdots\\ \underline{L}_{m,l}^{T}\end{array}\right\}+\left(\underline{\mu}^{-T}\otimes\hat{\underline{u}}^{T}(k\Delta\omega)\right)\left\{\begin{array}{c}\underline{G}_{1,l}^{T}\\ \vdots\\ \underline{G}_{m,l}^{T}\end{array}\right\}\\ +\underline{D}_{e,l}^{T}\hat{\underline{u}}(k\Delta\omega)+\underbrace{\left[\underline{\mu}^{*T}\quad\underline{\mu}^{-T}\right]}_{\underline{\mu}^{T}}\left\{\begin{array}{c}\underline{c}_l\\ \underline{d}_l\end{array}\right\}e^{-jk\Delta\omega T}-\underbrace{\left[\underline{\mu}^{*T}\quad\underline{\mu}^{-T}\right]}_{\underline{\mu}^{T}}\left\{\begin{array}{c}\underline{p}_l\\ \underline{q}_l\end{array}\right\}\end{array}\right]+CT\right\}=\sum_{k=0}^{N}\left\{\left(\underline{\mu}^{+}\otimes\hat{\underline{u}}(k\Delta\omega)\right)^{*}\left[\hat{e}_l\left(k\Delta\omega\right)\right]+CT\right\}$$



Institutional Repository - Library & Information Centre - University of Thessaly
24/04/2024 00:02:26 EEST - 3.141.244.201

For $\theta = G_{r,li}$

$$\frac{\partial \underline{x}^{r}\left(k\Delta\omega;\underline{\theta}\right)}{\partial G_{r,li}} = \underline{\delta}_i \underline{\delta}_i^{T} \mu_r^{-} \underline{\hat{u}}(k\Delta\omega) \Rightarrow \frac{\partial \underline{x}^{r*T}\left(k\Delta\omega;\underline{\theta}\right)}{\partial G_{r,li}} = \underline{\hat{u}}^{*T}(k\Delta\omega)\underline{\delta}_i \underline{\delta}_i^{T}\left(\mu_r^{-}\right)^{*} \tag{4.182}$$

Substituting (4.182) in (4.179) yields

$$\frac{\partial J(\underline{\theta})}{\partial G_{r,li}} = 0 \Rightarrow$$

$$\sum_{k=0}^{N}\left\{\left(\mu_r^{-}\right)^{*}\underline{\hat{u}}^{*T}(k\Delta\omega)\underline{\delta}_i\underline{\delta}_j^{T}\left[\underline{x}^{r}\left(k\Delta\omega;\underline{\theta}\right)-\underline{\hat{e}}\left(k\Delta\omega\right)\right]+CT\right\}=0 \;\Rightarrow\; \sum_{k=0}^{N}\left\{\left(\mu_r^{-}\right)^{*}\hat{u}_i^{*}(k\Delta\omega)\left[x_j^{r}\left(k\Delta\omega;\underline{\theta}\right)-\hat{e}_j\left(k\Delta\omega\right)\right]+CT\right\}=0 \Rightarrow$$

$$\sum_{k=0}^{N}\left\{\underbrace{\left(\mu_r^{-}\right)^{*}\hat{u}_i^{*}(k\Delta\omega)}_{\left(\mu^{-}\otimes\hat{u}\right)^{*}}\left[\begin{array}{l}\sum_{r=1}^{m}\left[\underline{L}_{r,l}^{T}\mu_r^{+}+\underline{G}_{r,l}^{T}\mu_r^{-}\right]\underline{\hat{u}}(k\Delta\omega)+\underline{D}_{c,l}^{T}\underline{\tilde{u}}(k\Delta\omega)\\ +\sum_{r=1}^{m}\left[c_{r,l}\mu_r^{+}+d_{r,l}\mu_r^{-}\right]e^{-jk\Delta\omega T}-\sum_{r=1}^{m}\left[p_{r,l}\mu_r^{+}+q_{r,l}\mu_r^{-}\right]\end{array}\right]+CT\right\}=\sum_{k=0}^{N}\left\{\left(\mu_r^{-}\right)^{*}\hat{u}_i^{*}(k\Delta\omega)\left[\hat{e}_j\left(k\Delta\omega\right)\right]+CT\right\}\Rightarrow$$

$$\sum_{k=0}^{N}\left\{\left(\underline{\mu}^{-}\otimes\underline{\hat{u}}(k\Delta\omega)\right)^{*}\left[\begin{array}{l}\underbrace{\left[\underline{\hat{u}}^{T}(k\Delta\omega)\mu_1^{+}\cdots\;\underline{\hat{u}}^{T}(k\Delta\omega)\mu_m^{+}\right]}_{\mu^{+T}\otimes\hat{u}^{T}(\omega)}\left\{\begin{array}{c}\underline{L}_{1,l}^{T}\\ \vdots\\ \underline{L}_{m,l}^{T}\end{array}\right\}+\\ \underbrace{\left[\underline{\hat{u}}^{T}(k\Delta\omega)\mu_1^{-}\cdots\;\underline{\hat{u}}^{T}(k\Delta\omega)\mu_m^{-}\right]}_{\mu^{-T}\otimes\hat{u}^{T}(\omega)}\left\{\begin{array}{c}\underline{G}_{1,l}^{T}\\ \vdots\\ \underline{G}_{m,l}^{T}\end{array}\right\}+\\ +\underline{D}_{c,j}^{T}\underline{\tilde{u}}(k\Delta\omega)+\left(\underline{c}_l^{T}\underline{\mu}^{+}+\underline{d}_l^{T}\underline{\mu}^{-}\right)e^{-jk\Delta\omega T}-\left(\underline{p}_l^{T}\underline{\mu}^{+}+\underline{q}_l^{T}\underline{\mu}^{+}\right)\end{array}\right]+CT\right\}=\sum_{k=0}^{N}\left\{\left(\underline{\mu}^{-}\otimes\underline{\hat{u}}(k\Delta\omega)\right)^{*}\left[\hat{e}_j\left(k\Delta\omega\right)\right]+CT\right\}\Rightarrow \tag{4.183}$$

$$\sum_{k=0}^{N}\left\{\left(\underline{\mu}^{-}\otimes\underline{\tilde{u}}(k\Delta\omega)\right)^{*}\left[\begin{array}{l}\left(\underline{\mu}^{+T}\otimes\underline{\hat{u}}^{T}(k\Delta\omega)\right)\left\{\begin{array}{c}\underline{L}_{1,l}^{T}\\ \vdots\\ \underline{L}_{m,l}^{T}\end{array}\right\}+\left(\underline{\mu}^{-T}\otimes\underline{\tilde{u}}^{T}(k\Delta\omega)\right)\left\{\begin{array}{c}\underline{G}_{1,l}^{T}\\ \vdots\\ \underline{G}_{m,l}^{T}\end{array}\right\}\\ +\underline{D}_{c,l}^{T}\underline{\tilde{u}}(k\Delta\omega)+\underbrace{\left[\underline{\mu}^{+T}\;\;\underline{\mu}^{-T}\right]}_{\mu^{T}}\left\{\begin{array}{c}\underline{c}_l\\ \underline{d}_l\end{array}\right\}e^{-jk\Delta\omega T}-\underbrace{\left[\underline{\mu}^{+T}\;\;\underline{\mu}^{-T}\right]}_{\mu^{T}}\left\{\begin{array}{c}\underline{p}_l\\ \underline{q}_l\end{array}\right\}\end{array}\right]+CT\right\}=\sum_{k=0}^{N}\left\{\left(\underline{\mu}^{-}\otimes\underline{\tilde{u}}(k\Delta\omega)\right)^{*}\left[\hat{e}_j\left(k\Delta\omega\right)\right]+CT\right\}$$



Institutional Repository - Library & Information Centre - University of Thessaly
24/04/2024 00:02:26 EEST - 3.141.244.201

For $\theta = D_{c,li}$

$$\frac{\partial \underline{\underline{y}}(k\Delta\omega)}{\partial D_{c,li}} = \underline{\delta}_l \underline{\delta}_i^T \, \hat{\underline{u}}(k\Delta\omega) \Rightarrow \frac{\partial \underline{\underline{y}}^{*T}(k\Delta\omega)}{\partial D_{c,li}} = \hat{\underline{u}}^{*T}(k\Delta\omega)\underline{\delta}_i \underline{\delta}_l^T = \hat{u}_i^*(k\Delta\omega)\underline{\delta}_l^T \tag{4.184}$$

Substituting (4.182) in (4.179) yields

$$\begin{aligned}
&\frac{\partial J(\underline{\theta})}{\partial D_{c,li}} = 0 \Rightarrow \\
&\sum_{k=0}^{N}\left\{\hat{\underline{u}}^{*T}(k\Delta\omega)\underline{\delta}_i\underline{\delta}_l^T\left[\underline{x}^r(k\Delta\omega;\underline{\theta}) - \hat{\underline{e}}(k\Delta\omega)\right] + CT\right\} = 0 \;\Rightarrow\; \sum_{k=0}^{N}\left\{\hat{u}_i^*(k\Delta\omega)\left[x_i^r(k\Delta\omega;\underline{\theta}) - \hat{e}_l(k\Delta\omega)\right] + CT\right\} = 0 \Rightarrow \\
&\sum_{k=0}^{N}\left\{\hat{u}_i^*(k\Delta\omega)\left[\begin{array}{l}\sum_{r=1}^{m}\left[\underline{L}_{r,l}^T\mu_r^+ + \underline{G}_{r,l}^T\mu_r^-\right]\hat{\underline{u}}(k\Delta\omega) + \underline{D}_{c,l}^T\tilde{\underline{u}}(k\Delta\omega) \\ +\sum_{r=1}^{m}\left[c_{r,l}\mu_r^+ + d_{r,l}\mu_r^-\right]e^{-jk\Delta\omega T} - \sum_{r=1}^{m}\left[p_{r,l}\mu_r^+ + q_{r,l}\mu_r^-\right]\end{array}\right] + CT\right\} = \sum_{k=0}^{N}\left\{\hat{u}_i^*(k\Delta\omega)\left[\hat{e}_l(k\Delta\omega)\right] + CT\right\} \Rightarrow \\
&\sum_{k=0}^{N}\left\{\hat{\underline{u}}^*(k\Delta\omega)\left[\begin{array}{l}\underbrace{\left[\hat{\underline{u}}^T(k\Delta\omega)\mu_1^+ \cdots \;\hat{\underline{u}}^T(k\Delta\omega)\mu_m^+\right]}_{\underline{\mu}^{+T}\otimes\hat{\underline{u}}^T(\omega)}\left\{\begin{array}{c}\underline{L}_{1,l}^T \\ \vdots \\ \underline{L}_{m,l}^T\end{array}\right\} + \\ \underbrace{\left[\hat{\underline{u}}^T(k\Delta\omega)\mu_1^- \cdots \;\hat{\underline{u}}^T(k\Delta\omega)\mu_m^-\right]}_{\underline{\mu}^{-T}\otimes\hat{\underline{u}}^T(\omega)}\left\{\begin{array}{c}\underline{G}_{1,l}^T \\ \vdots \\ \underline{G}_{m,l}^T\end{array}\right\} + \\ +\underline{D}_{c,l}^T\hat{\underline{u}}(k\Delta\omega) + \left(\underline{c}_l^T\underline{\mu}^+ + \underline{d}_l^T\underline{\mu}^-\right)e^{-jk\Delta\omega T} - \left(\underline{p}_l^T\underline{\mu}^+ + \underline{q}_l^T\underline{\mu}^-\right)\end{array}\right] + CT\right\} = \sum_{k=0}^{N}\left\{\hat{\underline{u}}^*(k\Delta\omega)\left[\hat{e}_l(k\Delta\omega)\right] + CT\right\} \Rightarrow \\
&\sum_{k=0}^{N}\left\{\hat{\underline{u}}^*(k\Delta\omega)\left[\begin{array}{l}\left(\underline{\mu}^{+T}\otimes\hat{\underline{u}}^T(k\Delta\omega)\right)\left\{\begin{array}{c}\underline{L}_{1,l}^T \\ \vdots \\ \underline{L}_{m,l}^T\end{array}\right\} + \left(\underline{\mu}^{-T}\otimes\hat{\underline{u}}^T(k\Delta\omega)\right)\left\{\begin{array}{c}\underline{G}_{1,l}^T \\ \vdots \\ \underline{G}_{m,l}^T\end{array}\right\} \\ +\underline{D}_{c,l}^T\hat{\underline{u}}(k\Delta\omega) + \underbrace{\left[\underline{\mu}^{+T} \quad \underline{\mu}^{-T}\right]}_{\underline{\mu}^T}\left\{\begin{array}{c}\underline{c}_l \\ \underline{d}_l\end{array}\right\}e^{-j\omega T} - \underbrace{\left[\underline{\mu}^{+T} \quad \underline{\mu}^{-T}\right]}_{\underline{\mu}^T}\left\{\begin{array}{c}\underline{p}_l \\ \underline{q}_l\end{array}\right\}\end{array}\right] + CT\right\} = \sum_{k=0}^{N}\left\{\hat{\underline{u}}^*(k\Delta\omega)\left[\hat{e}_l(k\Delta\omega)\right] + CT\right\}
\end{aligned} \tag{4.185}$$



Institutional Repository - Library & Information Centre - University of Thessaly
24/04/2024 00:02:26 EEST - 3.141.244.201

For $\theta = c_{r,l}$

$$\frac{\partial \underline{x}^r\left(k\Delta\omega;\underline{\theta}\right)}{\partial c_{r,l}} = \underline{\delta}_l \mu_r^+ e^{-j\omega T} \Rightarrow \frac{\partial \underline{x}^{r*T}\left(k\Delta\omega;\underline{\theta}\right)}{\partial c_{r,l}} = \underline{\delta}_l^T \left(\mu_r^+\right)^* e^{j\omega T} \tag{4.186}$$

Substituting (4.182) in (4.179) yields

$$\begin{aligned}
&\frac{\partial J(\underline{\theta})}{\partial c_{r,l}} = 0 \Rightarrow \\
&\sum_{k=0}^{N}\left\{\underline{\delta}_l^T \left(\mu_r^+\right)^* e^{jk\Delta\omega T}\left[\underline{x}^r\left(k\Delta\omega;\underline{\theta}\right) - \underline{\hat{e}}\left(k\Delta\omega\right)\right] + CT\right\} = 0 \;\Rightarrow\; \sum_{k=0}^{N}\left\{\left(\mu_r^+\right)^* e^{jk\Delta\omega T}\left[\partial x_l^r\left(k\Delta\omega;\underline{\theta}\right) - \hat{e}_l\left(k\Delta\omega\right)\right] + CT\right\} = 0 \Rightarrow \\
&\sum_{k=0}^{N}\left\{\left(\mu_r^+\right)^* e^{jk\Delta\omega T}\left[\begin{array}{l}\sum_{r=1}^{m}\left[\underline{L}_{r,l}^T \mu_r^+ + \underline{G}_{r,l}^T \mu_r^-\right]\underline{\hat{u}}(k\Delta\omega) + \underline{D}_{c,l}^T \underline{\hat{u}}(k\Delta\omega) \\ + \sum_{r=1}^{m}\left[c_{r,l}\mu_r^+ + d_{r,l}\mu_r^-\right]e^{-jk\Delta\omega T} - \sum_{r=1}^{m}\left[p_{r,l}\mu_r^+ + q_{r,l}\mu_r^-\right]\end{array}\right] + CT\right\} = \sum_{k=0}^{N}\left\{\left(\mu_r^+\right)^* e^{jk\Delta\omega T}\left[\hat{e}_l\left(k\Delta\omega\right)\right] + CT\right\} \Rightarrow \\
&\sum_{k=0}^{N}\left\{\left(\underline{\mu}^+\right)^* e^{jk\Delta\omega T}\left[\begin{array}{l}\underbrace{\left[\underline{\hat{u}}^T(k\Delta\omega)\mu_1^+ \cdots \underline{\hat{u}}^T(k\Delta\omega)\mu_m^+\right]}_{\underline{\mu}^{-T}\otimes\underline{\hat{u}}^T(\omega)}\left\{\begin{array}{c}\underline{L}_{1,l}^T \\ \vdots \\ \underline{L}_{m,l}^T\end{array}\right\} + \\ \underbrace{\left[\underline{\hat{u}}^T(k\Delta\omega)\mu_1^- \cdots \underline{\hat{u}}^T(k\Delta\omega)\mu_m^-\right]}_{\underline{\mu}^{-T}\otimes\underline{\hat{u}}^T(\omega)}\left\{\begin{array}{c}\underline{G}_{1,l}^T \\ \vdots \\ \underline{G}_{m,l}^T\end{array}\right\} + \\ +\underline{D}_{c,l}^T\underline{\hat{u}}(k\Delta\omega) + \left(\underline{c}_l^T\underline{\mu}^+ + \underline{d}_l^T\underline{\mu}^-\right)e^{-j\omega T} - \left(\underline{p}_l^T\underline{\mu}^+ + \underline{q}_l^T\underline{\mu}^-\right)\end{array}\right] + CT\right\} = \sum_{k=0}^{N}\left\{\left(\underline{\mu}^+\right)^* e^{jk\Delta\omega T}\left[\hat{e}_l\left(k\Delta\omega\right)\right] + CT\right\} \Rightarrow \\
&\sum_{k=0}^{N}\left\{\left(\underline{\mu}^+\right)^* e^{j\omega T}\left[\begin{array}{l}\left(\underline{\mu}^{+T}\otimes\underline{\hat{u}}^T(k\Delta\omega)\right)\left\{\begin{array}{c}\underline{L}_{1,l}^T \\ \vdots \\ \underline{L}_{m,l}^T\end{array}\right\} + \left(\underline{\mu}^{-T}\otimes\underline{\tilde{u}}^T(k\Delta\omega)\right)\left\{\begin{array}{c}\underline{G}_{1,l}^T \\ \vdots \\ \underline{G}_{m,l}^T\end{array}\right\} \\ +\underline{D}_{c,l}^T\underline{\hat{u}}(k\Delta\omega) + \underbrace{\left[\underline{\mu}^{+T} \;\; \underline{\mu}^{-T}\right]}_{\underline{\mu}^T}\left\{\begin{array}{c}\underline{c}_l \\ \underline{d}_l\end{array}\right\}e^{-jk\Delta\omega T} - \underbrace{\left[\underline{\mu}^{+T} \;\; \underline{\mu}^{-T}\right]}_{\underline{\mu}^T}\left\{\begin{array}{c}\underline{p}_l \\ \underline{q}_l\end{array}\right\}\end{array}\right] + CT\right\} = \sum_{k=0}^{N}\left\{\left(\underline{\mu}^+\right)^* e^{jk\Delta\omega T}\left[\hat{e}_l\left(k\Delta\omega\right)\right] + CT\right\}
\end{aligned} \tag{4.187}$$



Institutional Repository - Library & Information Centre - University of Thessaly
24/04/2024 00:02:26 EEST - 3.141.244.201

For $\theta = d_{r,l}$

$$\frac{\partial \underline{x}^r\left(k\Delta\omega;\underline{\theta}\right)}{\partial d_{r,l}} = \underline{\delta}_l \mu_r^- e^{-j\omega T} \Rightarrow \frac{\partial \underline{x}^{r*T}\left(k\Delta\omega;\underline{\theta}\right)}{\partial d_{r,l}} = \underline{\delta}_l^T \left(\mu_r^-\right)^* e^{j\omega T} \tag{4.188}$$

Substituting (4.182) in (4.179) yields

$$\begin{aligned}
&\frac{\partial J(\underline{\theta})}{\partial d_{r,l}} = 0 \Rightarrow \\
&\sum_{k=0}^{N}\left\{\underline{\delta}_l^T\left(\mu_r^-\right)^* e^{j\omega T}\left[\underline{x}^r\left(k\Delta\omega;\underline{\theta}\right) - \underline{\hat{e}}\left(k\Delta\omega\right)\right] + CT\right\} = 0 \;\Rightarrow\; \sum_{k=0}^{N}\left\{\left(\mu_r^-\right)^* e^{jk\Delta\omega T}\left[\partial x_l^r\left(k\Delta\omega;\underline{\theta}\right) - \hat{e}_l\left(k\Delta\omega\right)\right] + CT\right\} = 0 \Rightarrow \\
&\sum_{k=0}^{N}\left\{\left(\mu_r^-\right)^* e^{jk\Delta\omega T}\left[\begin{array}{l}\sum_{r=1}^{m}\left[\underline{L}_{r,l}^T \mu_r^+ + \underline{G}_{r,l}^T \mu_r^-\right]\underline{\hat{u}}(k\Delta\omega) + \underline{D}_{c,l}^T \underline{\hat{u}}(\omega) \\ +\sum_{r=1}^{m}\left[c_{r,l}\mu_r^+ + d_{r,l}\mu_r^-\right]e^{-jk\Delta\omega T} - \sum_{r=1}^{m}\left[p_{r,l}\mu_r^+ + q_{r,l}\mu_r^-\right]\end{array}\right] + CT\right\} = \sum_{k=0}^{N}\left\{\left(\mu_r^-\right)^* e^{jk\Delta\omega T}\left[\hat{e}_l\left(k\Delta\omega\right)\right] + CT\right\} \Rightarrow \\
&\sum_{k=0}^{N}\left\{\left(\underline{\mu}^-\right)^* e^{jk\Delta\omega T}\left[\begin{array}{l}\underbrace{\left[\underline{\hat{u}}^T(k\Delta\omega)\mu_1^+ \cdots \underline{\hat{u}}^T(k\Delta\omega)\mu_m^+\right]}_{\underline{\mu}^{+T}\otimes\underline{\hat{u}}^T(\omega)}\left\{\begin{array}{c}\underline{L}_{1,l}^T \\ \vdots \\ \underline{L}_{m,l}^T\end{array}\right\} + \\ \underbrace{\left[\underline{\hat{u}}^T(k\Delta\omega)\mu_1^- \cdots \underline{\hat{u}}^T(k\Delta\omega)\mu_m^-\right]}_{\underline{\mu}^{-T}\otimes\underline{\hat{u}}^T(\omega)}\left\{\begin{array}{c}\underline{G}_{1,l}^T \\ \vdots \\ \underline{G}_{m,l}^T\end{array}\right\} + \\ +\underline{D}_{c,l}^T\underline{\hat{u}}(k\Delta\omega) + \left(\underline{c}_l^T\underline{\mu}^+ + \underline{d}_l^T\underline{\mu}^-\right)e^{-jk\Delta\omega T} - \left(\underline{p}_l^T\underline{\mu}^+ + \underline{q}_l^T\underline{\mu}^-\right)\end{array}\right] + CT\right\} = \sum_{k=0}^{N}\left\{\left(\underline{\mu}^-\right)^* e^{jk\Delta\omega T}\left[\hat{e}_l\left(k\Delta\omega\right)\right] + CT\right\} \Rightarrow \\
&\sum_{k=0}^{N}\left\{\left(\underline{\mu}^-\right)^* e^{jk\Delta\omega T}\left[\begin{array}{l}\left(\underline{\mu}^{+T}\otimes\underline{\hat{u}}^T(k\Delta\omega)\right)\left\{\begin{array}{c}\underline{L}_{1,l}^T \\ \vdots \\ \underline{L}_{m,l}^T\end{array}\right\} + \left(\underline{\mu}^{-T}\otimes\underline{\hat{u}}^T(k\Delta\omega)\right)\left\{\begin{array}{c}\underline{G}_{1,l}^T \\ \vdots \\ \underline{G}_{m,l}^T\end{array}\right\} \\ +\underline{D}_{c,l}^T\underline{\hat{u}}(k\Delta\omega) + \underbrace{\left[\underline{\mu}^{+T} \quad \underline{\mu}^{-T}\right]}_{\underline{\mu}^T}\left\{\begin{array}{c}\underline{c}_l \\ \underline{d}_l\end{array}\right\}e^{-jk\Delta\omega T} - \underbrace{\left[\underline{\mu}^{+T} \quad \underline{\mu}^{-T}\right]}_{\underline{\mu}^T}\left\{\begin{array}{c}\underline{p}_l \\ \underline{q}_l\end{array}\right\}\end{array}\right] + CT\right\} = \sum_{k=0}^{N}\left\{\left(\underline{\mu}^-\right)^* e^{jk\Delta\omega T}\left[\hat{e}_l\left(k\Delta\omega\right)\right] + CT\right\}
\end{aligned} \tag{4.189}$$



Institutional Repository - Library & Information Centre - University of Thessaly
24/04/2024 00:02:26 EEST - 3.141.244.201

For $\theta = p_{r,l}$

$$\frac{\partial \underline{x}^{r}\left(k\Delta\omega;\underline{\theta}\right)}{\partial p_{r,l}} = \underline{\delta}_{l}\mu_{r}^{+} \Rightarrow \frac{\partial \underline{x}^{r*T}\left(k\Delta\omega;\underline{\theta}\right)}{\partial p_{r,l}} = \underline{\delta}_{l}^{T}\left(\mu_{r}^{+}\right)^{*} \tag{4.190}$$

Substituting (4.182) in (4.179) yields

$$\begin{aligned}
&\frac{\partial J\left(\underline{\theta}\right)}{\partial p_{r,l}} = 0 \Rightarrow \\
&\sum_{k=0}^{N}\left\{\underline{\delta}_{l}^{T}\left(\mu_{r}^{+}\right)^{*}\left[\underline{x}^{r}\left(k\Delta\omega;\underline{\theta}\right) - \underline{\hat{e}}\left(k\Delta\omega\right)\right] + CT\right\} = 0 \;\Rightarrow\; \sum_{k=0}^{N}\left\{\left(\mu_{r}^{+}\right)^{*}\left[x_{l}^{r}\left(k\Delta\omega;\underline{\theta}\right) - \hat{e}_{l}\left(k\Delta\omega\right)\right] + CT\right\} = 0 \Rightarrow \\
&\sum_{k=0}^{N}\left\{\left(\mu_{r}^{+}\right)^{*}\left[\begin{array}{l}\sum_{r=1}^{m}\left[\underline{L}_{r,l}^{T}\mu_{r}^{+} + \underline{G}_{r,l}^{T}\mu_{r}^{-}\right]\underline{\hat{u}}(k\Delta\omega) + \underline{D}_{c,l}^{T}\underline{\hat{u}}(\omega) \\ +\sum_{r=1}^{m}\left[c_{r,l}\mu_{r}^{+} + d_{r,l}\mu_{r}^{-}\right]e^{-jk\Delta\omega T} - \sum_{r=1}^{m}\left[p_{r,l}\mu_{r}^{+} + q_{r,l}\mu_{r}^{-}\right]\end{array}\right] + CT\right\} = \sum_{k=0}^{N}\left\{\left(\mu_{r}^{+}\right)^{*}\left[\hat{e}_{l}\left(k\Delta\omega\right)\right] + CT\right\} \Rightarrow \\
&\sum_{k=0}^{N}\left\{\left(\underline{\mu}^{+}\right)^{*}\left[\begin{array}{l}\underbrace{\left[\underline{\hat{u}}^{T}(k\Delta\omega)\mu_{1}^{+}\cdots\;\underline{\hat{u}}^{T}(k\Delta\omega)\mu_{m}^{+}\right]}_{\underline{\mu}^{+T}\otimes\underline{\hat{u}}^{T}(\omega)}\begin{Bmatrix}\underline{L}_{1,l}^{T}\\ \vdots \\ \underline{L}_{m,l}^{T}\end{Bmatrix} + \\ \underbrace{\left[\underline{\hat{u}}^{T}(k\Delta\omega)\mu_{1}^{-}\cdots\;\underline{\hat{u}}^{T}(k\Delta\omega)\mu_{m}^{-}\right]}_{\underline{\mu}^{-T}\otimes\underline{\hat{u}}^{T}(\omega)}\begin{Bmatrix}\underline{G}_{1,l}^{T}\\ \vdots \\ \underline{G}_{m,l}^{T}\end{Bmatrix} + \\ +\underline{D}_{c,l}^{T}\underline{\hat{u}}(k\Delta\omega) + \left(\underline{c}_{l}^{T}\underline{\mu}^{+} + \underline{d}_{l}^{T}\underline{\mu}^{-}\right)e^{-jk\Delta\omega T} - \left(\underline{p}_{l}^{T}\underline{\mu}^{+} + \underline{q}_{l}^{T}\underline{\mu}^{-}\right)\end{array}\right] + CT\right\} = \sum_{k=0}^{N}\left\{\left(\underline{\mu}^{+}\right)^{*}\left[\hat{e}_{l}\left(k\Delta\omega\right)\right] + CT\right\} \Rightarrow \\
&\sum_{k=0}^{N}\left\{\left(\underline{\mu}^{+}\right)^{*}\left[\begin{array}{l}\left(\underline{\mu}^{+T}\otimes\underline{\hat{u}}^{T}(k\Delta\omega)\right)\begin{Bmatrix}\underline{L}_{1,l}^{T}\\ \vdots \\ \underline{L}_{m,l}^{T}\end{Bmatrix} \div \left(\underline{\mu}^{-T}\otimes\underline{\hat{u}}^{T}(k\Delta\omega)\right)\begin{Bmatrix}\underline{G}_{1,l}^{T}\\ \vdots \\ \underline{G}_{m,l}^{T}\end{Bmatrix} \\ +\underline{D}_{c,l}^{T}\underline{\hat{u}}(k\Delta\omega) + \underbrace{\left[\underline{\mu}^{+T}\quad\underline{\mu}^{-T}\right]}_{\underline{\mu}^{T}}\begin{Bmatrix}\underline{c}_{l}\\ \underline{d}_{l}\end{Bmatrix}e^{-jk\Delta\omega T} - \underbrace{\left[\underline{\mu}^{+T}\quad\underline{\mu}^{-T}\right]}_{\underline{\mu}^{T}}\begin{Bmatrix}\underline{p}_{l}\\ \underline{q}_{l}\end{Bmatrix}\end{array}\right] + CT\right\} = \sum_{k=0}^{N}\left\{\left(\underline{\mu}^{*}\right)^{*}\left[\hat{e}_{l}\left(k\Delta\omega\right)\right] + CT\right\}
\end{aligned} \tag{4.191}$$



Institutional Repository - Library & Information Centre - University of Thessaly
24/04/2024 00:02:26 EEST - 3.141.244.201

For $\theta = q_{r,l}$

$$\frac{\partial \underline{x}^{r}\left(k\Delta\omega;\underline{\theta}\right)}{\partial q_{r,l}} = \underline{\delta}_l \mu_r^- \Rightarrow \frac{\partial \underline{x}^{r*T}\left(k\Delta\omega;\underline{\theta}\right)}{\partial q_{r,l}} = \underline{\delta}_l^T \left(\mu_r^-\right)^* \tag{4.192}$$

Substituting (4.182) in (4.179) yields

$$\begin{aligned}
&\frac{\partial J(\underline{\theta})}{\partial q_{r,l}} = 0 \Rightarrow \\
&\sum_{k=0}^{N}\left\{\underline{\delta}_l^T\left(\mu_r^-\right)^*\left[\underline{x}^{r}\left(k\Delta\omega;\underline{\theta}\right) - \underline{\hat{e}}\left(k\Delta\omega\right)\right] + CT\right\} = 0 \;\Rightarrow\; \sum_{k=0}^{N}\left\{\left(\mu_r^-\right)^*\left[x_l^{r}\left(k\Delta\omega;\underline{\theta}\right) - \hat{e}_l\left(k\Delta\omega\right)\right] + CT\right\} = 0 \Rightarrow \\
&\sum_{k=0}^{N}\left\{\left(\mu_r^-\right)^*\left[\begin{array}{l}\sum_{r=1}^{m}\left[\underline{L}_{r,l}^T\mu_r^+ + \underline{G}_{r,l}^T\mu_r^-\right]\hat{\underline{u}}(k\Delta\omega) + \underline{D}_{c,l}^T\hat{\underline{u}}(\omega) \\ +\sum_{r=1}^{m}\left[c_{r,l}\mu_r^+ + d_{r,l}\mu_r^-\right]e^{-jk\Delta\omega T} - \sum_{r=1}^{m}\left[p_{r,l}\mu_r^+ + q_{r,l}\mu_r^-\right]\end{array}\right] + CT\right\} = \sum_{k=0}^{N}\left\{\left(\mu_r^-\right)^*\left[\hat{e}_l\left(k\Delta\omega\right)\right] + CT\right\} \Rightarrow \\
&\sum_{k=0}^{N}\left\{\left(\underline{\mu}^-\right)^*\left[\begin{array}{l}\underbrace{\left[\hat{\underline{u}}^T(k\Delta\omega)\mu_1^+ \cdots \hat{\underline{u}}^T(k\Delta\omega)\mu_m^+\right]}_{\underline{\mu}^{+T}\otimes\hat{\underline{u}}^T(\omega)}\begin{Bmatrix}\underline{L}_{1,l}^T \\ \vdots \\ \underline{L}_{m,l}^T\end{Bmatrix} + \\ \underbrace{\left[\hat{\underline{u}}^T(k\Delta\omega)\mu_1^- \cdots \hat{\underline{u}}^T(k\Delta\omega)\mu_m^-\right]}_{\underline{\mu}^{-T}\otimes\hat{\underline{u}}^T(\omega)}\begin{Bmatrix}\underline{G}_{1,l}^T \\ \vdots \\ \underline{G}_{m,l}^T\end{Bmatrix} + \\ +\underline{D}_{c,l}^T\hat{\underline{u}}(k\Delta\omega) + \left(\underline{c}_l^T\underline{\mu}^+ + \underline{d}_l^T\underline{\mu}^-\right)e^{-jk\Delta\omega T} - \left(\underline{p}_l^T\underline{\mu}^+ + \underline{q}_l^T\underline{\mu}^-\right)\end{array}\right] + CT\right\} = \sum_{k=0}^{N}\left\{\left(\underline{\mu}^-\right)^*\left[\hat{e}_l\left(k\Delta\omega\right)\right] + CT\right\} \Rightarrow \\
&\sum_{k=0}^{N}\left\{\left(\underline{\mu}^-\right)^*\left[\begin{array}{l}\left(\underline{\mu}^{+T}\otimes\hat{\underline{u}}^T(k\Delta\omega)\right)\begin{Bmatrix}\underline{L}_{1,l}^T \\ \vdots \\ \underline{L}_{m,l}^T\end{Bmatrix} + \left(\underline{\mu}^{-T}\otimes\hat{\underline{u}}^T(k\Delta\omega)\right)\begin{Bmatrix}\underline{G}_{1,l}^T \\ \vdots \\ \underline{G}_{m,l}^T\end{Bmatrix} \\ +\underline{D}_{c,l}^T\hat{\underline{u}}(k\Delta\omega) + \underbrace{\left[\underline{\mu}^{+T} \quad \underline{\mu}^{-T}\right]}_{\underline{\mu}^T}\begin{Bmatrix}\underline{c}_l \\ \underline{d}_l\end{Bmatrix}e^{-jk\Delta\omega T} - \underbrace{\left[\underline{\mu}^{+T} \quad \underline{\mu}^{-T}\right]}_{\underline{\mu}^T}\begin{Bmatrix}\underline{p}_l \\ \underline{q}_l\end{Bmatrix}\end{array}\right] + CT\right\} = \sum_{k=0}^{N}\left\{\left(\underline{\mu}^-\right)^*\left[\hat{e}_l\left(k\Delta\omega\right)\right] + CT\right\}
\end{aligned} \tag{4.193}$$

where

$$\underline{c}_l = \begin{Bmatrix} c_{1,l} \\ \vdots \\ c_{m,l}\end{Bmatrix}, \underline{d}_l = \begin{Bmatrix} d_{1,l} \\ \vdots \\ d_{m,l}\end{Bmatrix}, \underline{p}_l = \begin{Bmatrix} p_{1,l} \\ \vdots \\ p_{m,l}\end{Bmatrix}, \underline{q}_l = \begin{Bmatrix} q_{1,l} \\ \vdots \\ q_{m,l}\end{Bmatrix}$$

### 4.8.2 System Of Linear Algebraic Equations (Second Approach of Second Step)

Taking the stationary condition

$$\frac{1}{V}\sum_{k=0}^{N}\left\{\frac{\partial \underline{x}^{r*T}\left(k\Delta\omega;\underline{\theta}\right)}{\partial\theta}\left[\underline{x}^{r}\left(k\Delta\omega;\underline{\theta}\right) - \underline{\hat{e}}\left(k\Delta\omega\right)\right] + CT\right\} = 0 \tag{4.194}$$



Institutional Repository - Library & Information Centre - University of Thessaly
24/04/2024 00:02:26 EEST - 3.141.244.201

the derivative $\frac{\partial \underline{x}^{r*T}(k\Delta\omega;\underline{\theta})}{\partial\theta}$ must be evaluated

$$\frac{\partial \underline{x}^{r*T}(k\Delta\omega;\underline{\theta})}{\partial \phi_{lr}} = \sum_{r\in I_{+}} \left\{ \begin{array}{l} \left(\frac{\underline{\delta}_l^T}{(jk\Delta\omega)-\lambda_r^*}\right)\left(\underline{u}^{*T}(k\Delta\omega)\underline{l}_{+}^{*} + e^{jk\Delta\omega T}\xi_r^*(\mathrm{T}) - \xi_r^*(0)\right) + \\ \left(\frac{\underline{\delta}_l^T}{\left((jk\Delta\omega)-\lambda_r^*\right)^*}\right)\left(\underline{u}^{*T}(k\Delta\omega)\underline{l}_{-} + e^{jk\Delta\omega T}\xi_r^*(\mathrm{T}) - \xi_r^*(0)\right) \end{array} \right\} \tag{4.195}$$

$$\frac{\partial \underline{x}^{r*T}(k\Delta\omega;\underline{\theta})}{\partial \psi_{lr}} = \sum_{r\in I_{+}} \left\{ \begin{array}{l} \left(\frac{-j\underline{\delta}_l^T}{(jk\Delta\omega)-\lambda_r^*}\right)\left(\underline{\hat{u}}^{*T}(k\Delta\omega)\underline{l}_{+}^{*} + e^{j\omega_k T}\xi_r^*(\mathrm{T}) - \xi_r^*(0)\right) \\ + \left(\frac{j\underline{\delta}_l^T}{\left((jk\Delta\omega)-\lambda_r^*\right)^*}\right)\left(\underline{\hat{u}}^{*T}(k\Delta\omega)\underline{l}_{-} + e^{j\omega T}\xi_r^*(\mathrm{T}) - \xi_r^*(0)\right) \end{array} \right\} \tag{4.196}$$

$$\frac{\partial \underline{x}^{r*T}(k\Delta\omega;\underline{\theta})}{\partial D_{c,li}} = \underline{\hat{u}}^{*T}(k\Delta\omega)\underline{\delta}_i\underline{\delta}_l^T = \hat{u}_i^*(k\Delta\omega)\underline{\delta}_l^T \tag{4.197}$$

Substituting (4.195) - (4.197) in (4.194) yields

$$\frac{\partial J(\underline{\theta})}{\partial \phi_{lr}} = 0 \Rightarrow$$

$$\sum_{k=1}^{N} \left\{ \begin{array}{l} \underbrace{\sum_{rel_{+}} \left\{ \left(\frac{1}{(j\omega_k)-\lambda_r^*}\right)\left(\underline{u}^{*T}(\omega_k)\underline{l}_{+}^{*} + e^{j\omega_k T}\xi_r^*(\mathrm{T}) - \xi_r^*(0)\right) + \left(\frac{1}{\left((j\omega_k)-\lambda_r^*\right)^*}\right)\left(\underline{u}^{*T}(\omega_k)\underline{l}_{-} + e^{j\omega_k T}\xi_r^*(\mathrm{T}) - \xi_r^*(0)\right) \right\}}_{A_r(\omega_k)} \cdot \\ \left\{ \begin{array}{l} \sum_{rel_{+}} \left[ \left( \underbrace{\frac{\underline{l}_{+}^T\hat{\underline{u}}(\omega_k)}{(j\omega_k)-\lambda_r}}_{term_{1,r}} + \underbrace{\frac{\underline{l}_{+}^{*T}\hat{\underline{u}}(\omega_k)}{(j\omega_k)-\lambda_r^*}}_{term_{2,r}} \right)\underline{\phi}_r + j\left( \frac{\underline{l}_{+}^T\hat{\underline{u}}(\omega_k)}{(j\omega_k)-\lambda_r} + \frac{\underline{l}_{+}^{*T}\hat{\underline{u}}(\omega_k)}{(j\omega_k)-\lambda_r^*} \right)\underline{\psi}_r \right] + \hat{\underline{u}}^T(\omega_k)\underline{D}_{c,l} + \\ \sum_{rel_{+}} \left[ \underbrace{\left( \frac{e^{-j\omega_k T}}{(j\omega_k)-\lambda_r} + \frac{e^{-j\omega_k T}}{(j\omega_k)-\lambda_r^*} \right)\xi_r(\mathrm{T})}_{term_{3,r}}\underline{\phi}_r + j\underbrace{\left( \frac{e^{-j\omega_k T}}{(j\omega_k)-\lambda_r} - \frac{e^{-j\omega_k T}}{(j\omega_k)-\lambda_r^*} \right)\xi_r(\mathrm{T})}_{term_{4,r}}\underline{\psi}_r \right] - \\ \sum_{r=1}^{n} \left[ \underbrace{\left( \frac{1}{(j\omega_k)-\lambda_r} + \frac{1}{(j\omega_k)-\lambda_r^*} \right)\xi_r(0)}_{term_{5,r}}\underline{\phi}_r + j\underbrace{\left( \frac{1}{(j\omega_k)-\lambda_r} - \frac{1}{(j\omega_k)-\lambda_r^*} \right)\xi_r(0)}_{term_{6,r}}\underline{\psi}_r \right] \end{array} \right\} + CT \end{array} \right\} =$$

$$\sum_{k=1}^{N} \left\{ \sum_{rel_{+}} \left\{ \left(\frac{1}{(j\omega_k)-\lambda_r^*}\right)\left(\underline{u}^{*T}(\omega_k)\underline{l}_{+}^{*} + e^{j\omega_k T}\xi_r^*(\mathrm{T}) - \xi_r^*(0)\right) + \left(\frac{1}{\left((j\omega_k)-\lambda_r^*\right)^*}\right)\left(\underline{u}^{*T}(\omega_k)\underline{l}_{-} + e^{j\omega_k T}\xi_r^*(\mathrm{T}) - \xi_r^*(0)\right) \right\} \hat{e}_l(\omega_k) + CT \right\} \Rightarrow$$

$$\sum_{k=1}^{N} \left\{ \sum_{rel_{+}} A_r(\omega_k) \left\{ \begin{array}{l} \sum_{rel_{+}} \left[ (term_{1,r} + term_{2,r})\underline{\phi}_r + j(term_{1,r} + term_{2,r})\underline{\psi}_r \right] + \hat{\underline{u}}^T(\omega_k)\underline{D}_{c,l} \\ + \sum_{rel_{+}} \left[ (term_{3,r})\underline{\phi}_r + j(term_{4,r})\underline{\psi}_r \right] - \sum_{rel_{+}} \left[ (term_{5,r})\underline{\phi}_r + j(term_{6,r})\underline{\psi}_r \right] \end{array} \right\} + CT \right\} = \sum_{k=0}^{N} \left\{ \sum_{rel_{+}} A_r(\omega_k)\hat{e}_l(\omega_k) + CT \right\} \tag{4.198}$$



Institutional Repository - Library & Information Centre - University of Thessaly
24/04/2024 00:02:26 EEST - 3.141.244.201

$$\frac{\partial J(\underline{\theta})}{\partial \psi_{lr}} = 0 \Rightarrow$$

$$\sum_{k=1}^{N}\left\{\underbrace{\sum_{r\in I_u}\left\{\left(\frac{-j}{(j\omega_k)-\lambda_r^*}\right)\left(\underline{u}^{*T}(\omega_k)\underline{l}_r^* + e^{j\omega_k T}\xi_r^*(\mathrm{T})-\xi_r^*(0)\right)+\left(\frac{j}{\left((j\omega_k)-\lambda_r^*\right)^*}\right)\left(\underline{u}^{*T}(\omega_k)\underline{l}_r + e^{j\omega_k T}\xi_r^*(\mathrm{T})-\xi_r^*(0)\right)\right\}}_{\mathrm{B}_r(\omega_k)}\right.$$

$$\left.\begin{aligned}&\sum_{r\in I_u}\left[\left(\underbrace{\frac{\underline{l}_r^T\hat{\underline{u}}(\omega_k)}{(j\omega_k)-\lambda_r}}_{term_{1,r}}+\underbrace{\frac{\underline{l}_r^{*T}\hat{\underline{u}}(\omega_k)}{(j\omega_k)-\lambda_r^*}}_{term_{2,r}}\right)\underline{\phi}_r + j\left(\frac{\underline{l}_r^T\hat{\underline{u}}(\omega_k)}{(j\omega_k)-\lambda_r}+\frac{\underline{l}_r^{*T}\hat{\underline{u}}(\omega_k)}{(j\omega_k)-\lambda_r^*}\right)\underline{\psi}_r\right]+\hat{\underline{u}}^T(\omega_k)\underline{D}_{v,l}+\\&\sum_{r\in I_u}\left[\underbrace{\left(\frac{e^{-j\omega_k T}}{(j\omega_k)-\lambda_r}+\frac{e^{-j\omega_k T}}{(j\omega_k)-\lambda_r^*}\right)}_{term_{3,r}}\xi_r(\mathrm{T})\underline{\phi}_r + j\underbrace{\left(\frac{e^{-j\omega_k T}}{(j\omega_k)-\lambda_r}-\frac{e^{-j\omega_k T}}{(j\omega_k)-\lambda_r^*}\right)}_{term_{4,r}}\xi_r(\mathrm{T})\underline{\psi}_r\right]-\\&\sum_{r\in I_u}^{n}\left[\underbrace{\left(\frac{1}{(j\omega_k)-\lambda_r}+\frac{1}{(j\omega_k)-\lambda_r^*}\right)}_{term_{5,r}}\xi_r(0)\underline{\phi}_r + j\underbrace{\left(\frac{1}{(j\omega_k)-\lambda_r}-\frac{1}{(j\omega_k)-\lambda_r^*}\right)}_{term_{6,r}}\xi_r(0)\underline{\psi}_r\right]\end{aligned}\right\}+CT\Bigg\}=$$

$$\sum_{k=1}^{N}\left\{\underbrace{\sum_{r\in I_u}\left\{\left(\frac{-j}{(j\omega_k)-\lambda_r^*}\right)\left(\underline{u}^{*T}(\omega_k)\underline{l}_r^* + e^{j\omega_k T}\xi_r^*(\mathrm{T})-\xi_r^*(0)\right)+\left(\frac{j}{\left((j\omega_k)-\lambda_r^*\right)^*}\right)\left(\underline{u}^{*T}(\omega_k)\underline{l}_r + e^{j\omega_k T}\xi_r^*(\mathrm{T})-\xi_r^*(0)\right)\right\}}_{\mathrm{B}_r(\omega_k)}\hat{e}_l(\omega_k)+CT\right\}\Rightarrow$$

$$\sum_{k=1}^{N}\left\{\sum_{r\in I_u}^{m}\mathrm{B}_r(\omega_k)\left\{\begin{aligned}&\sum_{r\in I_u}\left[\left(term_{1,r}+term_{2,r}\right)\underline{\phi}_r + j\left(term_{1,r}+term_{2,r}\right)\underline{\psi}_r\right]+\hat{\underline{u}}^T(\omega_k)\underline{D}_{e,l}\\&+\sum_{r\in I_u}\left[\left(term_{3,r}\right)\underline{\phi}_r + j\left(term_{4,r}\right)\underline{\psi}_r\right]-\sum_{r\in I_u}\left[\left(term_{5,r}\right)\underline{\phi}_r + j\left(term_{6,r}\right)\underline{\psi}_r\right]\end{aligned}\right\}+CT\right\}=\sum_{k=1}^{N}\left\{\sum_{r\in I_u}\mathrm{B}_r(\omega_k)\hat{e}_l(\omega_k)+CT\right\} \quad (4.199)$$

$$\frac{\partial J(\underline{\theta})}{\partial D_{e,l}} = 0 \Rightarrow$$

$$\sum_{k=1}^{N}\left\{\hat{\underline{u}}^*(\omega_k)\left\{\begin{aligned}&\sum_{r\in I_u}\left[\left(\underbrace{\frac{\underline{l}_r^T\hat{\underline{u}}(\omega_k)}{(j\omega_k)-\lambda_r}}_{term_{1,r}}+\underbrace{\frac{\underline{l}_r^{*T}\hat{\underline{u}}(\omega_k)}{(j\omega_k)-\lambda_r^*}}_{term_{2,r}}\right)\underline{\phi}_r + \Im\left(\frac{\underline{l}_r^T\hat{\underline{u}}(\omega_k)}{(j\omega_k)-\lambda_r}+\frac{\underline{l}_r^{*T}\hat{\underline{u}}(\omega_k)}{(j\omega_k)-\lambda_r^*}\right)\underline{\psi}_r\right]+\hat{\underline{u}}^T(\omega_k)\underline{D}_{e,l}+\\&\sum_{r\in I_u}\left[\underbrace{\left(\frac{e^{-j\omega_k T}}{(j\omega_k)-\lambda_r}+\frac{e^{-j\omega_k T}}{(j\omega_k)-\lambda_r^*}\right)}_{term_{3,r}}\xi_r(\mathrm{T})\underline{\phi}_r + j\underbrace{\left(\frac{e^{-j\omega_k T}}{(j\omega_k)-\lambda_r}-\frac{e^{-j\omega_k T}}{(j\omega_k)-\lambda_r^*}\right)}_{term_{4,r}}\xi_r(\mathrm{T})\underline{\psi}_r\right]-\\&\sum_{r\in I_u}\left[\underbrace{\left(\frac{1}{(j\omega_k)-\lambda_r}+\frac{1}{(j\omega_k)-\lambda_r^*}\right)}_{term_{5,r}}\xi_r(0)\underline{\phi}_r + j\underbrace{\left(\frac{1}{(j\omega_k)-\lambda_r}-\frac{1}{(j\omega_k)-\lambda_r^*}\right)}_{term_{6,r}}\xi_r(0)\underline{\psi}_r\right]\end{aligned}\right\}+CT\right\}= \quad (4.200)$$

$$\sum_{k=1}^{N}\left\{\hat{\underline{u}}^*(\omega_k)\hat{e}_l(\omega_k)+CT\right\}\Rightarrow$$

$$\sum_{k=1}^{N}\left\{\hat{\underline{u}}^*(\omega_k)\left\{\begin{aligned}&\sum_{r\in I_u}\left[\left(term_{1,r}+term_{2,r}\right)\underline{\phi}_r + j\left(term_{1,r}+term_{2,r}\right)\underline{\psi}_r\right]+\hat{\underline{u}}^T(\omega_k)\underline{D}_{e,l}\\&+\sum_{r\in I_u}\left[\left(term_{3,r}\right)\underline{\phi}_r + j\left(term_{4,r}\right)\underline{\psi}_r\right]-\sum_{r\in I_u}\left[\left(term_{5,r}\right)\underline{\phi}_r + j\left(term_{6,r}\right)\underline{\psi}_r\right]\end{aligned}\right\}+CT\right\}=\sum_{k=1}^{N}\left\{\hat{\underline{u}}^*(\omega_k)\hat{e}_l(\omega_k)+CT\right\}$$

where



Institutional Repository - Library & Information Centre - University of Thessaly
24/04/2024 00:02:26 EEST - 3.141.244.201

$$\underline{D}_{c,l} = \begin{Bmatrix} D_{c,l1} \\ \vdots \\ D_{c,lN_{in}} \end{Bmatrix} \in R^{N_{in}\times 1}, \quad \forall l = 1,\ldots,N_{out} \text{ and } \omega_k = k\Delta\omega\,,\ k = 1,\ldots,N\,.$$



Institutional Repository - Library & Information Centre - University of Thessaly
24/04/2024 00:02:26 EEST - 3.141.244.201

# Chapter 5

# Applications

## 5.1 Introduction

In the present study, the modal identification methodologies developed in previous chapters are used to analyze the dynamic modal characteristics of two bridges using real dynamic data. Simulated data are used for the validation of the methodologies through comparison of the estimated modal properties to the ones resulting from a 3 DOF and a 10 DOF spring mass chain model.

Further down, in Section 5.2, is presented the formulation of the response of a linear elastic structure, in the case when is supported at more than one point and is subjected to different input components. The formulation of the response to each input component depends on the fact that the multiple supports move independently of each other and induce quasi-static stresses that must be considered in addition to the dynamic response effects resulting from inertial forces. In Section 5.3 is presented the validation of the modal identification algorithms in time domain for both non-classically and classically damped modal models and in frequency domain for non-classically damped modal models using a 3 DOF and a 10 DOF spring mass chain model. In Section 5.4 the proposed identification methodologies are applied to the R/C bridge of Polymylos bridge for the low level, magnitude $M_L = 4.6$, earthquake event that occurred on 21/2/2007 (2:04:38 GMT) at a distance 35km Northeast of the bridge. The resulted values of the modal frequencies due to earthquake-induced vibrations are compared with the modal frequencies due to ambient vibrations estimated in other works. Finally, in Section 5.5 the proposed identification methodologies are also applied to the Vincent Thomas cable suspension bridge subjected to the 1987 Whittier earthquake. The resulted values of the modal frequencies and the damping ratios are also compared with the results given from other works in the previous years.

## 5.2 Response of Structures Subjected to Multiple Base Excitation

In the case when a linear elastic structure is supported at more than one point and is subjected to different input components, the formulation of the response to each input component depends on the fact that the multiple supports move independently of each other and induce quasi-static stresses that must be considered in addition to the dynamic response effects resulting from inertial forces.

To formulate the equations of motion (2.1) for the general case of base excitation, the following partition of the displacement vector is considered



Institutional Repository - Library & Information Centre - University of Thessaly
24/04/2024 00:02:26 EEST - 3.141.244.201

$$\underline{y} = \begin{Bmatrix} \underline{y}_s \\ \underline{y}_g \end{Bmatrix} \tag{5.1}$$

where $\underline{y}_s$ is the vector of the unknown nodal displacements and $\underline{y}_g$ is the vector of the given support displacements. In earthquake applications $\underline{y}_g$ consists of the independent input components that express, for example, the seismic excitation to which the structure is subjected. The equation of motion (2.1) is written

$$\begin{bmatrix} M_{ss} & M_{sg} \\ M_{gs} & M_{gg} \end{bmatrix} \begin{Bmatrix} \ddot{\underline{y}}_s(t) \\ \ddot{\underline{y}}_g(t) \end{Bmatrix} + \begin{bmatrix} C_{ss} & C_{sg} \\ C_{gs} & C_{gg} \end{bmatrix} \begin{Bmatrix} \dot{\underline{y}}_s(t) \\ \dot{\underline{y}}_g(t) \end{Bmatrix} + \begin{bmatrix} K_{ss} & K_{sg} \\ K_{gs} & K_{gg} \end{bmatrix} \begin{Bmatrix} \underline{y}_s(t) \\ \underline{y}_g(t) \end{Bmatrix} = \begin{Bmatrix} \underline{0} \\ \underline{0} \end{Bmatrix} \tag{5.2}$$

where the external forces are assumed to be zero, i.e. $\underline{u}(t) = \underline{0}$. The equilibrium equation expressing the motion of the response degrees of freedom can now be written in partitioned matrix form as follows

$$\begin{bmatrix} M_{ss} & M_{sg} \end{bmatrix} \begin{Bmatrix} \ddot{\underline{y}}_s(t) \\ \ddot{\underline{y}}_g(t) \end{Bmatrix} + \begin{bmatrix} C_{ss} & C_{sg} \end{bmatrix} \begin{Bmatrix} \dot{\underline{y}}_s(t) \\ \dot{\underline{y}}_g(t) \end{Bmatrix} + \begin{bmatrix} K_{ss} & K_{sg} \end{bmatrix} \begin{Bmatrix} \underline{y}_s(t) \\ \underline{y}_g(t) \end{Bmatrix} = \underline{0} \tag{5.3}$$

in which the motion vectors have been partitioned to separate the response quantities from the input, and the property matrices have been partitioned to correspond. The matrices that express forces in the response degrees of freedom due to motions of the supports are denoted with the subscript $g$. It is noted that (5.3) expresses the equilibrium of forces in the response degrees of freedom only, and that there are no external loads corresponding to these displacements.

An expression for the effective seismic loading is obtained by separating the support motion effects from the response quantities and transferring these input terms to the right hand side; thus the equation of motion of a structure excited at the base is considered to be:

$$M_{ss}\,\ddot{\underline{y}}_s + C_{ss}\,\dot{\underline{y}}_s + K_{ss}\,\underline{y}_s = -M_{sg}\,\ddot{\underline{y}}_g - C_{sg}\,\dot{\underline{y}}_g - K_{sg}\,\underline{y}_g \tag{5.4}$$

where $M_{ss}$, $C_{ss}$, $K_{ss}$ are the mass, damping and stiffness matrices of the system, $\underline{y}_s \equiv \underline{y}$ is the vector of motion at $N_s$ system degrees of freedom, $\underline{y}_g \equiv \underline{z}$ the vector of input motions at $N_{in}$ base degrees of freedom and $M_{sg}$, $C_{sg}$, $K_{sg}$ the mass, damping and stiffness matrices that couple the system and base degrees of freedom (DOFs).

The solution for the response to this input can be simplified if the total response motions are expressed as the combination of a quasi-static displacement vector $s$, plus a dynamic response vector $x$

$$\underline{y}_s = \underline{s} + \underline{x} \tag{5.5}$$



Institutional Repository - Library & Information Centre - University of Thessaly
24/04/2024 00:02:26 EEST - 3.141.244.201

The pseudostatic response represents the 'static' contributions of the individual support motions to the system response and is obtained by setting all time-derivative terms to zero in (5.4) and noting that the total displacements then are merely the quasi-static motions ($\underline{y} = \underline{s}$) given by

$$\underline{s} = D\,\underline{z} \tag{5.6}$$

where $D$ is the pseudostatic matrix, which expresses that response in all degrees of freedom due to unit support motions and is given by:

$$D = -K^{-1} K_{sf} \tag{5.7}$$

The dynamic component in (5.5) accounts for the contributions of the system's fixed-base modal vibrations about its pseudostatic reference position. Thus, the equations of motion of the dynamic response components $x$ are obtained by substituting (5.5) into (5.4) and satisfy the equation

$$M\,\ddot{\underline{x}} + C\,\dot{\underline{x}} + K\,\underline{x} = -(M\,D + M_{sg})\,\ddot{\underline{z}} - (C\,D + C_{sg})\,\dot{\underline{z}} \tag{5.8}$$

It is noted that there is no stiffness term in the effective forces on the right side; it drops out because of the definition of the pseudostatic displacement matrix given by (5.7). It is also recognized that this relationship will eliminate any effective input associated with a stiffness-proportional component of the viscous damping. In fact, it can be demonstrated by numerical experiment that the entire velocity-dependent part of this effective input is negligible in comparison to the contribution due to inertia if the viscous damping ratio has any reasonable value (Clough and Penzien, 1993). Consequently, (5.8) may be written in the following approximate form:

$$M\,\ddot{\underline{x}} + C\,\dot{\underline{x}} + K\,\underline{x} = -(M\,D + M_{sg})\,\ddot{\underline{z}} \tag{5.9}$$

It is worth pointing out that equation (5.9) is of the same form as equation (2.1) with $L$ in (2.1) replaced by $M\,D + M_{sg}$ and $\underline{u}(t)$ replaced by $\ddot{\underline{z}}(t)$. So the modal analysis and identification methods developed in this Thesis are directly applicable to structures subjected to different acceleration excitations at multiple supports.



Institutional Repository - Library & Information Centre - University of Thessaly
24/04/2024 00:02:26 EEST - 3.141.244.201

## 5.3 Validation of Modal Identification Algorithm using Simulated Data

The implemented algorithms, concerning the case of earthquake excitation, was validated by using simulated data from a 3-DOF and a 10 DOF spring mass chain model shown in Figure 1. The structures are excited at the base by specifying the base acceleration $\ddot{\underline{y}}_g$.

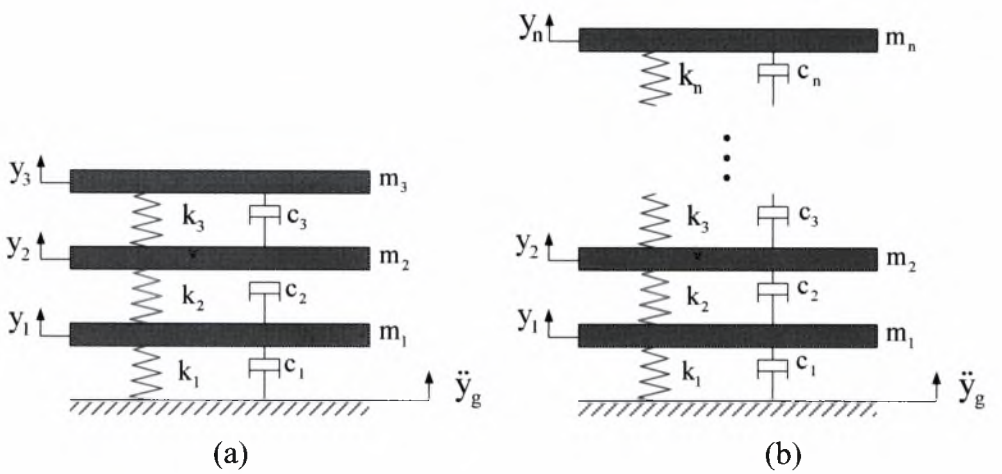


**Figure 1:** Spring mass chain-like models, (a) 3 DOF, (b) $n$ DOF

The optimal modal parameters $\underline{\theta}$, were estimated by using both the time domain approach, for both non-classically and classically damped modal models, and the frequency domain approach for non-classically damped modal models. The simulated data are generated by enforcing at the base of the model the El Centro earthquake acceleration and by computing the responses at all DOFs of the model. The available acceleration time history of the El Centro earthquake and its Fourier transform is shown in Figure 2.

The simulated absolute acceleration responses for selected floors computed by solving the equations of motion for the 3 DOF and the 10 DOF models are shown in Figure 3 and Figure 4, respectively, along with the Fourier transforms of the responses. These simulated data are used in the analysis that follows to validate the effectiveness of the modal identification algorithms.

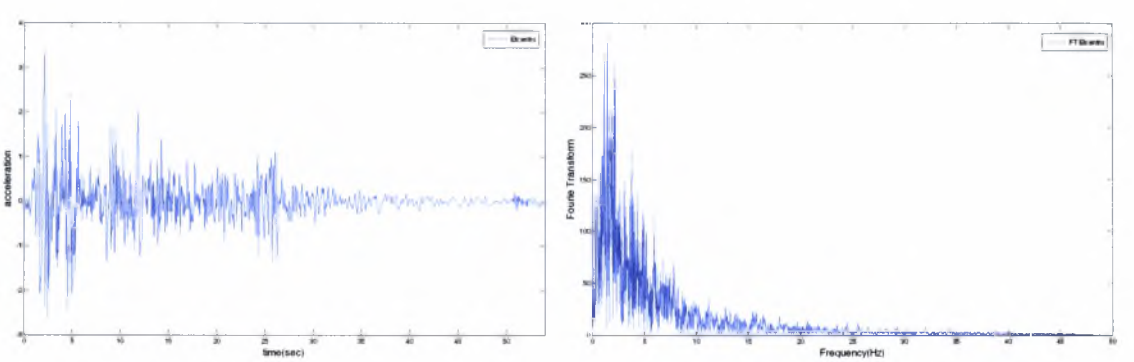


**Figure 2:** (a) El Centro Acceleration time history and (b) El Centro Fourier transformation



Institutional Repository - Library & Information Centre - University of Thessaly
24/04/2024 00:02:26 EEST - 3.141.244.201

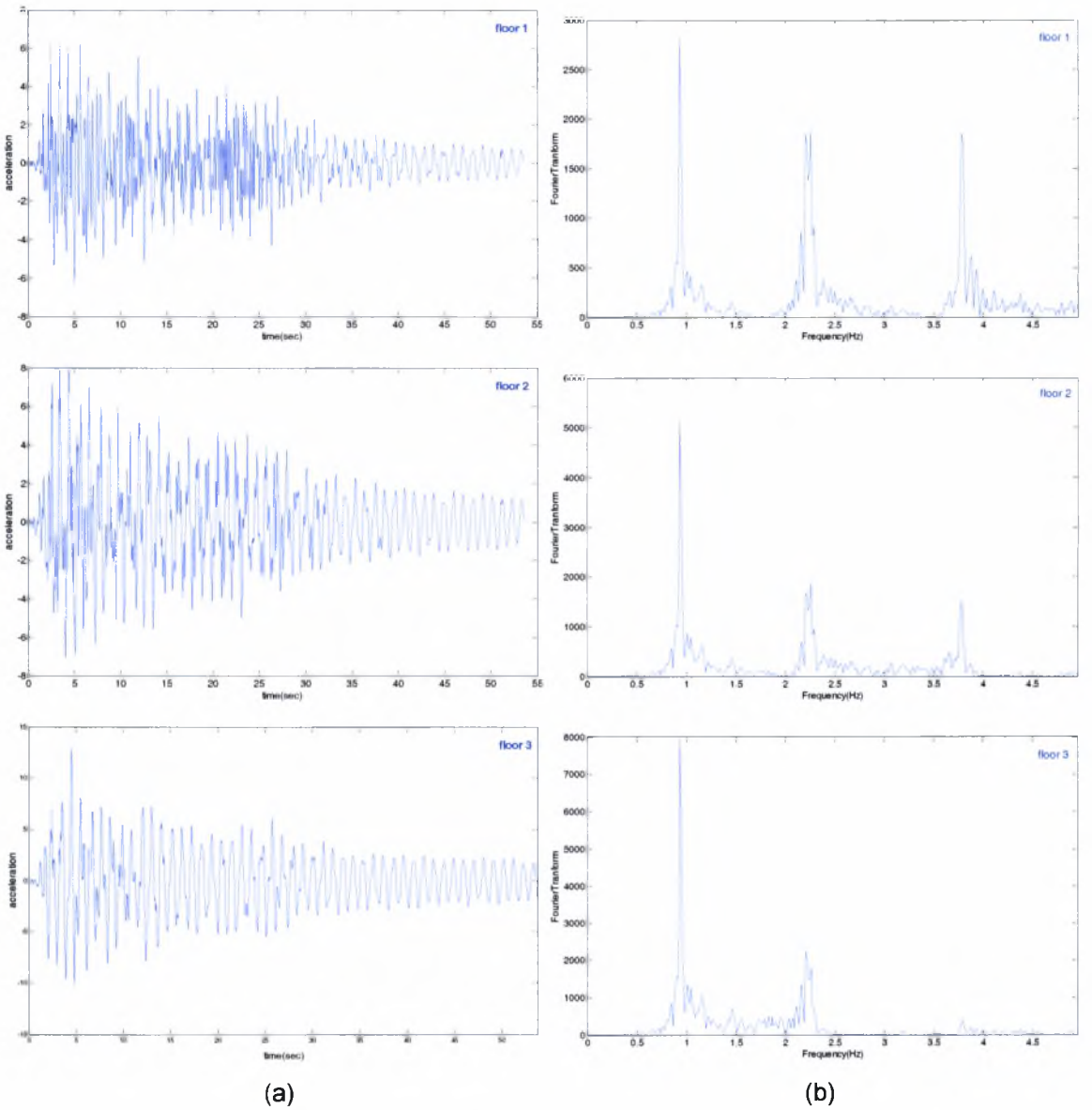


**Figure 3:** Simulated responses for the 1st, 2nd and 3rd floor of the 3 DOF model: (a) absolute accelerations, (b) Fourier transform of absolute accelerations



Institutional Repository - Library & Information Centre - University of Thessaly
24/04/2024 00:02:26 EEST - 3.141.244.201

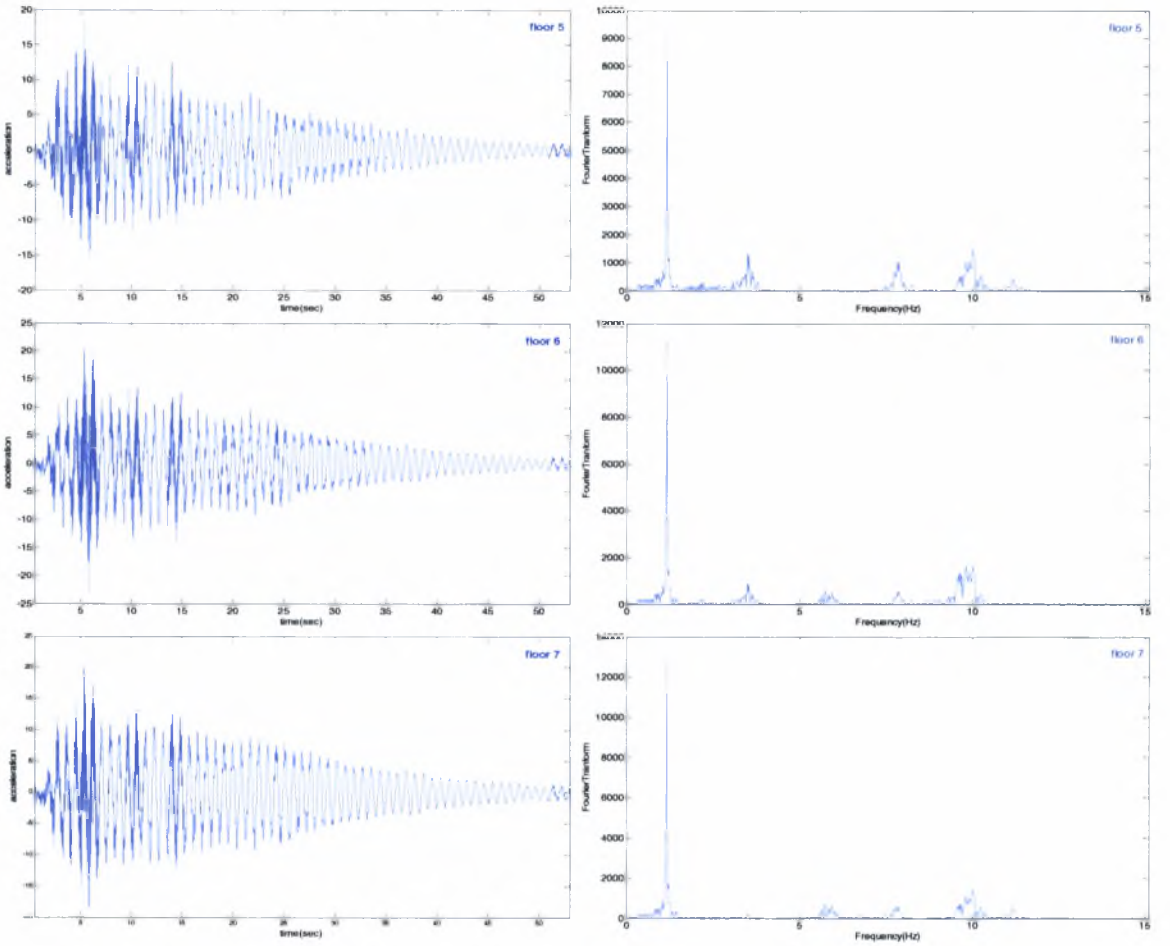


(a) (b)

**Figure 4:** Simulated responses for the 5th, 6th and 7th floor of the 10 DOF model: (a) absolute accelerations, (b) Fourier transform of absolute accelerations

**Table 1:** Comparison of optimal and real parameter values for Stabilization Diagram (First Step)

| | Spring Mass Chain-like Model | | | | Estimated Optimal Parameter Values | | | |
|---|---|---|---|---|---|---|---|---|
| | 3 DOF | | 10 DOF | | Stabilization Diagram | | | |
| | | | | | 3 DOF | | 10 DOF | |
| | $\omega$ Hz | $\zeta$ (%) | $\omega$ Hz | $\zeta$ (%) | $\omega$ Hz | $\zeta$ (%) | $\omega$ Hz | $\zeta$ (%) |
| 1 | 0.95 | 1.00 | 1.17 | 1.00 | 0.95 | 1.02 | 1.17 | 1.01 |
| 2 | 2.25 | 1.00 | 3.49 | 1.00 | 2.25 | 1.00 | 3.49 | 1.00 |
| 3 | 3.78 | 1.00 | 5.72 | 1.00 | 3.78 | 1.00 | 5.72 | 1.01 |
| 4 | | | 7.79 | 1.00 | | | 7.79 | 1.00 |
| 5 | | | 9.64 | 1.00 | | | 9.66 | 1.00 |
| 6 | | | 10.05 | 1.00 | | | 10.05 | 1.00 |
| 7 | | | 11.23 | 1.00 | | | 11.23 | 1.00 |
| 8 | | | 12.52 | 1.00 | | | 12.52 | 1.00 |
| 9 | | | 13.46 | 1.00 | | | 13.46 | 1.01 |
| 10 | | | 14.04 | 1.00 | | | 14.06 | 1.05 |



Institutional Repository - Library & Information Centre - University of Thessaly
24/04/2024 00:02:26 EEST - 3.141.244.201

The estimated modal characteristics (modal frequencies and damping ratios), which result from the stabilization diagrams obtained in the first step of the modal identification algorithms, are summarized in Table 1 and they are compared to the modal characteristics of the model that was used to generate the simulated data. The stabilization diagrams are used to distinguish between physical and mathematical modes, shown in Figure 5 and in Figure 6 for the 3-DOF and the 10 DOF spring mass chain model, respectively.

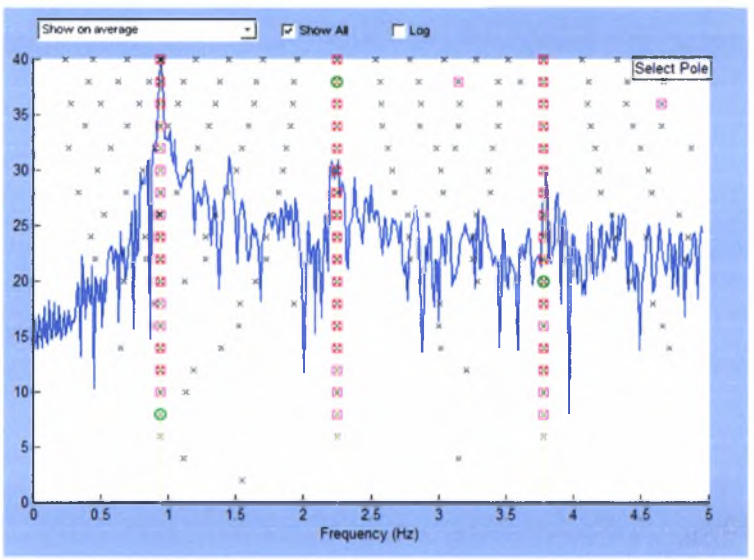


(a)

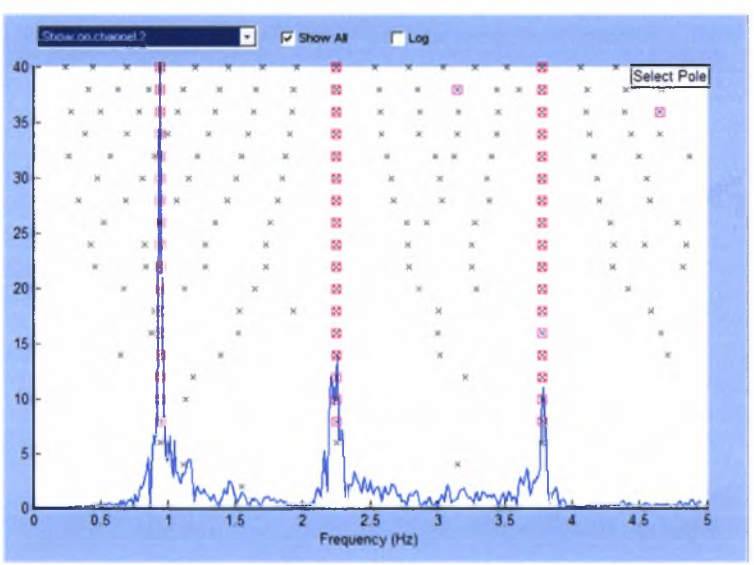


(b)

**Figure 5:** Stabilization Diagram for the3-DOF chain spring mass model: (a) Average of the Fourier Transforms of 3 floors, (b) Fourier Transform of 1st floor



Institutional Repository - Library & Information Centre - University of Thessaly
24/04/2024 00:02:26 EEST - 3.141.244.201

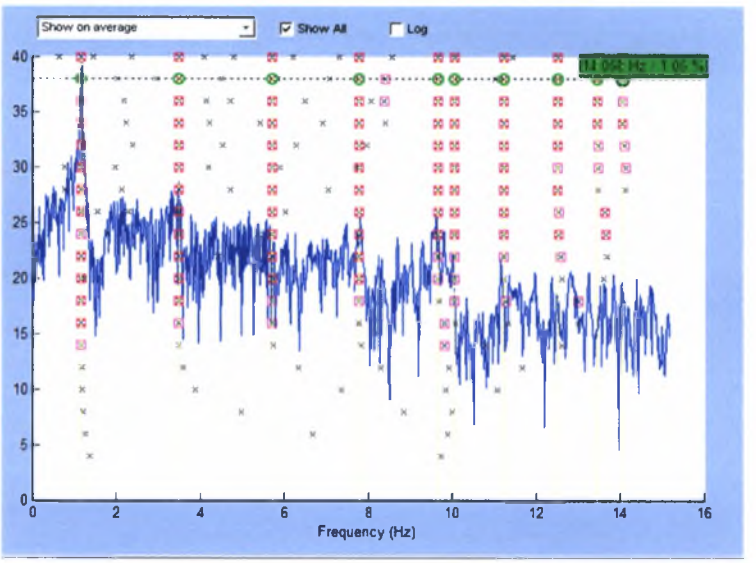


(a)

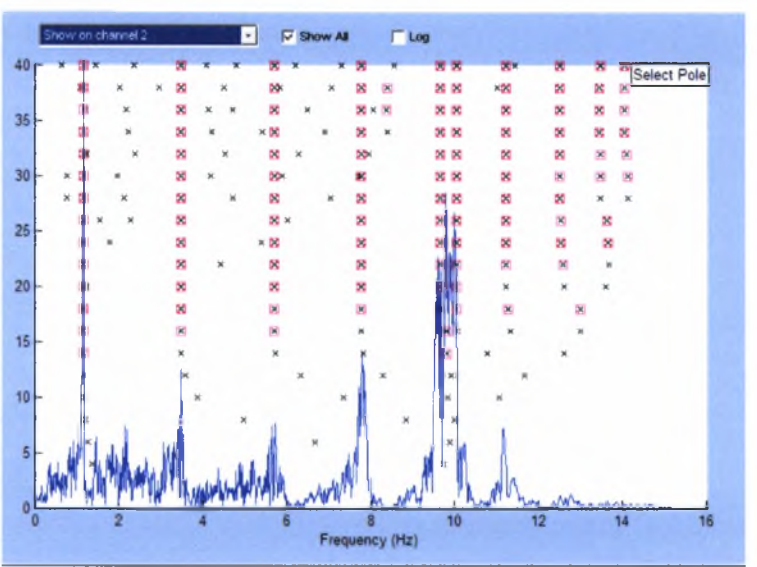


(b)

**Figure 6:** Stabilization Diagram for the 10-DOF chain spring mass model: (a) Average of the Fourier Transforms of 10 floors, (b) Fourier Transform of 1$^{st}$ floor

In Figure 5 and Figure 6 the stabilized poles are pointed with a red square for each polynomial order. It is observed that the estimated modal frequencies and damping ratios were accurately identified (no major discrepancies between the modal frequencies and damping ratios resulted from the Stabilization Diagrams and the modal identification algorithm), which validates the effectiveness of the Stabilization Diagrams.



Institutional Repository - Library & Information Centre - University of Thessaly
24/04/2024 00:02:26 EEST - 3.141.244.201

**Table 2:** Comparison of optimal parameter values

| | Optimal Parameter Values | | | | | | | | | | | |
|---|---|---|---|---|---|---|---|---|---|---|---|---|
| | Time Domain (classically damped) | | | | Time Domain (non-classically damped) | | | | Frequency Domain (non-classically damped) | | | |
| | 3 DOF | | 10 DOF | | 3 DOF | | 10 DOF | | 3 DOF | | 10 DOF | |
| | $\omega$ Hz | $\zeta$ (%) | $\omega$ Hz | $\zeta$ (%) | $\omega$ Hz | $\zeta$ (%) | $\omega$ Hz | $\zeta$ (%) | $\omega$ Hz | $\zeta$ (%) | $\omega$ Hz | $\zeta$ (%) |
| 1 | 0.95 | 1.00 | 1.17 | 1.00 | 0.95 | 1.00 | 1.17 | 1.01 | 0.95 | 1.01 | 1.17 | 1.02 |
| 2 | 2.25 | 1.00 | 3.49 | 1.00 | 2.25 | 1.01 | 3.49 | 1.00 | 2.25 | 1.00 | 3.51 | 0.99 |
| 3 | 3.78 | 1.00 | 5.72 | 1.00 | 3.78 | 1.07 | 5.72 | 1.06 | 3.78 | 1.00 | 5.72 | 0.97 |
| 4 | | | 7.79 | 1.00 | | | 7.79 | 1.00 | | | 7.78 | 0.99 |
| 5 | | | 9.64 | 1.00 | | | 9.66 | 1.03 | | | 9.66 | 1.01 |
| 6 | | | 10.05 | 1.00 | | | 10.05 | 1.00 | | | 10.05 | 0.97 |
| 7 | | | 11.23 | 1.00 | | | 11.23 | 2.00 | | | 11.23 | 0.77 |
| 8 | | | 12.52 | 1.00 | | | 12.52 | 2.00 | | | 12.52 | 0.75 |
| 9 | | | 13.46 | 1.00 | | | 13.46 | 2.00 | | | 13.46 | 0.75 |
| 10 | | | 14.04 | 1.00 | | | 14.04 | 2.00 | | | 14.04 | 0.76 |

The estimated modal characteristics for time domain approach and frequency domain approach are presented in Table 2. In Figure 7 it is observed that an accurate fit resulted from the convergence of the acceleration time histories predicted from the optimal modal model to the "measured" acceleration time histories for the 3-DOF and the 10 DOF chain spring mass model, which validates the effectiveness of the modal identification methodology. A similar fit is observed in Figure 8 for the Fourier Transforms of the accelerations.



Institutional Repository - Library & Information Centre - University of Thessaly
24/04/2024 00:02:26 EEST - 3.141.244.201

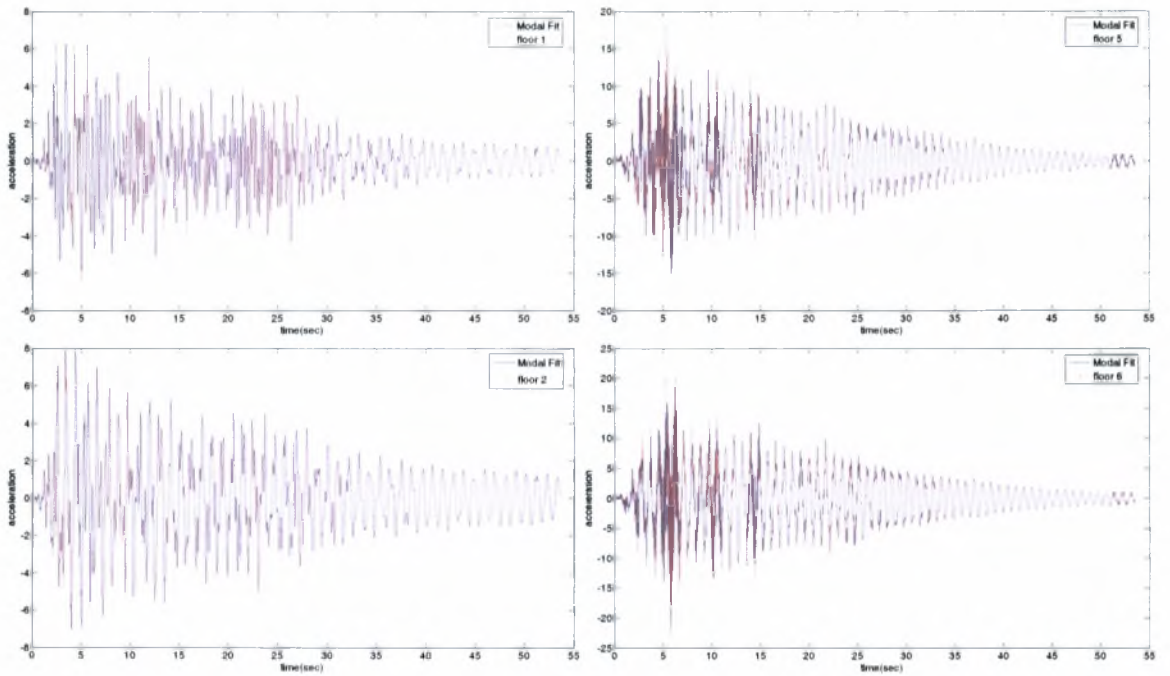


(a) (b)

**Figure 7:** Comparison between measurement data and modal model predictions (time histories of accelerations) (a) at the 1st and 2nd floor of the 3-DOF chain spring mass model and (b) at the 5th and 6th floor of the 10-DOF chain spring mass model

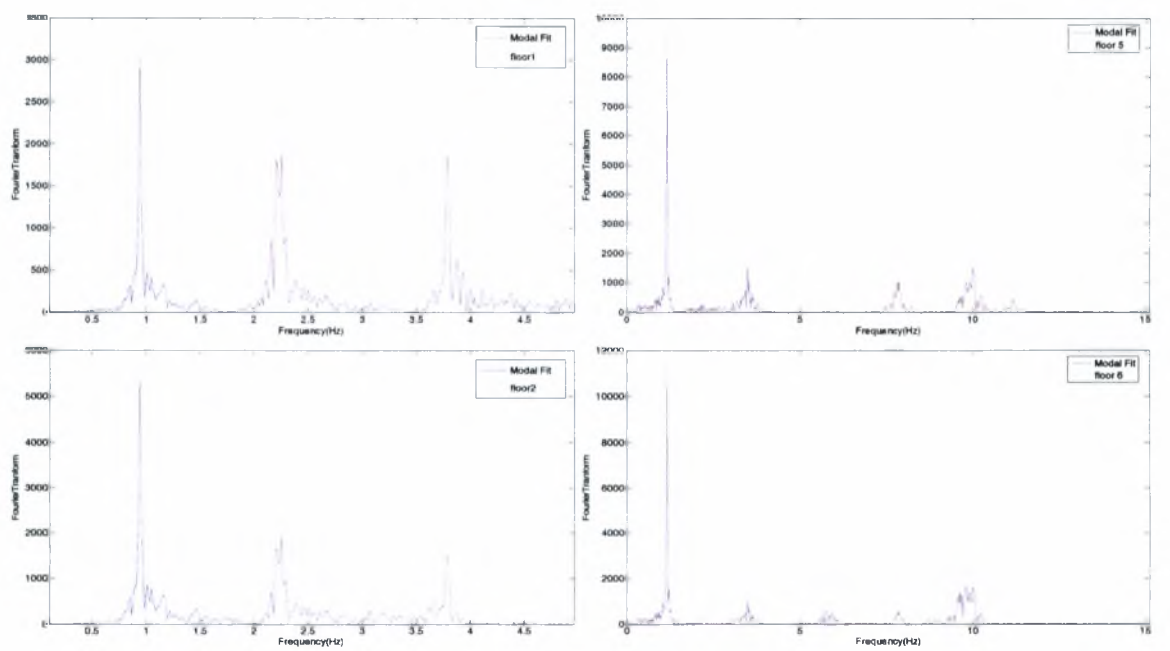


(a) (b)

**Figure 8:** Comparison between measurement data and modal model predictions (Fourier Transforms of accelerations) (a) at the 1st and 2nd floor of the 3-DOF chain spring mass model and (b) at the 5th and 6th floor of the 10-DOF chain spring mass model



Institutional Repository - Library & Information Centre - University of Thessaly
24/04/2024 00:02:26 EEST - 3.141.244.201

The modal identification algorithm for time domain (non-classically and classically damped) and frequency domain was based on a number of modes for each chain spring mass model. It is obvious that the proposed optimization algorithms work effectively, since it correctly and accurately identifies the dynamic properties of the two models. In particular, for the 3 DOF model both modal frequencies and modal damping ratios were estimated very accurately for all the modes by all the proposed optimization algorithms. For the 10 DOF model, it is observed that for the first 6 modes the modal frequencies were estimated very accurately and the damping ratios were estimated quite accurately. In contrast, for the highest modes only the time domain methodology for classically damped modal models was accurately identified the values of the damping ratios of the model. This may be due to the fact that the El Centro earthquake used to create the simulated data did not excite adequately these highest modes. Also, because of the fact that the response for the general case of non-classically damped modal models, for both time and frequency domain methodologies, is described by complex-valued parameters such as the modeshapes and the participation factors, the number of the parameters involved in the nonlinear optimization process of such systems increases. Hence, the identification algorithm for non-classically damped modal models, cannot estimate accurately the values of the damping ratios for these modes.

## 5.4 Polymylos Bridge, Greece

This section applies the developed modal identification methodologies for estimating the dynamic modal characteristics of a representative bridge on the Egnatia Odos motorway, using earthquake induced vibration measurements. Egnatia Motorway is a new, 670 km long highway, that transverses Northern Greece in an E-W direction. The R/C bridge of Polymylos that were instrumented with special accelerometer arrays are the 9th Ravine Bridge on the Veroia - Polymylos section (Figure 9). The bridge has two, almost identical, statically independent branches, one for each traffic direction, one of which was instrumented. Modal identification results (modal frequencies modal damping ratios and modeshape components) for the Polymylos bridge are estimated for the low level, magnitude $M_L = 4.6$, earthquake event that occurred on 21/2/2007 (2:04:38 GMT) at a distance 35km Northeast of the bridge.

### 5.4.1 Bridge Description and Instrumentation

The T-shaped 9$^{th}$ Polymylos bridge is curved in plan and has a total length of 170m. The deck cross section is a box girder of height varying parabolically from 9m at the central pier to 4m at the two abutments. It is supported monolithically by a central pier (M1), of 35m height, which is founded on a massive rectangular R/C rock socket at its basement and continues with two transverse flanges for the rest of its height. Each of the two 85m-long cantilever parts of the deck girder rests on each abutment through special elastomeric bearings that allow free sliding in the



Institutional Repository - Library & Information Centre - University of Thessaly
24/04/2024 00:02:26 EEST - 3.141.244.201

longitudinal direction (to accommodate thermal expansions/contractions), while functioning as normal elastomeric pads in the transverse (radial) direction.

**Figure 9:** View of Polymylos bridge

Two 12-channel Kinemetrics K2 ® recording units were installed on the northern branch of the 9$^{th}$ Polymylos bridge (on deck level at the middle of the total bridge deck), each supporting 12 uniaxial Kinemetrics Episensor ® accelerometers (± 2g full scale) installed on both sides of the bridge deck. The recording units have a 19-bit resolution, a sampling rate capacity of up to 200sps and a dynamic range of 108 dB @ 200 sps. Fifteen sensors were installed on the deck, three on the basement of the central pier and three on each of the two abutments (at the support level of the elastomeric bearings), as shown in Figure 10. Thus, the nine sensors monitor the earthquake-induced excitations at the two abutments and the basement of the pier. The particular layout of the instrumentation permits the analysis of earthquake-induced response of the bridge. The 3 to 4-letter sensor labels follow the following convention: The last letter denotes the orientation of the uniaxial sensor (L: longitudinal, T: transverse, V: vertical). The previous one denotes the side of the bridge deck on which the sensor lies (R: right, L : left). Finally, the first one or two letters denote the bridge section that the sensor lies on (first letters U1 and U3 refer here to the abutment level where the elastomeric bearings are seated, U2 refers to the base of the central pier and all other letters refer to positions on the level of the bridge deck). The numbers next to each sensor label denotes the length of the cable used to connect the sensor to each recording unit. Among the 15 accelerometers located on the bridge deck, 8 record in the vertical, 1 in the longitudinal and the rest 6 in the transverse direction.



Institutional Repository - Library & Information Centre - University of Thessaly
24/04/2024 00:02:26 EEST - 3.141.244.201

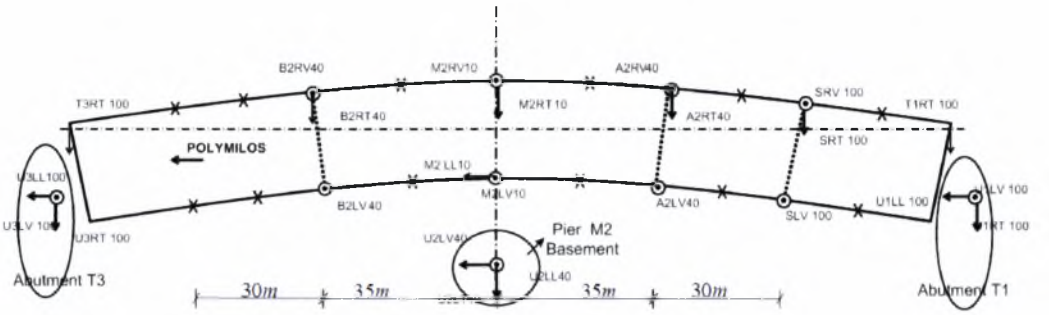


**Figure 10:** Instrumentation layout of Polymylos bridge

The modal identification carried out in the time domain and in the frequency domain using the measurements of the 24 accelerometers which were installed on the northern branch of the 9th Polymylos bridge. In particular, in the time domain the modal identification carried out using both non-classically damped and classically damped modal models. From the 15 accelerometers located on the bridge deck, accelerometers A2LV, A2RV and M2RV were excluded because they were damaged during the earthquake event. The accelerometer U1LV which monitors the earthquake-induced excitations at the right abutment of the bridge was also excluded for the same reason.

### 5.4.2 Modal Identification

Using all the eight (8) available input sensors which monitor the earthquake-induced excitations at the two abutments and the basement of the pier and all twelve (12) available output sensors, the values of the modal frequencies and modal damping ratios resulted from Stabilization Diagrams are presented in Figure 11 for: (a) the Fourier Transform of the accelerations of all vertical sensors, and (b) the Fourier Transform of the accelerations of all transverse sensors. After distinguishing the physical from the mathematical poles the values of the modal frequencies and modal damping ratios are presented in Table 3. Eight values of modal frequencies and modal damping ratios were identified. These values for the modal frequencies and the damping ratios were used for applying the next two steps described in Chapters 3 and 4 and estimating the modeshape components and participation factors on the measured locations of the bridge.



Institutional Repository - Library & Information Centre - University of Thessaly
24/04/2024 00:02:26 EEST - 3.141.244.201

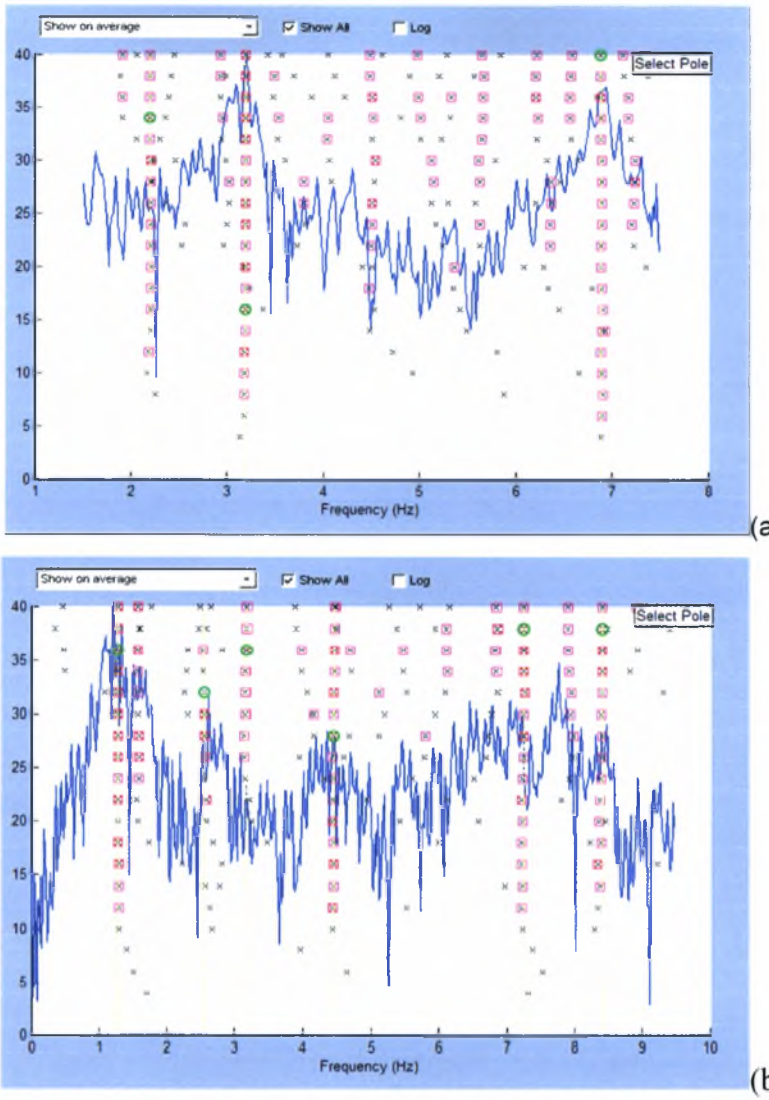


**Figure 11:** Stabilization Diagram for the Polymylos bridge: (a) Vertical Sensors, (b) Transverse sensors

**Table 3:** Identified modal frequencies $\omega$ and damping ratios $\zeta$ of the Polymylos Bridge, obtained by the Stabilization Diagram for Earthquake Vibrations

| Mode | Polymylos Bridge Stabilization Diagram | |
|---|---|---|
| | $\omega$ Hz | $\zeta$ (%) |
| 1st Transverse | 1,28 | 2.07 |
| 1st Bending (deck) | 2.19 | 0.42 |
| 2nd Transverse | 2.56 | 4.39 |
| 2nd Bending (deck) | 3.19 | 0.66 |
| 3rd Transverse | 4.46 | 1.46 |
| 3rd Bending (deck) | 6.89 | 0.66 |
| 4th Transverse | 7.25 | 1.20 |
| 1st Torsional | 8.4 | 0.58 |



Institutional Repository - Library & Information Centre - University of Thessaly
24/04/2024 00:02:26 EEST - 3.141.244.201

In Table 4 the values for the modal frequencies and damping ratios resulted from the identification algorithms for non-classically and classically damped modal models in time and frequency domain are presented and compared with the values identified using ambient vibration measured data presented in the work by Ntotsios et al. (2007).

Comparing the modal frequencies and damping ratios resulted from the Stabilization Diagrams and the modal identification algorithm for time and frequency domain it is observed that there are no major discrepancies. This validates that the values of the modal frequencies and the modal damping ratios which result from the Stabilization Diagrams constitute a very good approach of the optimal values that result from the modal identification algorithm.

**Table 4:** Identified and design FE model predicted modal frequencies $\omega$ and damping ratios $\zeta$ of the Polymylos bridge for Earthquake Vibrations

| Mode | Polymylos Bridge | | | | | | Ambient Vibrations (Ntotsios et. al, 2007) |
|---|---|---|---|---|---|---|---|
| | Earthquake Vibrations | | | | | | |
| | *Frequency Domain (non-classically damped)* | | *Time Domain (non-classically damped)* | | *Time Domain (classically damped)* | | |
| | $\omega$ Hz | $\zeta$ (%) | $\omega$ Hz | $\zeta$ (%) | $\omega$ Hz | $\zeta$ (%) | $\omega$ Hz |
| 1st Transverse | 1.26 | 2.07 | 1.29 | 1.8 | 1.29 | 1.8 | 1.13 |
| 1st Bending (deck) | 2.19 | 0.47 | 2.19 | 0.4 | 2.20 | 0.6 | 2.13 |
| 2nd Transverse | 2.61 | 3.86 | 2.57 | 4.12 | 2.56 | 3.5 | 2.22 |
| 2nd Bending (deck) | 3.19 | 0.61 | 3.19 | 0.66 | 3.20 | 0.7 | 3.07 |
| 3rd Transverse | 4.45 | 1.55 | 4.30 | 2.49 | 4.23 | 3.2 | 4.10 |
| 3rd Bending (deck) | 6.88 | 0.58 | 6.89 | 0.44 | 6.89 | 0.6 | 6.66 |
| 4th Transverse | 7.17 | 1.38 | 7.24 | 1.2 | 7.24 | 1.2 | 6.78 |
| 1st Torsional | 8.41 | 0.73 | 8,39 | 2,1 | | | - |

From the earthquake vibration data, it is noted that eight (8) modes were successfully and reliably identified for the Polymylos bridge: four transverse modes, three bending modes and one torsional. In Table 4, comparing the modal damping ratios, resulted from time domain and frequency domain, it is observed that the bending modes have significantly lower values of damping, of the order of 0.4% to 0.7%, than the damping values of the lower transverse modes which are of the order of 1.2% to 4.12%. The higher damping values observed for the lower transverse modes can be attributed to the energy dissipation arising from the higher modal deformation levels of the elastomeric bearings at the ends of the bridges which dominate the motion of these modes. Also, soil damping could also have contributed to the higher damping values observed for these modes.

Comparing the modal frequencies resulted from non-classically damped case and classically damped case for the time domain it is observed that there are no major discrepancies. For the



Institutional Repository - Library & Information Centre - University of Thessaly
24/04/2024 00:02:26 EEST - 3.141.244.201

modal damping ratios of bending modes, it is observed that the resulted values from non-classically damped case have lower values of the order of 0.4%-0.6% than the values resulted from classically damped case which are of the order of 0.6%-0.7%. For the transverse modes it is observed that the resulted damping ratios from non-classically and classically damped case of 1$^{st}$ and 4$^{th}$ mode have the same values, while the resulted damping ratios of the rest two modes have different values.

Comparing the results from time domain and frequency domain using non-classically damped modal models it is observed that the modal frequency of the 3$^{rd}$ transverse mode resulted from the time domain has lower value of the order of 4.23 Hz than the value resulted from the frequency domain which are of the order of 4.30 Hz. For the rest modes there are no major discrepancies between the values of the modal frequencies. Differences are also observed for the modal damping ratios for the transverse modes of the order of 0.26% - 0,94% and of the order of 0.05% - 0.14% for the bending modes.

From the results in Table 4, it is observed that the modal frequencies due to earthquake vibrations are 4% to 15% higher than the modal frequencies identified in Ntotsios et. al (2007) from the ambient vibrations. No conclusive explanation can be given for these differences without making assumptions about the bridge behavior within the measured vibration levels. These differences could be attributed to the nonlinear softening hysteretic behavior of the structural components, especially the elastomeric bearings. The results in Ntotsios et. al (2007) reveal that the peak acceleration responses for the earthquake induced vibrations are 1.4 to 3.8 times lower than the peak acceleration responses of the ambient vibrations (Table 5). Accepting that the estimation of the equivalent modal frequencies is dominated by the peak vibration levels, this could justify a higher secant stiffness of the elastomeric bearings for the lower earthquake peak vibration levels which results in stiffer structures and thus justifies the increase in the equivalent values of the modal frequencies observed in Table 4 for earthquake induced vibrations. However, this explanation cannot be used to justify the higher modal frequency values observed for the modes associated with bending of the deck since these modes are not affected by the bearing stiffness. It is unlikely that similar softening nonlinear effects will arise by the deformation of the pier and deck elements in these low vibration levels.

In Ntotsios et. al (2007) the values of the modal frequencies were also identified using much shorter duration segments of the ambient vibrations recordings shown in Figure 12, selected so that the peak acceleration levels are the same as or smaller that the peak acceleration of the earthquake recordings. The estimated values of the modal frequencies obtained by analyzing these short duration segments were found to be almost identical to the values of the modal frequencies that were estimated using the whole, approximate 30 minutes, segment of the records shown in Figure 12. This verifies that at the low vibration levels considered, the aforementioned differences in the peak acceleration levels between the ambient and the earthquake induced vibrations cannot justify the large differences in the modal frequencies observed in Table 4.



Institutional Repository - Library & Information Centre - University of Thessaly
24/04/2024 00:02:26 EEST - 3.141.244.201

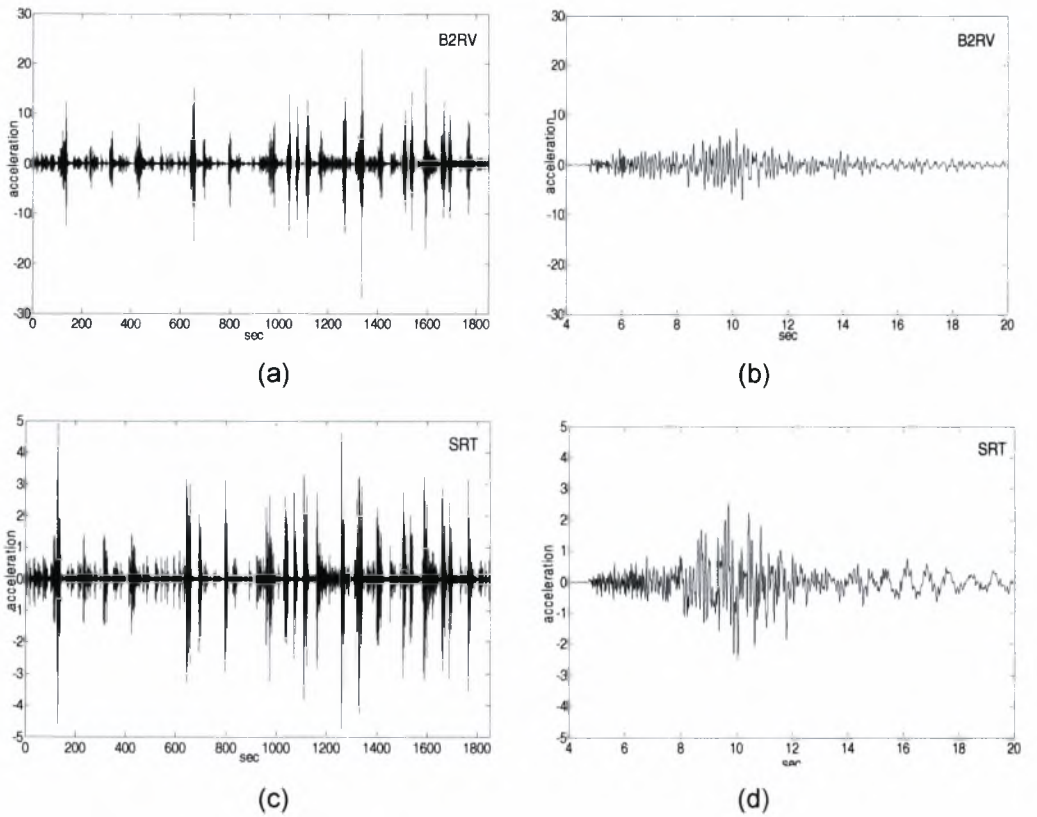


**Figure 12:** Accelerations time history measurements from ambient (Ntotsios et. al, 2007) and earthquake vibrations at sensors B2RV and SRT, (a,c) ambient, (b,d) earthquake

**Table 5:** Comparison of Peak and RMS response acceleration obtained from Ambient (AV) and Earthquake (EV) induced Vibrations (Ntotsios et. al, 2007)

| | Peak response ($cm/sec^2$) | | | RMS ($cm/sec^2$) | | |
|---|---|---|---|---|---|---|
| Channel | AV | EV | AV/EV | AV | EV | AV/EV |
| B2LV | 23.2470 | 7.1062 | 3.2714 | 0.9181 | 1.9397 | 0.4733 |
| M2LL | 2.1767 | 1.0009 | 2.1747 | 0.0922 | 0.2407 | 0.3830 |
| M2LV | 11.2310 | 2.9575 | 3.7975 | 0.6044 | 0.7350 | 0.8223 |
| SLV | 15.9950 | 6.6148 | 2.4181 | 0.8847 | 2.0163 | 0.4388 |
| T3RT | 5.9160 | 3.3652 | 1.7580 | 0.1825 | 0.7129 | 0.2561 |
| B2RV | 26.9220 | 7.3206 | 3.6776 | 0.9704 | 1.7120 | 0.5668 |
| B2RT | 7.7054 | 2.3919 | 3.2215 | 0.2928 | 0.6667 | 0.4392 |
| M2RT | 4.3362 | 2.5179 | 1.7221 | 0.2582 | 0.6141 | 0.4204 |
| A2RT | 5.5674 | 2.5210 | 2.2084 | 0.2559 | 0.5911 | 0.4329 |
| SRV | 17.4100 | 12.3900 | 1.4052 | 0.9418 | 2.5206 | 0.3737 |
| SRT | 4.9252 | 2.5542 | 1.9283 | 0.2783 | 0.5786 | 0.4810 |
| T1RT | 1.2481 | 2.3865 | 0.5230 | 0.0401 | 0.6104 | 0.0657 |

In contrast to the peak vibration levels, the levels of the RMS response in Table 5 of the approximately 30 minutes ambient acceleration measurements are 0.25 to 0.82 times the corresponding root mean square earthquake response levels. Accepting that the estimation of the



Institutional Repository - Library & Information Centre - University of Thessaly
24/04/2024 00:02:26 EEST - 3.141.244.201

equivalent modal frequencies in Table 4 is dominated by the RMS vibration levels, the modal frequencies due to higher RMS earthquake vibration levels are expected to decrease if softening of the elastomeric bearings take place, which is not consistent with the opposite increasing trend observed in Table 4.

A more reasonable explanation that can account for the differences in the identified values of the modal frequencies in Table 4 is soil structure interaction effects (Safak 1995). In this work (earthquake vibration case), the modal properties of the system were identified using as input acceleration the eight recordings at the two abutments and the base of the central pier and as output accelerations the twelve available recordings along the bridge deck. Thus, ignoring the rigid body rotation of the central pier foundation at the low vibration levels measured, the modal frequencies identified by the input-output earthquake vibration measurements are those of the fixed base bridge, excluding the effects of soil-structure interaction since the base motion of the abutment and the pier foundation were used as input accelerations in the modal identification process. In contrast, in Ntotsios et. al (2007) for the ambient vibration case, the modal properties of the system, obtained from the ambient measurements due to excitations from the traffic and wind loads, were identified using only the twelve output accelerations recorded along the bridge deck. Thus, the modal frequencies due to ambient vibrations correspond to the dynamic characteristics of the combined system consisting of the bridge and accounting for soil structure interaction effects. This interaction effect is due to the additional soil flexibility provided at the base supports of the bridge. The presence of this effect is also supported from the non-zero vibration levels recorded at the base of the pier and the top of the side abutments during ambient measurements. Thus, soil-structure interaction effects cause the combined soil-foundation-superstructure system to appear as less stiff than the superstructure (fixed-based bridge) itself, resulting in lower values of the modal frequencies which is consistent with the results observed in Table 4.

Representative measured modeshapes ($1^{st}$ bending and $1^{st}$ transverse) are shown in Figure 13 for the Polymylos Bridge obtained by the time domain identification algorithm using non-classically damped modal models. The identified modeshapes are in general complex valued. Figure 14 represents in polar plots two representative modeshapes ($1^{st}$ bending and $1^{st}$ transverse) based on earthquake-induced vibrations. These plots have the advantage to show directly the extent of non-classically damping characteristics of a modeshape. If all components of a modeshape vector are collinear (in phase or 180 degrees out of phase) then this mode is said to be classically (or proportionally) damped. On the contrary, the more these modeshape components are scattered in the complex plane, the more the mode is non-classically (or non-proportionally). For example, in Figure 14 it is observed that the $1^{st}$ transverse mode (1.29 Hz) is nearly classically damped. In Figure 15 the earthquake-induced accelerations and the accelerations predicted by the optimal modal model for selected sensors are compared. In Figure 16 the Fourier transform (FT) of the earthquake-induced accelerations and the FT of the accelerations predicted by the optimal modal model for selected sensors are compared. A very



Institutional Repository - Library & Information Centre - University of Thessaly
24/04/2024 00:02:26 EEST - 3.141.244.201

good fit is observed, validating the effectiveness of the proposed modal identification software based on earthquake recordings. All Figures of the modeshapes are shown in the appendices.

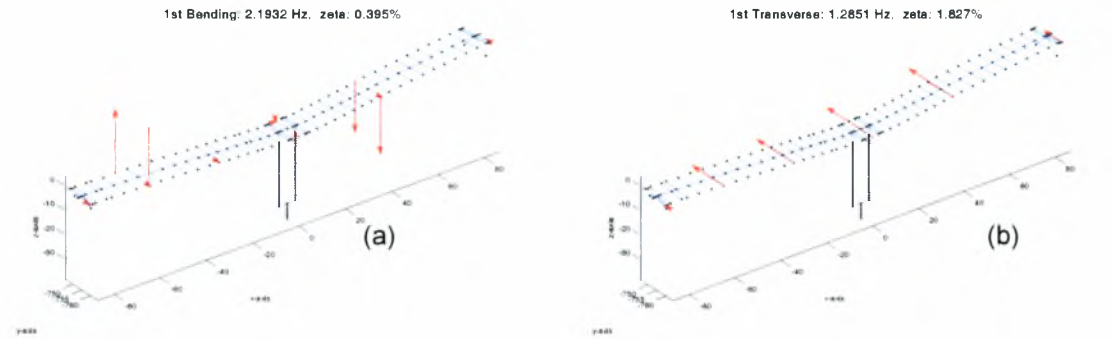


**Figure 13:** (a) 1st bending and (b) 1st transverse modeshape of the Polymylos bridge

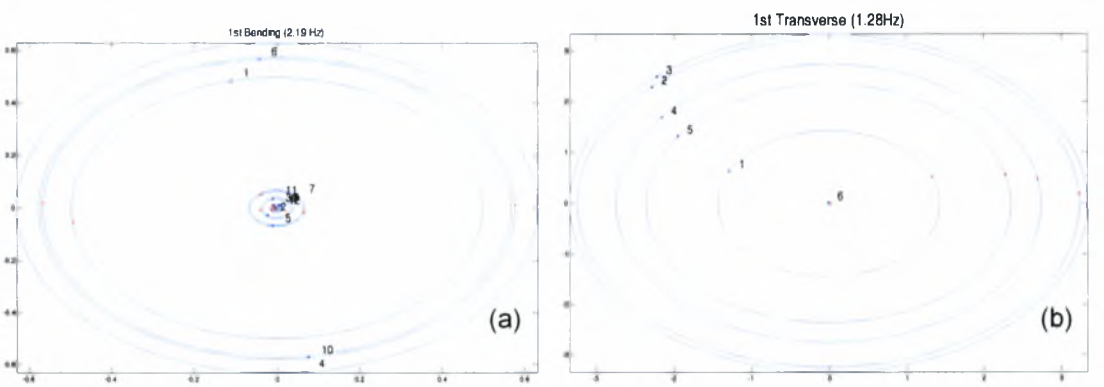


**Figure 14:** Polar plots representation of (a) 1st bending and (b) 1st transverse of the Polymylos Bridge

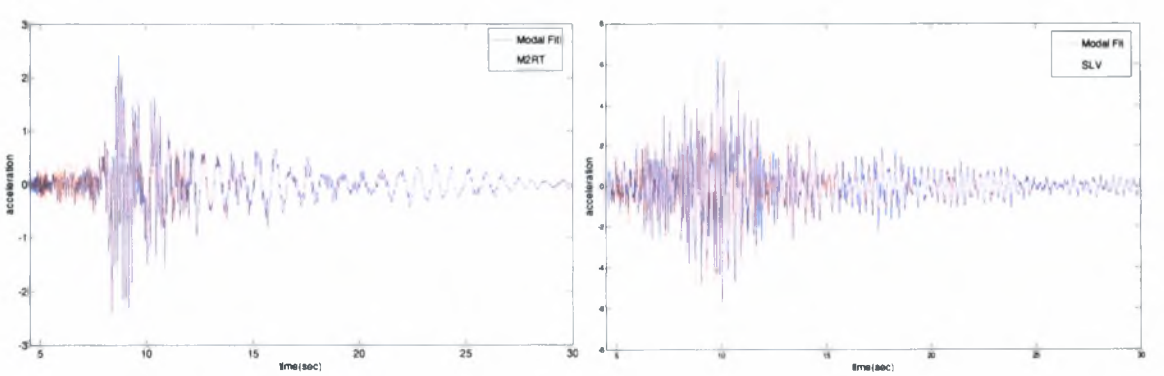


**Figure 15:** Comparison between measured and optimal modal model predicted accelerations recordings for selected sensors of the Polymylos Bridge



Institutional Repository - Library & Information Centre - University of Thessaly
24/04/2024 00:02:26 EEST - 3.141.244.201

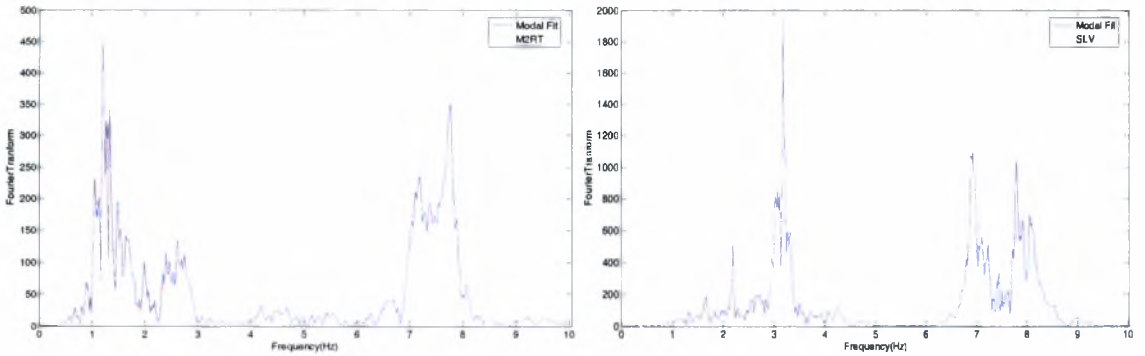


**Figure 16:** Comparison between measured and optimal modal model predicted Fourier Transforms of accelerations recordings for selected sensors of the Polymylos Bridge

## 5.5 Vincent Thomas Bridge, Los Angeles, California

The Vincent Thomas Bridge is a 6060 feet (1847 m) long bridge crossing the Los Angeles Harbor in the U.S. state of California (Figure 17). It is a cable-suspension bridge, consisting of a main span of approximately 457 m, two suspended side spans of 154 m each, and a 10-span approach of approximately 545 m length on either end. The roadway accommodates four lanes of traffic. The bridge was completed in 1964, and in 1980 was instrumented with 26 accelerometers as part of a seismic upgrading project. The measurement data from the sensor's network were obtained by the Center for Engineering Strong Motion Data (CESMD).

**Figure 17:** View of Vincent Thomas Bridge



Institutional Repository - Library & Information Centre - University of Thessaly
24/04/2024 00:02:26 EEST - 3.141.244.201

Figure 18 shows the layout of the location of the 26 sensors mounted on the bridge. Thirteen sensors were installed on the deck and three sensors on the top of the east tower, three sensors on the bottom of the west tower, four on the bottom of the east tower and three sensors on the eastern cable anchorage, as shown in Figure 18. Thus, the ten sensors monitor the earthquake-induced excitations at the bottom of the two towers and at the eastern cable anchorage. Notice that the eastern half of the bridge is more densely instrumented. This is because the analog recorder is housed in the eastern cable anchorage. The particular layout of the instrumentation permits the analysis of earthquake-induced response of the bridge. Among the 16 accelerometers located on the bridge deck and at the top of the towers, 6 record in the vertical, 3 in the longitudinal and the rest 7 in the transverse direction.

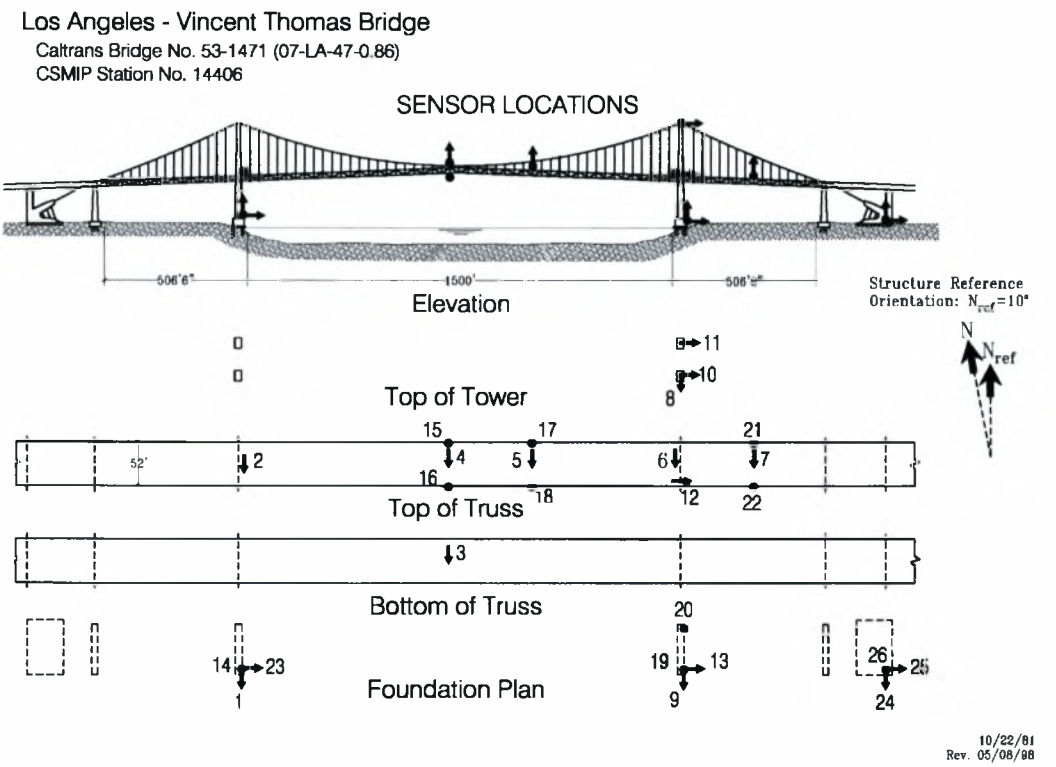


**Figure 18:** Instrumentation layout of Vincent Thomas Bridge (**http://www.strongmotioncenter.org**)

The modal identification carried out in the time domain and in the frequency domain using non-classically damped modal models for the 1987 Whittier earthquake $(M_L = 6.1)$. As it is mentioned in previous works (Lus et al., 1999, Smyth et al., 2003), the measurements of the earthquake-induced excitations and accelerations of the bridge were highly non-stationary for the Whittier earthquake. It is also known that the response of the bridge was highly non-linear during the peak times. Therefore, in the study of Lus et al. (1999) the final 50 sec of the records was used, in which the strong ground accelerations have died out. In this study, for the identification of



Institutional Repository - Library & Information Centre - University of Thessaly
24/04/2024 00:02:26 EEST - 3.141.244.201

structural parameters of the Vincent Thomas Bridge, the inputs were the accelerations of the ten (10) sensors located at the base of the structure and the outputs were the accelerations of five (5) vertical sensors. In the study of Smyth et al. (2003) the identification of structural parameters of the Vincent Thomas Bridge for the 1987 Whittier earthquake was done using the last 40 sec of the records in order to compare their results with the results from the study of Lus et al. (1999). The inputs were the same as in the study of Lus et al. (1999) but the outputs were the accelerations of all sensors on the deck of the bridge and on the towers.

In this work the identification of structural parameters of the Vincent Thomas Bridge was done for the recorded time lengths of 80 sec, using for inputs the accelerations of the ten (10) sensors located at the base of the structure and for outputs the accelerations of all sensors. Modal identification results (modal frequencies and modal damping ratios) for the Vincent Thomas Bridge are shown in Table 6 compared with the values identified by Lus et al (1999) and Smyth et al. (2003). In Table 6 are also presented the values of the modal frequencies and modal damping ratios resulted from the Stabilization Diagram (Step 1). In contrast with the two aforementioned studies (Lus et al., 1999, Smyth et al., 2003), in this work the identification of structural parameters of the Vincent Thomas Bridge was done for the recorded time lengths of 80 sec and therefore this is a more challenging identification problem. In the study of Smyth et al. (2003), several modal frequencies have been highlighted with a '*' symbol for comparison with similar results in Lus et al. (1999). Similar to this, in Table 6 the same modal frequencies have been highlighted with the '*' symbol for comparison with the resulted modal frequencies and damping ratios from the modal identification algorithm which have been developed in this thesis. As it is mentioned in the study of Smyth et al. (2003), these modes exhibited a significant vertical component in the modeshapes. This is consistent with the results of this work. This can be shown in Figure 20 in which two representative modeshapes in 0.211 Hz and 0.950 Hz are presented where a significant vertical component is observed.

Using all ten (10) input sensors which monitor the earthquake-induced excitations at the bottom of the two towers and at the eastern cable anchorage and all sixteen (16) output sensors, the values of the modal frequencies and modal damping ratios resulted from Stabilization Diagrams are presented in Figure 19 for: (a) the average of the Fourier Transforms of accelerations of all the output sensors, (b) the Fourier Transform of acceleration of a selected vertical sensor, and (c) the Fourier Transform of acceleration of a selected transverse sensor. It is observed that there are no clearly results for the modal frequencies and modal damping ratios. This is may be due to the existence of to many closely spaced and overlapped modes. Thus, in this case is up to the user to choose the optimal values of the modal frequencies and modal damping ratios. In Table 6, the "selected" values of the modal frequencies and modal damping ratios are presented and further down they are compared with the corresponding optimal values resulted from the modal identification algorithm in the time and in the frequency domain.



Institutional Repository - Library & Information Centre - University of Thessaly
24/04/2024 00:02:26 EEST - 3.141.244.201

**Table 6:** Identified modal frequencies $\omega$ and damping ratios $\zeta$ of the Vincent Thomas Bridge

| Vincent Thomas Bridge (Whittier earthquake) | | | | | | | | | |
|---|---|---|---|---|---|---|---|---|---|
| Modal Identification Algorithm | | | | | | | | | |
| Stabilization Diagram | | *Time Domain (non-classically damped)* | | *Frequency Domain (non-classically damped)* | | Smyth et al. (2003) All sensors *(records of the last 40 sec)* | | Lus et al. (1999) Vertical sensors *(records of the last 50 sec)* | |
| $\omega$ Hz | $\zeta$ (%) | $\omega$ Hz | $\zeta$ (%) | $\omega$ Hz | $\zeta$ (%) | $\omega$ Hz | $\zeta$ (%) | $\omega$ Hz | $\zeta$ (%) |
| | | | | 0.211 | 0.10 | *0.212 | 1.20 | 0.234 | 1.5 |
| | | | | - | - | *0.242 | 1.70 | 0.388 | 38.2 |
| | | 0.384 | 73.22 | 0.317 | 0.07 | *0.317 | -4.30 | 0.464 | 9.7 |
| | | 0.514 | 66.32 | 0.529 | 4.12 | 0.531 | 10.20 | 0.576 | 9.9 |
| | | | | 0.581 | 3.73 | *0.570 | 0.06 | 0.617 | 14.5 |
| 0.626 | 8.77 | | | 0.626 | -3.15 | *0.636 | 4.20 | 0.617 | 76.8 |
| | | 0.662 | 0.72 | 0.671 | 1.83 | 0.672 | 0.10 | 0.769 | 29.7 |
| | | | | - | - | 0.734 | 2.40 | 0.804 | 1.4 |
| | | 0.829 | 4.59 | 0.822 | 6.11 | *0.818 | 1.90 | 0.857 | 11.6 |
| | | 0.938 | 1.41 | 0.950 | 0.65 | *0.958 | 2.90 | 0.947 | 4.3 |
| 1.012 | 5.94 | 0.983 | 1.69 | 1.022 | 1.49 | 1.027 | -1.90 | | |
| 1.136 | 9.13 | 1.111 | 1.83 | 1.107 | 0.93 | *1.111 | 1.30 | | |
| | | 1.170 | 1.56 | 1.157 | 0.58 | *1.159 | 1.70 | | |
| | | 1.414 | 6.06 | 1.397 | 3.90 | 1.391 | 2.30 | | |
| | | | | 1.547 | 0.83 | 1.554 | -1.30 | | |
| 2.102 | 6.95 | 2.292 | 0.73 | 2.274 | 1.33 | | | | |
| 3.458 | 6.80 | | | 3.428 | 2.75 | | | | |
| 4.361 | 2.83 | | | 4.333 | 0.75 | | | | |
| 4.573 | 2.38 | | | 4.572 | 0.47 | | | | |
| 5.548 | 2.79 | | | 5.674 | 0.19 | | | | |



Institutional Repository - Library & Information Centre - University of Thessaly
24/04/2024 00:02:26 EEST - 3.141.244.201

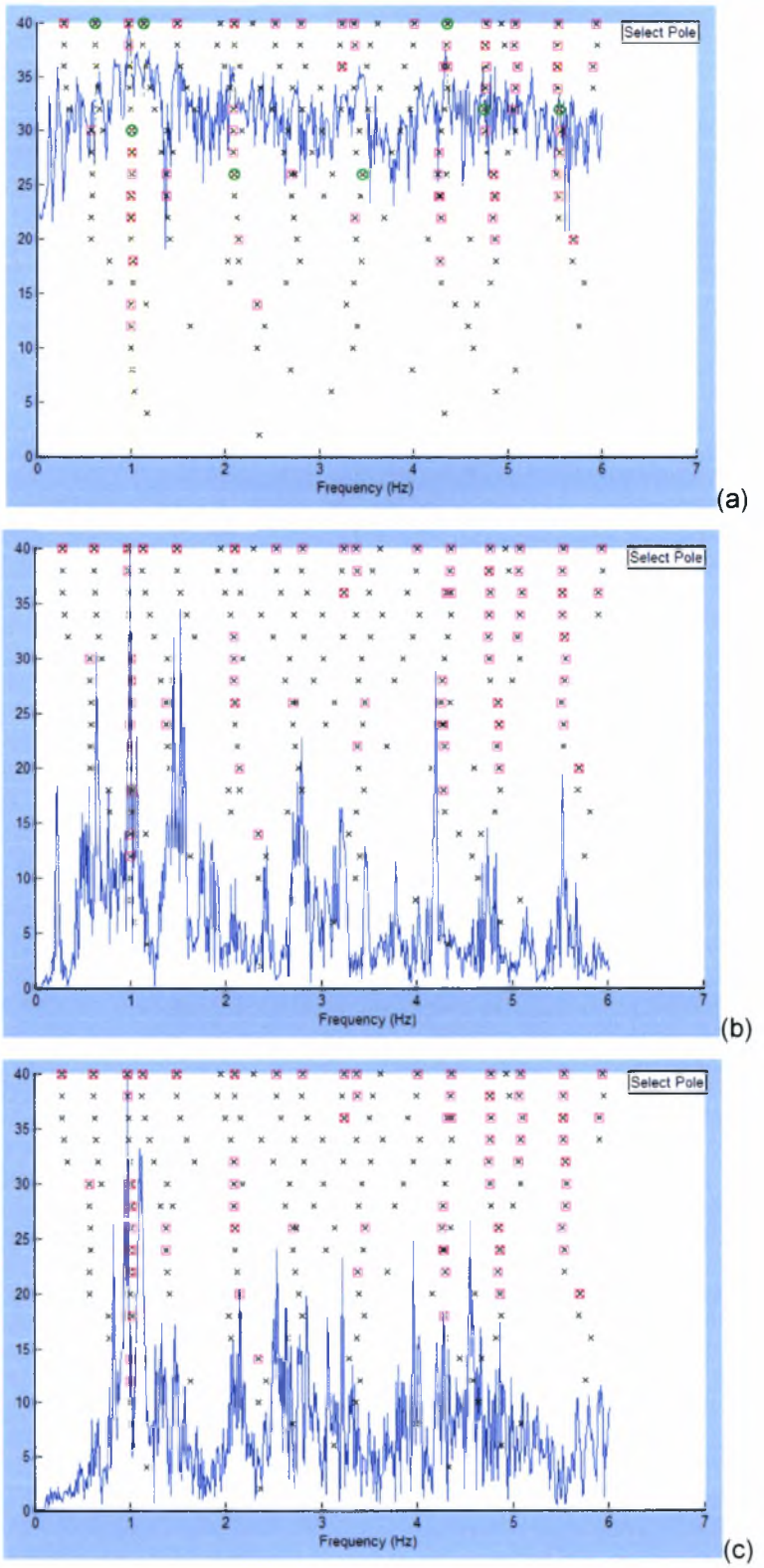


**Figure 19:** Stabilization Diagram for the Vincent Thomas Bridge: (a) average of the Fourier Transforms of accelerations of: all sensors, (b) Fourier Transform of acceleration of the vertical sensor 16, and (c) Fourier Transform of acceleration of the transverse sensor 5



Institutional Repository - Library & Information Centre - University of Thessaly
24/04/2024 00:02:26 EEST - 3.141.244.201

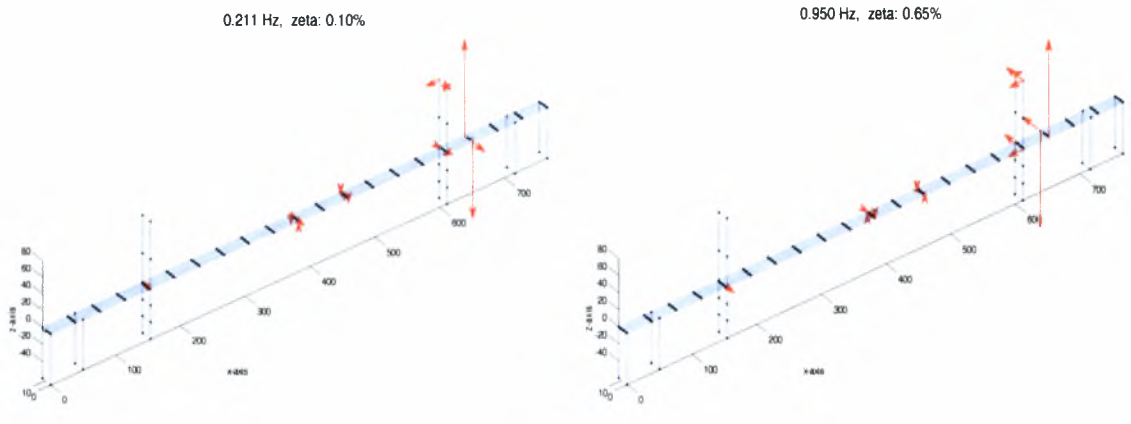


**Figure 20:** Two representative modeshapes in 0.211 Hz and 0.950 Hz of the Vincent Thomas Bridge

Comparing the modal frequencies and damping ratios resulted from the Stabilization Diagrams and the modal identification algorithm for time and frequency domain it is observed that Stabilization Diagrams does not provide good estimates of the optimal values of the modal frequencies. In contrast, it is observed that the resulted values from the Stabilization Diagrams of the modal damping ratios have major discrepancies compared with the optimal values of the modal damping ratios from the identification algorithm in time and frequency domain. This may be due to the presence of many closely spaced and overlapped modes combined with the presence of instrumentation noise and the affect of "leakage" in the computation of the FFTs of the measured time histories.

In Table 6 it is observed that the number of the modal frequencies (and damping ratios) identified in the frequency domain is greater than the number of identified modal frequencies (and damping ratios) in the time domain. In particular, it should be noted that time domain identification algorithm cannot identify the lower and higher frequencies, in a frequency band of 0-6Hz, and that for the low frequencies very high damping estimates are obtained. This may indicate that the particular time domain methodology have problems to reliably identify modal frequencies (and damping ratios) when they are closely spaced and overlapped. In contrast, 18 modes were successfully and reliably identified by the frequency domain identification algorithm.

The identification method employed in Lus et al. (1999) is constrained to give only positive damping estimates and does not therefore yield the few negative damping estimates obtained in the study of Smyth et al. (2003). In this thesis high damping estimates are observed in the results from time domain identification algorithm for two modes. This points the difficulties associated with accurate estimation of damping from this type of data set in the time domain algorithm. It has to be mentioned that in this work the identification was done for the recorded time lengths of 80 sec which complicates more the identification process. In Table 6, it is observed that the values of the modal frequencies resulted from frequency domain identification algorithm are similar to the values which resulted from the analysis in the study of Smyth et al. (2003), while the modal



Institutional Repository - Library & Information Centre - University of Thessaly
24/04/2024 00:02:26 EEST - 3.141.244.201

damping ratios have major differences. This evidence that the frequency domain methodology which has been developed in this work is more efficient than the time domain methodology for from this type of data set.

Further down representative measured modeshapes in polar plots (0.211 Hz and 0.950 Hz) are shown in Figure 21 for the Vincent Thomas Bridge obtained by the frequency domain identification algorithm using non-classically damped modal models. In Figure 22 the earthquake-induced accelerations and the accelerations predicted by the optimal modal model for selected sensors are compared. In Figure 23 the Fourier transform (FT) of the earthquake-induced accelerations and the FT of the accelerations predicted by the optimal modal model for selected sensors are compared, for the frequency band 0-1.6 Hz.

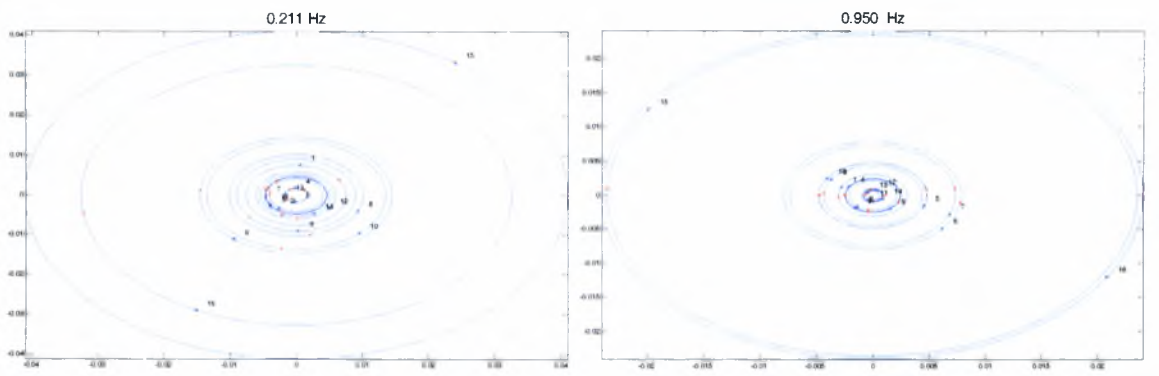


**Figure 21:** Polar plots of two representative modeshapes in 0.211 Hz and 0.950 Hz of the Vincent Thomas Bridge

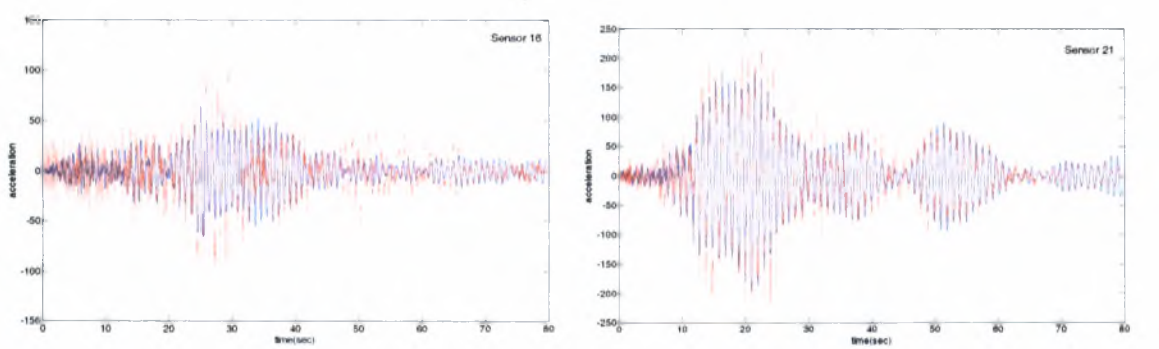


**Figure 22:** Comparison between measured and optimal modal model predicted accelerations recordings for selected sensors of the Vincent Thomas Bridge



Institutional Repository - Library & Information Centre - University of Thessaly
24/04/2024 00:02:26 EEST - 3.141.244.201

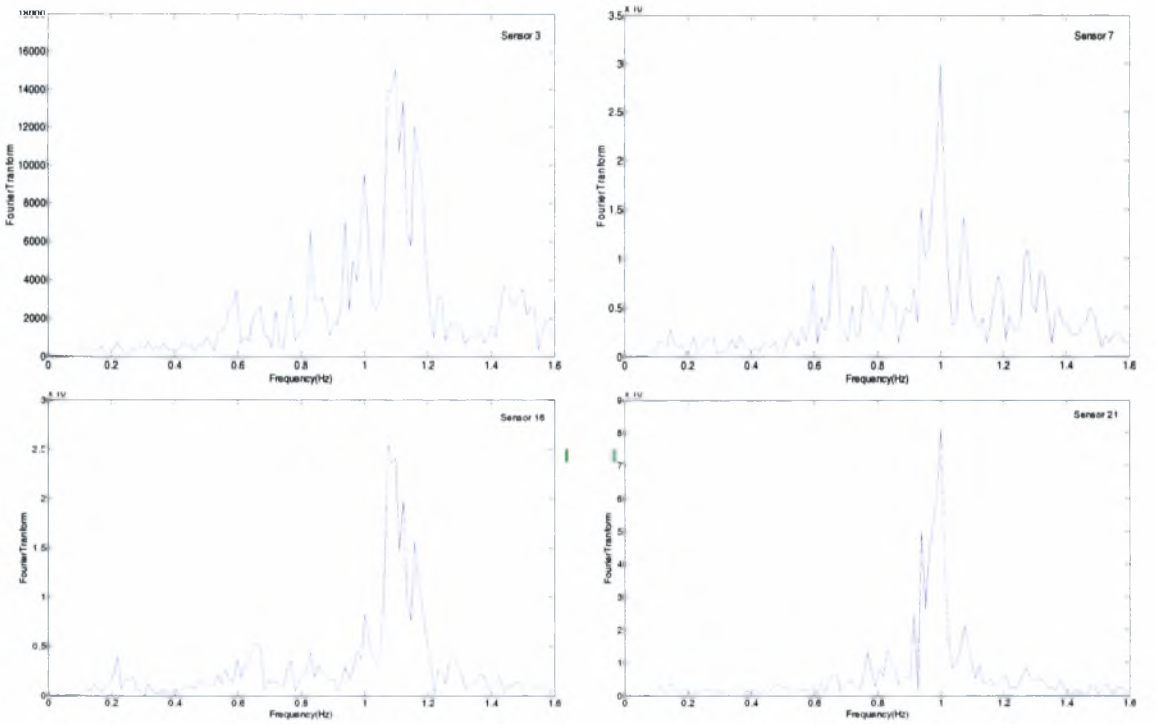


**Figure 23:** Comparison between measured and optimal modal model predicted Fourier Transforms of accelerations recordings for the frequency band 0-1.6 Hz for selected sensors of the Vincent Thomas Bridge



Institutional Repository - Library & Information Centre - University of Thessaly
24/04/2024 00:02:26 EEST - 3.141.244.201

## 5.6 Appendix

Modeshapes of Polymylos bridge

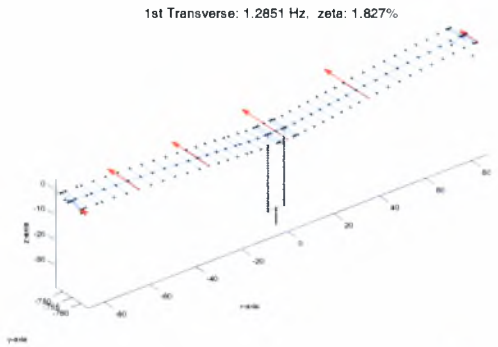


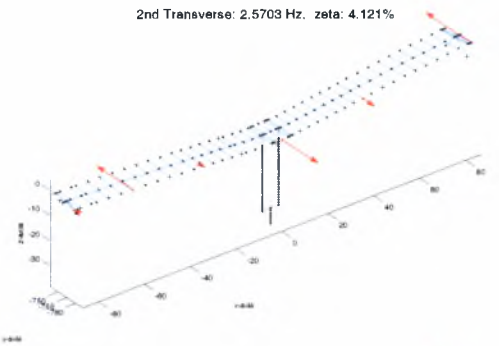


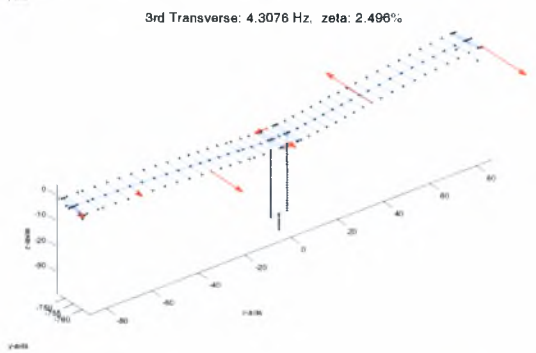


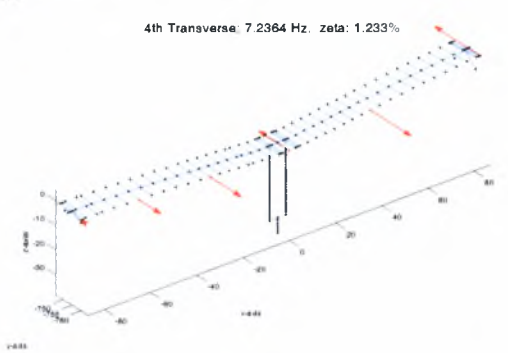


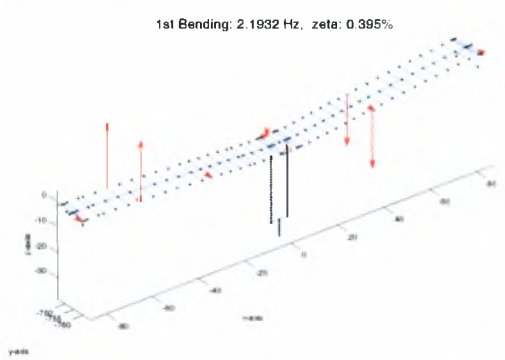


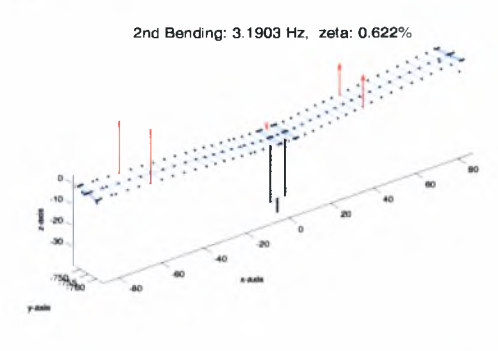


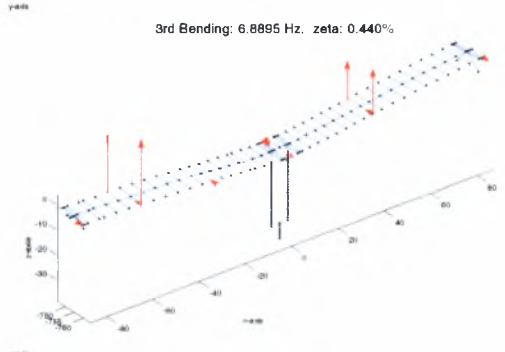


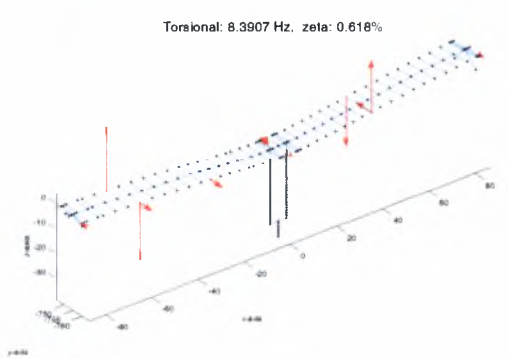




Institutional Repository - Library & Information Centre - University of Thessaly
24/04/2024 00:02:26 EEST - 3.141.244.201

## Polar Plots of Modeshapes of Polymylos bridge

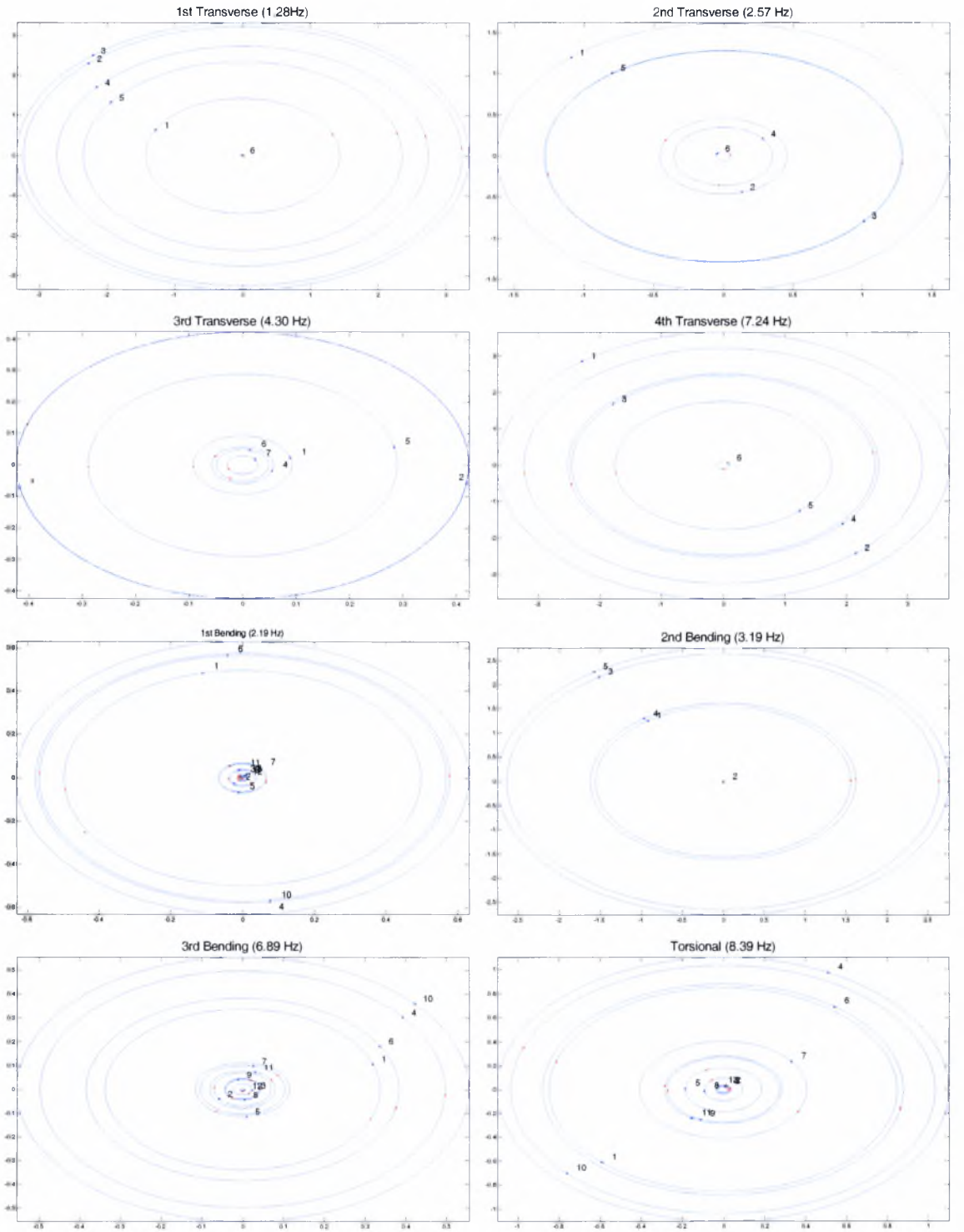




Institutional Repository - Library & Information Centre - University of Thessaly
24/04/2024 00:02:26 EEST - 3.141.244.201

Time Histories of Polymylos bridge

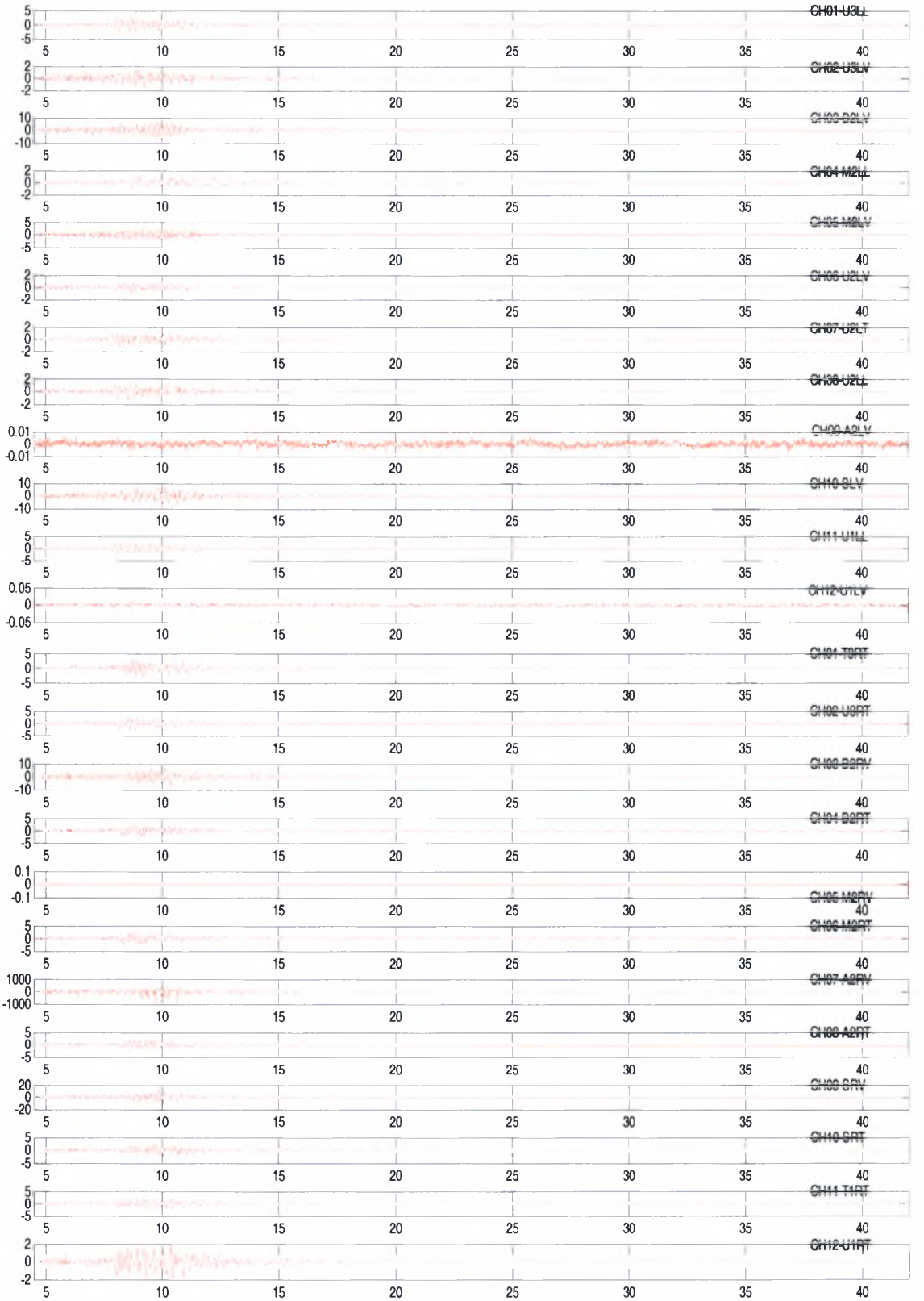




Institutional Repository - Library & Information Centre - University of Thessaly
24/04/2024 00:02:26 EEST - 3.141.244.201

# Chapter 6

# Conclusions

Modal identification methodologies for estimating the dynamic modal characteristics of civil engineering structures have been developed in this thesis using earthquake induced vibration measurements. The main objective of this work has been to determine the modal and other parameters of non-classically damped modal models used to describe the response of linear structures subjected to multiple base excitations.

The identification has been performed by analysis in the time domain and in the frequency domain. The methods developed by McVerry (1980) in the frequency domain and Beck and Jennings (1980) in the time domain, have been extended in this work to treat non-classically damped modal models. Additionally, time domain methodology for identifying the modal and other parameters of classically damped modal models has been also developed. The optimal values of the modal parameters, such as modal frequencies, modal damping ratios and modeshapes, were obtained by the implementation of an output error methodology. In time domain analysis, the optimal values were obtained by minimizing a measure of fit between the output measured acceleration time histories and the predicted acceleration time histories by a modal model. In frequency domain analysis, the optimal values were obtained by minimizing a measure of fit between the theoretical Fourier transform of the model response to the Fourier transform of the measured response acceleration.

In particular, the modal identification methodology have been developed in a three step approach. In the first step, the PolyMAX or polyreference least-squares complex frequency domain method, developed by Peeters et. al (2004), has been extended in order to treat non-classically damped modal models describing a system's response characteristics based on earthquake-induced vibration data. . In the second step, the resulted values of modal frequencies and modal damping ratios from the first step were used for the time and the frequency domain methodologies, in order to compute the modeshape components and the participation factors. Finally, the solution of a nonlinear optimization problem using initial conditions from the previous steps improves the modal estimates and it is recommended for the identification of closely spaced and overlapped modes.

The number of variables to be optimized depends on the number of contributing modes. In order to overcome the problem of the large number of variables involved, improve the robustness, and accelerate convergence, a modal sweep approach was proposed for which each mode was optimized separately while the contribution from the rest of the modes was held constant. In addition, for time domain and frequency domain analysis analytically evaluated gradients of the



Institutional Repository - Library & Information Centre - University of Thessaly
24/04/2024 00:02:26 EEST - 3.141.244.201

cost function have been implemented in to the modal identification algorithm accelerating more the convergence.

The modal model identification methods were implemented in Matlab software. The software was validated using simulated data from a 3 DOF and 10 DOF spring mass chain model. It was observed that an accurate fit resulted from the convergence of the acceleration time histories predicted from the optimal modal model to the "measured" acceleration time histories for the 3-DOF and the 10 DOF spring mass chain model and a similar fit was observed for the Fourier Transforms of the accelerations. It was also observed that the estimated modal frequencies and damping ratios resulted from the Stabilization Diagrams were accurately identified (no major discrepancies between the modal frequencies and damping ratios resulted from the Stabilization Diagrams and the modal identification algorithm), which validates their effectiveness.

The modal model identification methods were also applied to two bridges in order to identify their modal properties. The identification methodology applied to the R/C bridge of Polymylos subjected to a low level magnitude earthquake event reliably identified eight of the lower modes. The results showed that the damping values of the bending modes are of the order of 0.4% to 0.7% which is significantly lower than the damping values of the transverse modes. This is attributed to the higher damping provided by the elastomeric bearings for the latter modes. Comparing the modal frequencies due to earthquake-induced vibrations estimated in this work, with the modal frequencies due to ambient vibrations estimated in other works, showed that they are 4% to 15% higher. This is attributed mainly to the soil-structure interaction effects contributing to the dynamics of the bridge systems during ambient excitation. These effects are not present in the identified dynamics of the system based on earthquake-induced vibrations due to the use of the input acceleration measurements of the base of the piers and the abutments.

The identification methodologies were also applied to the Vincent Thomas cable suspension bridge subjected to the 1987 Whittier earthquake. Despite the fact that the Whittier earthquake was highly non-stationary and the bridge response was highly nonlinear during the peak times, 18 of the bridge modes were identified using the frequency domain methodology. The time domain methodology showed lack of reliability especially for the identification of the lower closely spaced and overlapped modes. The values of the modal frequencies and the damping ratios estimated in the present work were also compared with the results given from other works in the previous years. This comparison showed that the values for the modal frequencies are similar, while the modal damping ratios have major discrepancies.

Through the application of identification methods to these real structures, a great degree of experience was gained, developing intuition of the way the techniques lead to the desired result and of the problems that emerge in the process.



Institutional Repository - Library & Information Centre - University of Thessaly
24/04/2024 00:02:26 EEST - 3.141.244.201

## References


[1] Arici Y, Mosalam KM (2003) System identification of instrumented bridge systems. Earthquake Engineering and Structural Dynamics 32: 999–1020.

[2] Beck JL (1978) Determining models of structures from earthquake records. Report No. EELRL 78-01, Earthquake Engineering Research Laboratory, California Institute of Technology, Pasadena, CA.

[3] Beck JL, Jennings PC (1980) Structural identification using linear models and earthquake records. Earthquake Engineering and Structural Dynamics 8: 145-160.

[4] Chaudhary MTA, Abe M, Fujino Y (2000) System identification of two base-isolated buildings using seismic records. Journal of Structural Engineering (ASCE) 126(10): 1187-1195.

[5] Chaudhary MTA, Abe M, Fujino Y (2002) Investigation of atypical seismic response of a base-isolated bridge. Engineering Structures 24: 945–953.

[6] Christodoulou K, Papadimitriou C (2007) Structural identification based on optimally weighted modal residuals. Mechanical Systems and Signal Processing 21: 4-23.

[7] Clough RW, and Penzien J (1993) Dynamics of structures. McGraw-Hill.

[8] Ewins DJ (2000) Modal Testing: Theory, Practice and Application, Second edition. Research Studies Press LTD.

[9] Lin CC, Hong LL, Ueng JM, Wu KC, and Wang CE (2005) Parametric identification of asymmetric buildings from earthquake response records. Smart Materials and Structures 14: 850-861.

[10] Liu H, Yanga Z, Gaulkeb MS (2005) Structural identification and finite element modeling of a 14-story office building using recorded data. Engineering Structures 27: 463–473

[11] Lus H, Betti R, Longman RW (1999) Identification of Linear Structural Systems using Earthquake-Induced Vibration Data. Earthquake Engineering and Structural Dynamics 28: 1449–1467.

[12] Mahmoudabadi M, Ghafory-Ashtiany M, and Hosseini M (2007) Identification of modal parameters of non-classically damped linear structures under multi-component earthquake loading. Earthquake Engineering and Structural Dynamics 36: 765-782.

[13] McVerry GH (1980) Structural identification in the frequency domain from earthquake records. Earthquake Engineering and Structural Dynamics 8: 161-180.

[14] Mottershead JE, Friswell MI (1993) Model updating in structural dynamics: A survey. Journal of Sound and Vibration 167: 347-375.




Institutional Repository - Library & Information Centre - University of Thessaly
24/04/2024 00:02:26 EEST - 3.141.244.201

[15] Ntotsios E, Karakostas Ch, Lekidis V, Panetsos P, Nikolaou I, Papadimitriou C, and Salonikos Th (2007) Structural Identification of Egnatia Odos Bridges based on Ambient and Earthquake Induced Vibrations. Bulletin of Earthquake Engineering

[16] Papadimitriou C, Levine-West M, and Milman M (1997) Structural Damage Detection Using Modal Test Data. Proc. International Workshop on Structural Health Monitoring: Current Status and Perspectives, F-K. Chang (Ed), Technomic Publishing Co 678-689.

[17] Papadimitriou C, Pavlidou M, Christodoulou K, Karamanos SA, (2002) Optimal Sensor Configuration Methodology for Structural Identification. 1st European Workshop on Structural Health Monitoring, Paris, France.

[18] Peeters B, Van der Auweraer H, Guillaume P, and Leuridan J (2004) The PolyMAX frequency-domain method: a new standard for modal parameters estimation. Shock and Vibration 11: 395-409.

[19] Smyth AW, Pei J-S, Masri SF (2003) System identification of the Vincent Thomas suspension bridge using earthquake records. Earthquake Engineering and Structural Dynamics 32: 339–367.

[20] Tan RY, Cheng WM (1993) System identification of a non-classically damped linear system. Computers and Structures 46:67–75.

[21] Safak E (1993) Response of a 42-storey steel-frame building to the $M_s = 7.1$ Loma Prieta earthquake. Engineering Structures 15: 403-421

[22] Safak E (1995) Detection and identification of soil-structure interaction in buildings from vibration recordings. Journal of Structural Engineering (ASCE) 121(5): 899-906.

[23] Siringoringo DM, Fujino Y (2007) Dynamic characteristics of a curved cable-stayed bridge identified from strong motion records. Engineering Structures 29: 2001-2017

[24] Werner SD, Beck JL, Levine MB (1987) Seismic response evaluations of Meloland road overpass using 1979 Imperial Valley earthquake records. Earthquake Engineering and Structural Dynamics 15: 249-274.

[25] Wilson JC (1986) Analysis of the observed seismic response of an highway bridge. Earthquake Engineering and Structural Dynamics 14: 339–354.



Institutional Repository - Library & Information Centre - University of Thessaly
24/04/2024 00:02:26 EEST - 3.141.244.201

ΠΑΝΕΠΙΣΤΗΜΙΟ ΘΕΣΣΑΛΙΑΣ
ΒΙΒΛΙΟΘΗΚΗ
ΠΑΝΕΠΙΣΤΗΜΙΟ
ΘΕΣΣΑΛΙΑΣ
0040000091591
Institutional Repository - Library & Information Centre - University of Thessaly
24/04/2024 00:02:26 EEST - 3.141.244.201

Institutional Repository - Library & Information Centre - University of Thessaly
24/04/2024 00:02:26 EEST - 3.141.244.201